UNIVERSITÀ DEGLI STUDI DI CAMERINO
SCHOOL OF ADVANCED STUDIES

DOCTORAL COURSE IN
CHEMICAL AND PHARMACEUTICAL SCIENCES AND BIOTECHNOLOGY
CHEMICAL SCIENCES
XXXIV CYCLE

CHEMISTRY, TECHNOLOGY AND OPTIMIZATION OF FORMULATIONS AND PHYSICAL-CHEMICAL PARAMETERS IN FOOTWEAR SOLE INDUSTRY AND SYNTHESIS OF NEW METAL-SUPPORTED CATALYSTS

PHD STUDENT
DR. RICCARDO VALLESI

SUPERVISORS
PROF. CARLO SANTINI
PROF. MAURA PELLEI

CO-SUPERVISORS
LUIGI LUCENTINI
ANTONIO QUATRINI

ACADEMIC YEARS 2018/2019 - 2020/2021

Preface

My PhD work is not a classical one: it involves both industrial and academic experiences. The first part of this work describes the period I spent in Delta Spa. It is located in the industrial zone of Civitanova Marche (MC). This particular part of Marche region is known as “sole valley” because the main production is outsole for footwear. Delta is one of the most historic companies in soles production: it was founded in 1972 and Mr Luigi Lucentini is the CEO. Actually, Delta Spa has its main stake in Civitanova Marche (13000 m^2 over a total area of 40000 m^2) and it has some international participations (Delta HK is one of the most important). His first main activity was the production of PolyUrethane (PU) soles; however, due to the increase of technological knowledge and financial investments in research and development, the company has expanded his production to other materials (Rubber, Ethylene Vinyl Acetate (EVA), Thermoplastic PolyUrethane (TPU)). The propriety has always believed in external resources to increase and better know the properties and quality of the final product. Having in mind this aim, the collaboration between Delta and University of Camerino in this PhD project makes it work. The second part of this thesis involves inorganic chemistry of carbenes and allylic oxidation of alkenes (Kharasch-Sosnovsky reaction) catalysed by copper(II) complexes. I spent this period in the research group of Professor Maura Pellei and Professor Carlo Santini at the School of Science and Technology, Chemistry Division of the University of Camerino. Carbene chemistry is useful in many applications: in this family, a special role is played by N-Heterocyclic carbenes (NHCs). They show interesting properties and uses in material chemistry. Derivatives of NHCs having a borate counter anion have been synthesized and they have been studied as carbene precursors for NHCs-silver(I) complexes. Kharasch-Sosnovsky reaction is Cu(II) C-H oxidation for allylic functionalization. Newly ligands and relative copper(II) complexes were synthetized and their relative catalytic activity were studied.

Table of contents

List of figures

List of tables

List of schemes

List of equations

List of abbreviations

Ac	Accelerators
ACN	AcryloNItrile
BIIR	BromoButyl Rubber
BR	Butadiene Rubber
CB	Carbon Black
CB-DBP	Carbon Black DiButyl Phtalate
CIIR	ChloroButyl Rubber
CTAB	Cetyl Trimethylene Ammonium Bromide
CV	Constant Viscosity
DP	Degree of Polymerization
DSC	Differential Scanning Calorimetry
EDG	Electron Donating Group
ENR	Epoxidized Natural Rubber
EO	Ethylene Oxide
EPDM	Ethylene-Propylene Diene Monomer
E-SBR	Emulsion-type SBR
EtOAc	Ethyl Acetate
EVA	Ethylene Vinyl Acetate
EWG	Electron Withdrawing Group
HDI	1,6-Hexamethylene Diisocyanate
HDS	Highly Dispersible Silica
HexOH	1-Hexanol
HNBR	Hydrogenated Nitrile Rubber
IIR	Butyl Rubber
IR	Isoprene Rubber
IUPAC	International Union of Pure and Applied Chemistry
LATZ	Low Ammonia Latex Concentrate
LDPE	Low Density PolyEthylene
MDI	Methylene Diisocyanate
MeCN	Acetonitrile
MH	Moment Highest
ML	Moment Lowest
MW	Molecular Weight
MW	Microwave
NBR	Nitrile Butadiene Rubber
NEXAFS	Near Edge X-ray Absorption Fine Structure
NHC	N-Heterocylcle Carbene
NR	Natural Rubber
PET	PolyEthylene Terephtalate
Phr	Part of Hundred of Rubber
PO	Propylene Oxide

PP	PolyPropylene
PU	PolyUrethane
PVA	PolyVinylAlcohol
PVC	PolyVinylChloride
RSS	Ribbed Smoked Sheet
SBR	Styrene Butadiene Rubber
S-SBR	Solution-type SBR
TDI	Toluene Diisocyanate
TESPT	bis(triethoxysilylpropyl)tetrasulfane
T_g	Glass Transition temperature
THF	TetraHydroFuran
TPE	ThermoPlastic Elastomers
TPU	ThermoPlastic Polyurethane
TR	thermoplastic Rubber
TSR	Technical Specified Rubbers
UV	UltraViolet light
XAFS	X-ray Absorption Fine Structure Spectroscopy
XPS	X-ray Photoelectron Spectroscopy

1. Polymers

1.1 Introduction

Everyday life is based on natural and, from the half of the last century, synthetic polymers. For example, in footwear industry, some polymers are used in sole production: from Styrene Butadiene Rubber (SBR) to Thermoplastic Rubber (TR), from PolyUrethane (PU) to Ethylene Vinyl Acetate (EVA), all these polymers are used to obtain different products with distinctive properties. Regarding soles industry, besides considering polymer properties, an economic view must be made in order to make the best product at a reasonable price. The word "polymer" derives from two Greek words, "poly" and "mer". Poly means "many" while "mer" "part". From the etymology of the word, we can understand that polymers are formed by a lot of units. According to the definition of IUPAC, polymers are "substances composed of macromolecules, very large molecules with molecular weights ranging from a few thousand to as high as millions of grams/mole". The structural units of these macromolecules are called monomers which are linked together by a process called polymerization. Due to the complex structure and high Molecular Weight (MW), it's almost impossible to write down a polymer chain; however, it is generally used to write down the monomer(s) of the final polymer (**Fig. 1**):

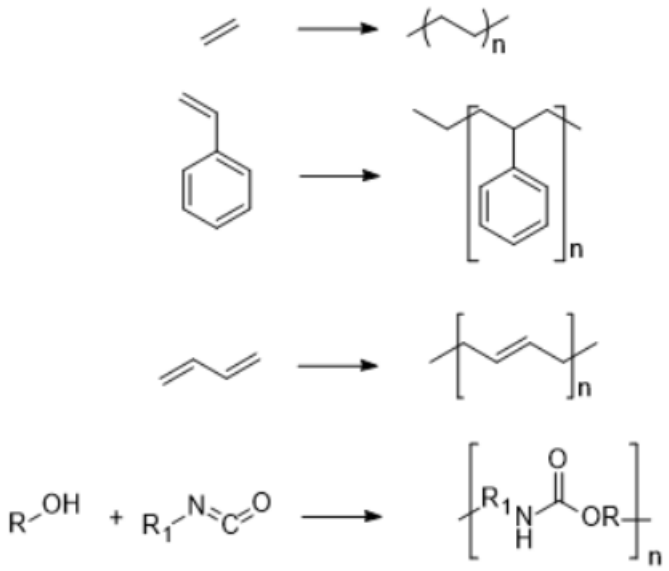

Fig. 1. Examples of polymers.

Fig. 1 shows, respectively, polyethylene, polystyrene, polybutadiene and polyurethane. The last one is interesting because, differently from the other polymers reported in **Fig. 1**, it is formed from the reaction of two different monomers (polyol and isocyanate).

1.2 History and milestones

Interestingly, the word polymer is introduced at the beginning of 19th century by the pioneering work of Bezelius.[1] Other important discoveries have been made in the same century: isolation of isoprene rubber and polymerization of styrene are one of the most important.[2,3] With the development of industrial sector at the beginning of 20th century, novel synthetic polymers have been introduced to the market: Bakelite, discovered by Leo Backeland,[4] and polybutadiene rubber. In parallel with it, academic research on polymer structure made some important advantages: the theory of German chemist Staudinger is one of the most important and the Sweden Academy has recognized him the 1930 Nobel Prize in Chemistry.[5] The idea of Staudinger was to explain the polymer characteristic properties by the presence of ordinary intermolecular forces between the high MW molecules. In his work, he introduced the word "macromolecule" (*makromolectül*).[6] The first successful application of Staudinger's theory was the synthetic production process of nylon and neoprene rubber.[7]
A huge impact on polymer chemistry was made by the Second World War. Substituting the natural rubber was the main aim of polymer chemistry: synthetic rubbers were developed in these years. Post-war years were characterized by two important milestones: Ziegler-Natta catalysts and Flory's equation for polymer behaviour. The authors have been awarded of the Nobel Prize in Chemistry, respectively, in 1963 and 1974.[5] Ziegler discovered new coordination catalysts for initiating polymerization reaction: those catalysts were used in the synthesis of new controlled stereochemical polymers by Natta.[8,9] Flory introduced a new method for quantitative estimation of determining the behaviour of polymers, e.g. chemical phenomena like crosslinking or properties of macromolecules in bulk or solution.[10]
Nowadays, the "green" thinking is also making his way in polymer chemistry. Researchers are focusing their interest in finding new ways for production of synthetic polymers without the use of toxic agents. Due to the market demand and variety, polymer industry has also developed important materials to increase performances and worker security; example are non-flammable and biodegradable polymers.

1.3 Basic concepts of polymers

An oligomer (*oligos* means few in Greek) is a low MW polymer formed by few monomers. Homochain polymers derived from alkene addition: their structure or backbone is formed only by a single type of carbon with a single or a group of atoms. Contrarily, an heterochain polymer has in his composition different type of atoms. The chain length(s) and molecular weight are very important parameters. Related to them, there is the definition of "degree of polymerization" which describes the total number of structural units, including the presence of any groups. However, in real situation, it's easier and more convenient to use the "average degree of polymerization", because, during a polymerization reaction, the final result is a distribution of MW, not a maximum limit in chain length. If polymer contains the same structural unit (monomer), it is called homopolymer. If different monomers (two or more) react together and form a polymer chain, then a copolymer is obtained. In **Fig. 2**, there is an example scheme for copolymers:

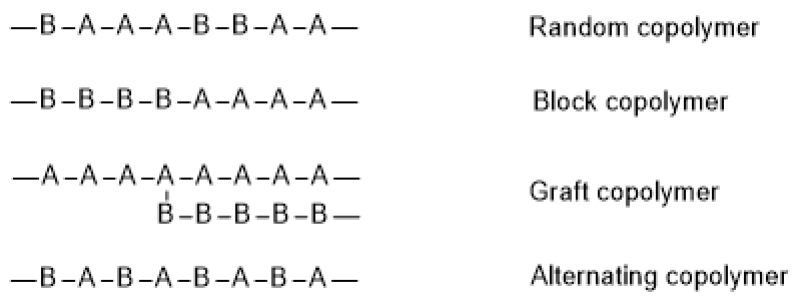

Fig. 2. Example for copolymers.

Assuming A and B as different monomers, several combinations can be possible:

- if the monomer distribution is random, a random copolymer is obtained;
- if the monomers are distributed in blocks, then a block copolymer is obtained;
- if one polymer is linked on the backbone of the other, a graft copolymer is produced;
- if the distribution of the monomers is an alternate fashion, then an alternating copolymer is obtained.

There are several other ways for describing a polymer. If the special arrangement or disposition is taking into consideration, then linear, branched or network/crosslinked polymers are obtained (**Fig. 3**):

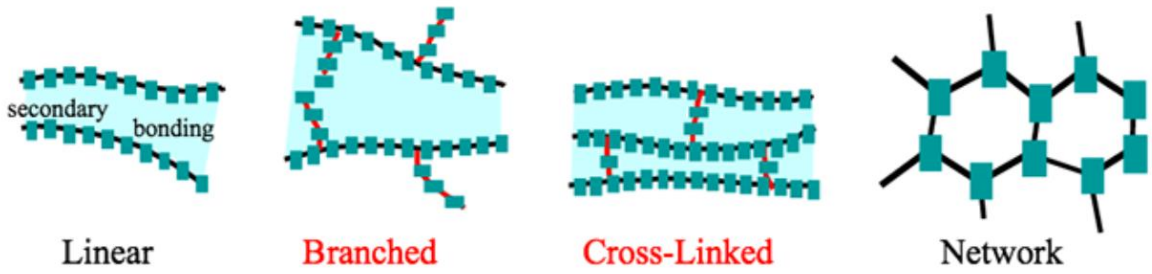

Fig. 3. Different arrangements for polymers.

As the name suggests, a linear polymer has no branched point other the substituents on the monomer. The typical example of a branched polymer is a graft polymer (see **Fig. 2**): however, a branched polymer can be also a homopolymer. In LDPE case, the branched is due to side reactions during polymerization.[11]

Generally, in sole industry, rubber is used for articles production as starting material which is shaped into a mould during the so-called vulcanization process. Vulcanizing rubber is one of the most important examples of network polymers. In vulcanization process, linear or branched polymer chains (elastomeric compound having free double bonds) are linked together by covalent bonds (sulphur bridges). From this example, an important phenomenon is observed: polymer chains lose their flowing behaviour due to crosslink reactions. As a matter of fact, the final polymer cannot be moulded or melted: in polymer chemistry, they are called “thermosetting polymers”. Their main characteristics are two:

1. swelling in the presence of a solvent (solvent molecules can penetrate the network);
2. they are insoluble because of the increase of MW during crosslink reaction.

Regarding thermic behaviour, when the temperature increases, they don’t soften and become impossible to process. This kind of materials has to be worked in one step process to obtain the desired product. A disadvantage is that they can’t be reused in the same process: for recycling purpose, they must be treated to be used in other formulations as filler for improve physical proprieties or for an aesthetic function. On the other side, thermoplastic polymers are polymers usually not crosslinked: they can be dissolved in solvents and, in most situations, they can flow. Considering their thermic behaviour, thermoplastic compounds became soft and liquid increasing temperature. In this way, it can be moulded. Interestingly, in case of reaching a temperature below its softening point in the cooling process, they became rigid and can be used as a final article. Differently from the other type, they can be recycled infinite

times increasing temperature. In polymer chemistry, the glass transition temperature (commonly known as T_g) is the temperature when the change from a liquid to a glassy state occurs in the polymer. In thermoplastics, for example, below T_g, the compound is hard and it has specific functions while, above T_g, it is soft and easy to process.

1.4 Polymerization processes

The first classification of addition and condensation polymers was introduced by Carothers and it is based on the chemical structure and composition of the final product.[12] On one hand, addition polymers, according to this definition, contain the same atoms as the monomer, while, on the other, condensation ones contain fewer atoms because of the by-products formed during polymerization process. The problem with this classification is related to the fact that the same polymer can be synthesized both with addition and condensation reactions.

In order to avoid ambiguity, nowadays, the mechanism of polymerization is taken into account instead of chemical composition. In this view, a step-growth reaction (or step reaction) is a process where polymer chains are built in a stepwise fashion by the random union of monomers to form higher species throughout the monomer matrix. Differently, a chain-growth reaction (or chain-step reaction) is a process where the MW increases as the monomer molecules react and stops as the growing chain come to an end. Obviously, some facts have to be taken into account:

1. polymers having the same repeating units but formed with different processes do not have the same properties in most cases;
2. the polymerization processes have a great influence on the physical and mechanical properties; however, as the molecular weight increases, the differences will be less significant.

1.4.1 Step-growth polymerization (or step polymerization)

Step-growth kinetics describe polymerization processes where the MW of the polymer increases in a stepwise manner as the time increase (**Fig. 4**):

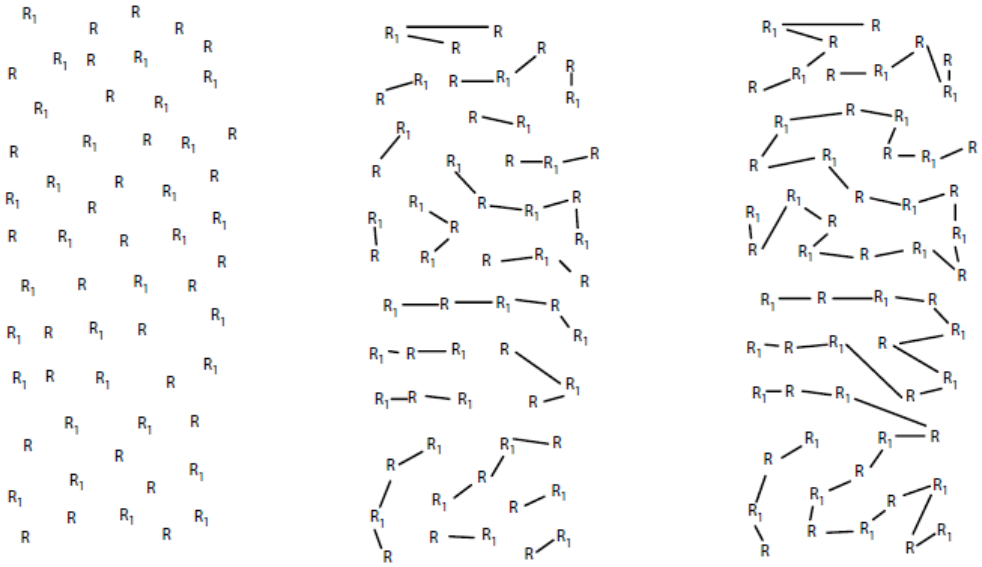

Fig. 4. Stepwise growth reaction (from left to right).

For example, if two functional groups A and B react together and form group X, two possible approaches are possible (**Scheme 1**):

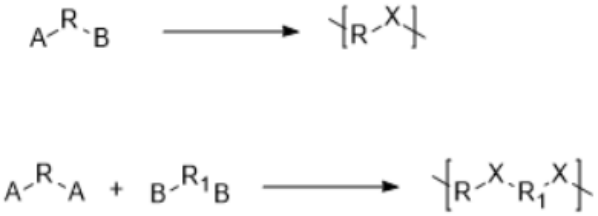

Scheme 1. Approaches for step growth reactions.

The typical example of the first approach is the formation of polyamide from ω-aminocarboxyl acid. The formation of polyurethanes and the polyesterification of diols and diacids are examples of the second approach. In the latter case (polyesterification), the polymerization occurs anywhere in the monomer matrix where two monomers have the right characteristics (proper orientation and energy). The ester is formed with the loss of a water molecule: the formed moiety can further react due to the presence of still-reactive carboxyl and hydroxyl functional groups. As a result, the MW increase is not too large while monomer molecules are rapidly consumed. This situation can be explained with an example: considering a system of 12 monomers containing two functional groups A and B (hydroxy acids for example). if A and B react as shown in **Fig. 5**, the DP (degree of polymerization:

number of initial molecules/number of remaining molecules) is 1.3. **Fig. 6** shows 75% of the consumption of the monomer molecules: in this situation, the DP is 1.7.

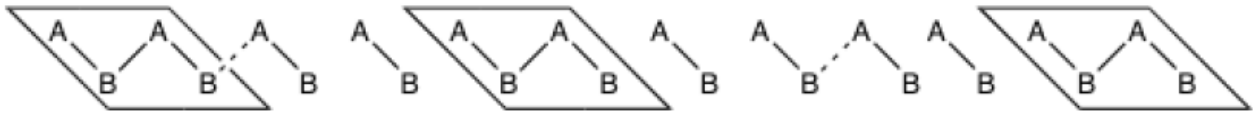

Fig. 5. Reaction mode of A and B.

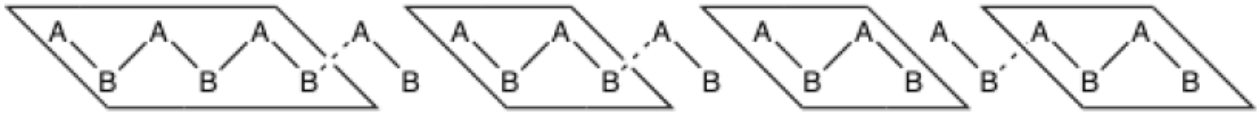

Fig. 6. 75% of the consumption of the monomer molecules.

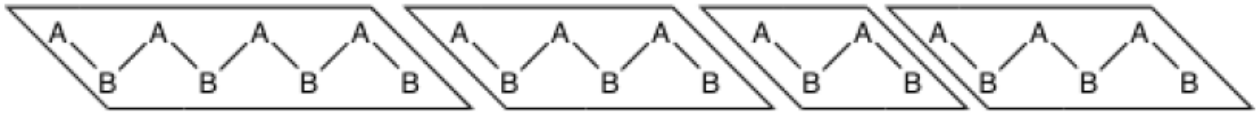

Fig. 7. Final situation of A-B reaction.

DP still remains low with all molecules reacted (**Fig. 7**). However, each oligomer in **Fig. 7** can further react because of the presence of reactive end groups; for this reason, the polymerization will have a stepwise behaviour. Each step of the process will be mechanistically the same and the rate will decrease as more functional groups are consumed. The main consequence is that the MW will increase slowly even in the case of high levels of monomer conversion. When the reactive end group concentration become too low, the molecular weight will stop its increase and this fact is also influenced by the viscosity of reaction medium. The conversion of monomer is related to the degree of polymerization by **Equation 1**, where p is the reaction conversion:

$$Degree\ of\ polymerization = \frac{1}{1 - \mathrm{p}}$$

Equation 1. Relation between conversion of monomers and DP.

This formula was firstly developed by Carothers and it describes an essential aspect of step-growth polymerizations.

1.4.2 Chain-growth polymerization (or chain polymerization)

Chain polymerization, specifically addition ones, are generally rapid and, in contrast with stepwise ones, the concentration of monomer decreases in a continuous way during the reaction and the first formed species have a high MW. Usually, a process like this has three steps (at least) that are respectively called initiation, propagation and termination. From the nature of the initiator, the reactions can be classified as cationic, anionic, free radical or coordination catalysed polymerizations:

1. Cationic polymerization: it is one of the most ancient. The first species produced in this type of reaction are carbocations. A combination of a pure Lewis acid and a trace of a Lewis base is necessary to have a proton, which is the true initiator. These polymerizations can take place at a very low temperature because of their low activation energy. The stability of the carbocations is a fundamental aspect to consider in initiation and propagation steps. Vinyl monomers with EDG are more suitable for this polymerization. Butyl rubber is one of the most important polymers produced with this type of reaction: it is used for inner tubes and sealants and it is the product of the copolymerization of isobutylene with 10% of isoprene (**Scheme 2**):

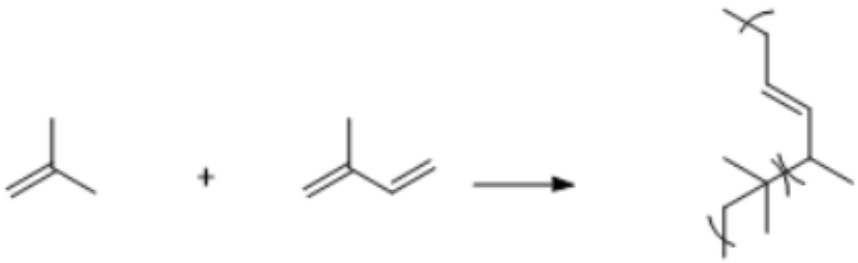

Scheme 2. Butyl rubber polymerization.

2. Anionic polymerization: the first examples of this type of polymerization were described in the beginning of last century for the synthesis of elastomers from butadiene. Similarly to cationic processes, the same three steps are in anionic ones (initiation, propagation and termination). Vinyl monomers with electron withdrawing groups (EWGs) are usually polymerized using this approach. A typical example of this

type of polymerization is the production of synthetic *cis*-1,4-polyisoprene in the presence of hexane and n-butyllithium;

3. Polymerization with complex coordination catalysts: the typical example is the synthesis of stereoregular and crystalline polypropylene (PP) made by Natta using a complex coordination complex, successively called Ziegler-Natta catalyst. Generally, these types of catalyst are a combination of a transition metal compound from Periodic Table groups 4B to 7B and an organometallic compound of a 1A to 3A metal;
4. Radical chain polymerization: many synthetic elastomers like SBR (Styrene Butadiene Rubber) and plastics like LDPE (Low Density PolyEthylene) are prepared using this method. As seen in the other reactions, even in this class of processes there are three common steps: initiation, propagation and termination. The initiators are radical species produced in different ways (heat, UV and visible light (**Scheme 3**), redox agents, electricity etc) by homolytic cleavage of covalent bonds.

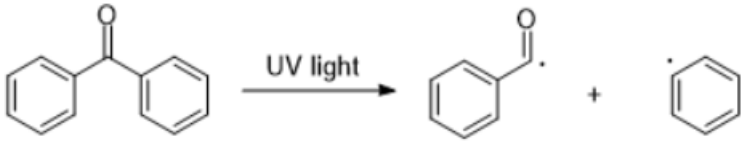

Scheme 3. Generation of radicals from diphenylketone.

Initiation starts with the addition of a free radical to a vinyl monomer. In the case of branched monomers, like styrene, the addition can happen hypothetically in two sites; however, in this case, due to steric and resonance factors, the addition takes place at the carbon not directly attached to phenyl group. Propagation is a bimolecular reaction where a new radical species (derived from the initiation step) attacks a monomer structure. The formation of the polymer chain is due to the repetition of this step. Unlike the other types of reactions, termination usually occurs when two radicals couple: the final configuration is head-to-head at the juncture of the two radicals. In some cases, disproportionation is the preferred way of termination. It involves chain transfer to a hydrogen atom from one chain end to the free radical chain of another growing chain, having as a result an unsaturated chain end in one of the dead polymer

chains. Several factors influence the termination step: among all, reaction and monomer conditions.

2. Polymer morphology and chemical structure

The properties of a specific polymer are deeply connected to its size and shape. The latter is also strongly influenced by the size of the structural units and the intermolecular forces between the chains. There are many ways to describe the structure or the morphological nature of polymers. Firstly, the description of the polymer structure can be made in terms of levels:

1. the primary structure is the precise sequence of the components of the chain;
2. the secondary structure describes the conformation of polymer chain;
3. the tertiary structure represents the shaping or folding of the considered polymer;
4. the quaternary structure is the shape of the tertiary structures that can be different or similar.

Secondly, the morphological nature can be described by two morphologies which are called amorphous and crystalline. The latter definition is not "really" corrected: because polymers with commercial and production purposes never reach 100% crystallinity, the term "semicrystalline" describes better the reality. In the next sections, a deeper look inside the structural and chemical features in polymer chemistry will be made.

2.1 Intermolecular forces

The chemical structure and the molecular weight are at the base of the final properties of any polymer.[13,14] Before talking about intermolecular forces, a consideration on molecular weight has to be made. Useful mechanical properties are reached when polymers have a certain MW. In this view, there is a direct relation between MW and chemical structure: the desired mechanical properties are obtained if there is a proper chemical structure that ensures the desired molecular weight. In the mechanical properties' definition, a huge role is played by intermolecular forces. There are several types of these forces:

- Van der Waals forces: they are responsible for the van der Waals corrections to the ideal gas relationship. Usually, they are in the range from 0.25 to 0.5 mm and they are inversely proportional to 2 or greater power of the distance. Examples of these interactions are the high-boiling points of polar molecules such as water or amines;

- Dipole-dipole interactions: they are in the energy order of 8-25 kJ/mol and they come from electrostatic attraction between two atoms. Another characteristic is their temperature dependence;
- London or dispersion forces: this type of forces come from the presence of induced dipole-induced dipole interactions. 8 kJ/mol is the energy value for London forces and it remains almost constant. Differently from dipole-dipole interactions, they are temperature-independent and they are more frequently present in nonpolar polymers;
- Hydrogen bonding: it is a special type of dipole force: it is common when a hydrogen, next to a highly electronegative element, is closer to another highly electronegative element (oxygen or nitrogen for example). For molecules such as hydrogen fluoride (HF), hydrogen bonding is very strong and it can reach energy values of about 40 kJ/mol. PU polymers typically show a strong hydrogen bonding character that results in the formation of strong fibres.

A huge drawback of these interactions is the fact that intermolecular forces drop off easily increasing the separation distance. Polymer molecules must be able to pack together in a very short distance to maximize cohesive strength. In the case of rubber bands, it can be shown considering the stretching situation. Before the stretch, the rubber band has low modulus and poor resistance to applied force because of the random distribution of its molecules. On stretching situation, the orientation of molecules is directed along a common axis and, as a result, they are efficiently packed together. When rubber band reaches 600% elongation, the modulus is at least 200 times higher than the unstretched one.

2.2 Glass transition temperature (T_g)

Polymer compounds show other transitions than melting. The most important is the glass transition (T_g). A general polymer usually undergoes different thermal transitions. In a low temperature situation, polymers are brittle and they have a glassy behaviour because chain movement is prevented due to the insufficient energy. If the temperature is raised, the chain mobility is higher. The glass transition temperature is the temperature which "starts" the movement of the chain for a polymer containing amorphous and crystalline segments or that is only amorphous.[15] If heating is continued, the polymer will melt to a flowable liquid and it will probably lose its elastomeric properties. T_g is one of the fundamental polymer properties

for its behaviour and processing. Considering the molecular level at glass transition temperature, it is estimated that 20-50 chain atoms are involved in the long-range molecular motion. In order to have this situation, the so-called “free volume”, defined as the space between atoms, must increase: the major consequence is the increase of specific volume. A measure of T_g can be estimated by knowing the temperature where this change takes place. Other significative differences can be noted at microscopic level during glass transition. Among them, enthalpy change can be measured by calorimetry, while mechanical measurements can be used for determination of the decrease of modulus (or stiffness). As already said, chemical structure is important in determining T_g: however, aging factors, such as UV light and oxidation, and MW usually influence the change of T_g. Higher the molecular weight is, lower is the free volume because of the presence of fewer chain ends. Example of this situation is the T_g of polystyrene. At MW of 3000, its value is about 40 °C. When the molecular weight is 300000, it increases at 100 °C.[16] Taking into consideration all these factors, T_g has to be considered an approximation and literature data should be taken with caution.[17] Considering a general polymer, structural effects that influence T_g could be generalized. Taking into account that any compound with a C-C single bonds can exist in an infinite number of conformations (if rotation freedom is paired) and the fact that T_g is a function of rotational freedom, in the case of substituted polymers, it can be shown that the bulkier are the substituents on polymer backbone, the less is rotational freedom and, as a result, T_g is higher. Besides rotation, a discrete effect is also made by substituents volume and group polarity. The classic example of the effect of volume substituents is the difference in T_g of polypropylene (methyl substituents) and polystyrene (styrene substituents) while for the effect of group polarity interesting examples can be PVC (polyvinylchloride) and PVA (polyvinylalcohol). For practical use, polymer T_g should be sufficiently higher than the temperature of intended work environment. In the case of elastomers, the glass transition temperature is below room temperature.

2.3 The amorphous state

An amorphous polymer contains structural chains that are not arranged in a crystalline and well-ordered way.[18] It is a characteristic polymeric behaviour at a temperature above their meting point. Vitrification is the phaenomenon where, upon cooling, a molten polymer retains

its amorphous state. Amorphous polymers are glass-like. Tobolsky described amorphous state as resembling, on a molecular scale, a bowl of cooker spaghetti.[19] Obviously there are some differences between solid and liquid amorphous state: the former describes a situation where molecular motions are restricted to very short rotations and/or vibrations, while in the latter molecular conformational freedom arises from the possibility of rotation about chemical bonds.[20] When a certain level of rotational freedom is achieved, the amorphous polymer can be deformed. Rheology describes this type of situations: it is the branch of science that study glow and deformation. Even if it is more interesting for an engineer point of view, the polymer chemist must have a comprehensive base of knowledge of rheologic aspects of amorphous state. The application of a force is required to cause the deformation of a polymer. If the applied force is withdrawn quickly, the polymer chains tend to return to the initial undisturbed state. This process is called relaxation. This behaviour shows a certain level of elasticity of the amorphous liquid. However, because of chain entanglement and frictions, viscosity of the polymer could be high. Polymers can be seen as viscoelastic compounds according to their dual nature, elastic and viscous one.[21] Shear is the applied force rheologists are most concerned with: it is the force applied to one side of a surface in a parallel direction to the surface. In molten state, the flow of molecules past each other is a direct cause of shear. The rapidity and the readiness of molecules flow is a function of:

- molecular weight because of the entanglement of the chains;
- molecular structure because of the intermolecular forces strength;
- temperature (how much kinetic energy they have).

The more readily the flow is, the more rapid the final product is fabricated and more economic it is. However, in molten or solution state, viscosity is the measure of flow resistance. Two important principles are used in order to determine it:

1. dissolving the polymer in an appropriate solvent and directly measuring the solution viscosity about a Brookfield type viscometer;
2. using the instrument directly to the material.

Different types of viscometers with different machinery are present in the market; among them, the cone-plate one is the most used. When the molten polymer is contained between the two parts of the sample chamber (the bottom and the cone plate, the latter rotating at a constant velocity), the shear stress can be measured.

2.4 Crystallinity

Crystallinity in a polymer compound may be found in at least two situations: in the first one, crystalline form can be present if polymeric structure is highly stereoregular with no or little presence of chain branching, while in the second one, they can be present if there are strong dipole-dipole interactions, formed by highly polar groups.[22-24] Low MW polymers usually don't show such crystallinity, while in high MW compounds there are polymer matrix regions where chains set themselves in a thermodynamically stable order. A different number of ways can induce crystallinity:

1. heating (molten polymer);
2. cooling;
3. annealing (heating process under vacuum or inert atmosphere preventing oxidation);
4. evaporation of polymer solutions;
5. drawing (stretching a polymer sample at a temperature above its T_g).

It is important to underline that each of these including-crystallization methods allows polymer chains to orient themselves into a crystalline morphology but losing their rotational and vibrational freedom. Nucleation is the onset of crystallization and it can probably occur along the matrix as soon as polymer molecules start to align or at a surface of a foreign impurity (for example: nucleating agents). The first way is called homogeneous nucleation, while the second one is called heterogeneous nucleation. Obviously, crystalline polymers have different properties than amorphous ones. They are stiffer, tougher, more solvent resistant and opaque and, if crystallinity degree is higher, these properties are higher. They are strictly related to the more effective intramolecular forces among the closely packed molecules. Crystalline and semicrystalline polymers have melting points in a narrow range which can be conveniently determined by thermal and DSC analyses. The obtained values are defined as crystalline melting point, T_m. As already said for T_g, T_m is not an exact value, but it can differ because of methods or rate of heating.

2.5 Physical and chemical crosslinking

The most important mechanism for forming and retaining different shapes is crosslinking. This process decreases molecular freedom by linking ad "jointing" polymer chains through covalent or ionic bonds (chemical crosslinking) or through chain entanglements or formation

of crystalline portions within an amorphous region of polymer matrix (physical crosslinking). Regarding chemical crosslinking, sometimes it can be called curing and, generally, it is generally divided in two categories:

1. crosslinking during polymerization by the use of polyfunctional monomers;
2. crosslinking in a separate process after the branched or linear polymer is formed.

The final result could have the same structural chain features in the case of former situation or completely different ones in the case of the latter one. The major consequence of chemical crosslinking process is insolubility: if previously soluble, after crosslink reaction, polymer will swell in the presence of solvent. In this context, solvent molecule penetrates the crosslinked network and a gel is formed. The swelling level mostly depends on two factors: crosslinking degree and polymer-solvent affinity. If the particles of the resulting gel are small in the order of 300-1000 μm, they form a microgel, behaving as solvent-suspended tightly packed spheres.

A useful quantity to use with network polymers is crosslink density. It is defined as the number of crosslinked monomer units per chains according to **Equation 2**:

$$\Gamma = \frac{(\bar{M}_n)_0}{(\bar{M}_n)_c}$$

Equation 2. Crosslinking density.

In **Equation 2**, $(\bar{M}_n)_0$ is the average MW of uncrosslinked polymer and $(\bar{M}_n)_c$ is the average MW between crosslinks. Higher is Γ, more rigid is the considered polymer. Embrittlement is the result of high values of crosslink density. Elastomers commonly used in rubber industry have low crosslinked density values (one crosslinked per one hundred monomer units) together with highly flexible structural chains allowing huge deformations. The behaviour of these compounds is the result of different factors: among all MW, morphology, polymer structure and Γ value are important while entanglements, chain ends and loops have no or little importance in the ideal elastic behaviour.[25]

The main disadvantage of chemical crosslinking reactions is the fact that, once crosslinked, the polymer cannot be dissolved or moulded. The main consequence is the impossibility of recycling of these products. Physical crosslinking is the main solution to overcome this problem and chain entanglement is one of the means to create crosslinks. The idea behind this

approach is introducing strong intermolecular attraction forces between polymer structural chains: in this optic, the final result is a thermoplastic material with the properties of a thermosetting one. An example is gelatine, an animal-derived protein with elastic-like characteristics. One of the milestones in physical crosslinking history is the introduction of block copolymers technology from the second half of the last century.[26,27] The aim of this process is to synthesize ABA-type block copolymers, where A and B block differ in their structures. The typical example is considering polybutadiene and polystyrene. Due to their incompatibility, polystyrene block, which is a "long chain flexible" polymer, aggregates and forms separate phases called microdomains within the matrix. Homopolymers, having an amorphous atactic meddle block and a semicrystalline isotactic and syndiotactic one, show the same behaviour. Microdomains impart the characteristic elastic properties so that they are responsible of the flow properties of thermoplastics. These types of compounds are called thermoplastic elastomers (TPE).[28,29] The most important TPEs are Ethylene-Propylene Diene Monomer (EPDM), Thermoplastic Polyurethanes (TPU) and poly(ethylene terephtalate) (PET).

2.6 Polymer blends

The definition "polymer blends" is not new in material chemistry: it is a concept taken from rubber industry. A polyblend (or polymer blend) is a physical mixture of two or more different polymers or copolymers without the presence of any covalent bond.[30-32] This approach has been renewed in the last thirty years due to demand for engineering plastics and special elastomers. Polymer blends are a useful way of balancing research costs and specific needs because, instead of developing a new product, the desired proprieties are obtained by a simply mixing procedure. Numerous technologies have been developed to prepare blends:

- Mechanical blends: this approach involves the mixing of two or more polymers at temperatures above their T_g (amorphous compounds) or T_m (semicrystalline compounds);
- Solution-cast blends: it involves two steps: the first one is the dissolution of the polymer in a common solvent, while the second is the remove of the solvent;

- Mechanochemical blends: block and graft components are produced in this way. Mixing at high shear rates of the polymers causes the start of degradation process. Free radicals are formed; they combine together and form complex mixtures;
- IPN (Interpenetrating Polymer Network): a crosslinked polymer is swollen with different monomers. Successively, monomers are polymerized and crosslinked;
- Semi-IPN (or pseudo IPN): the first step is the mixing of a polyfunctional monomer with thermoplastic polymer. Monomers, in the second step, are polymerized to network polymers;
- Latex blends: in this approach, latexes are mixed together and, successively, they are coagulated. Latexes are fine dispersions of polymer in water;
- IEN (Interpenetrating Elastomeric Networks): a latex polyblend is crosslinked after coagulation process;
- SIN (Simultaneous Interpenetrating Networks): in this approach, different monomers are mixed together. The successive simultaneous homopolymerization and crosslinking processes are made by a noninteracting mechanism.

In real applications, most of the times polymers are incompatible: usually, they separate into discrete phases on being mixed. However, an increasing number of completely miscible has been developed. Some differences are clearly visible in miscible and immiscible blends, having the former a single T_g intermediate between those of the individual components and the latter separate T_g characteristic of each component. Miscibility is fundamental for commercial purposes.

3. Rubber

Elastomeric compounds are generally known as rubbers. This term identifies a macromolecule polymer class whose main feature is its high elasticity. Due to their viscoelastic nature, elastomers are able of losing kinetic energy. If stress is applied on rubber compounds, deformation is the main result; however, the initial parameters (dimensions and forces) are recovered as soon as the external strain is removed.[33] A measure of the absorbed energy during the elastomer deformation is known as hysteresis. As previously said, rubbers have a low hysteresis value. The main characteristics of rubber compounds are not present in the raw material, but they derived from chemical crosslinking processes called vulcanization.

Goodyear, in 1839, discovered that the addition of sulphur to rubber compounds induces crosslinks reactions.[34] Elastomer structure after vulcanization reaction is amorphous, so macromolecules will have rotation freedom and flexibility (**Scheme 4**).

Scheme 4. Example of vulcanization.

3.1 History

Natural rubber is the first type of elastomeric compound used in history. Natural rubber had been known by the Indians in pre-Colombian era. The first kind of natural rubber was extracted by a typical Brazilian tree known as "Hevea Brasiliensis". The name of this extract was "*caoutchouc*" and it is also used in present days (**Figure 8**):

Fig. 8. Caoutchouc extraction.

The first articles produced with this extra were vessels and his use as waterproof clothing made natural rubber known across Europe. However, the huge transport cost and plantation costs were the main disadvantages for European market. Some of the problems were solved in 1783 when it was discovered that resin was able to dissolve NR: this discovery opened the

“first elastomeric market”. However, at that time, some of the most important properties of NR were unknown: the main problems were the stickiness (at room temperature) and the brittleness (at higher temperatures) of rubber objects. In 1839, a crucial and fundamental discovery were made by Goodyear: vulcanization. With addition of sulphur and heat, rubber molecules generate crosslink and, consequently, viscosity of rubber compound is increased. Vulcanization process solves the problem of stickiness and brittleness. Successively, tyres were invented and the demand for natural rubber was so high that there was no available compound for all of it. Two approaches were used in that time: the first one involved the finding of new area of plantations like Panama, Philippines and South Asia, while the other the creation of synthetic routes for the fabrication of rubber. The first step of the latter approach was the discovery of isoprene units made by Wiliams (**Figure 9**):

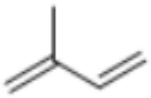

Fig. 9. Isoprene unit.

The first composition of natural rubber (C_5H_8) was defined by German scientists before the outcome of World War I. After the War, macromolecular theory proposed by Carothers made a huge impact on polymer science. The same chemist proposed a synthetic route for the chloro-derivative of isoprene called Chloroprene (or Neoprene) (**Scheme 5**):

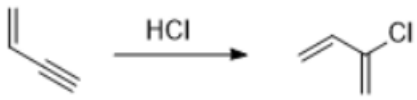

Scheme 5. Production of Chloroprene.

In 1933, the first synthetic copolymer was developed by Bock and Tschunkur by substituting the 25% of butadiene with styrene. This was the first example of SBR and it was called Buna-S. In 1934, Konrad and Tschunkur developed Buna-N by substituting styrene with acrylonitrile (**Figure 10**):

Fig. 10. Buna S and Buna N compounds.

The main characteristics for Buna-S are higher resistance and life than NR, while for Buna-N its high solvent- and oil-resistance. Numerous discoveries were made up today: among them, oil-extended rubber is one of the most important.

3.2 Rubber types

3.2.1 Natural rubber

The unit structure of NR is *cis*-1,4 polyisoprene and, as previously said, it comes in latex form by a variety of trees (**Table 1**):

Species	**Family**
Castilla elastica	Moracea
Hevea brasilensis	Euphorbiaceae
Parthenium argentatum	Compositae
Funtomia elastica	Apocymaceae

Table 1. Plant sources of natural rubber.

Hevea brasiliensis is the most important plant for NR: it is indigenous to Amazonian forests region and it prefers warm environment with a certain degree of humidity. The typical density of plants is 4,5-5k trees per km^2.[35]

Natural rubber is recovered from the tree in form of latex, which is composed by numerous intercellular ducts (latex vessels). The turgor pressure, which is the hydrostatic pressure inside the vessel, reaches approximately the value of 1,9 MPa.[36] Extraction of latex is made by tapping: this process involves making a cut of about 30° from horizontal to vertical direction in a region very close to the cambium, without injuring it. Tapping operation is made at regular intervals and usually in the morning, because it is the moment that turgor pressure reaches its maximum. The composition of extracted natural latex is shown in **Table 2**:

Constituents	Percentage (%)
Rubber	30-40
Resins	1,5-3
Minerals	0,7-0,9
Carbohydrates	0,8-1
Proteins	1-1,5
Water	55-60

Table 2. Composition of latex.

The collected latex is sieved and collected in a talk in the factory: the first operation is essential to remove contaminants. The storage conservation, on one side, must guarantee from bacterial activity and, on the other, to enhance stability. In order to reach these aims, preservers are added. Ammonia and combination of primary and secondary preservers (LATZ system) are the most employed. As successive operation, latex is concentrated in order to enrich the rubber component. Evaporation, creaming and centrifuging are the most used processes. Concentration of latex is required from various economic reasons (economy of transportation and the preference of high content of rubber of consuming history). The final operations are dependent on the desired performance of the final material. Numerous approaches are used. Field coagulum crepe, pale latex crepe, sole crepe, ribbed smoked sheet (RSS) and technically specified rubbers (TSR) are more frequently used. The latter one guarantees quality consistency, stability for important parameters, easy handling and minimum space for storage.[37]

Natural rubber can be chemically or physically modified. This need is due to development of synthetic rubbers, so it is a way of offering an alternative in the market. Some of the modified natural rubber-based compounds are not commercially available, while others have made a huge impact on the market. Constant Viscosity (CV) and epoxidized NR are the most important chemical modified NR-based compounds.

Constant viscosity natural rubber has been studied to overcome the crosslinking reaction of the randomly distributed carbonyl groups along rubber structural chains, which causes

hardening and, as a consequence, an increase of viscosity.[38] Hydroxylamine salts are added before coagulation and this treatment is used to main the same viscosity during time. The available Mooney viscosity range goes from 60 to 65 units.

The first epoxidized natural rubber was proposed by Baker's research group and Gelling.[39] Epoxidation in the latex stage gives NR improved oil- and hydrocarbon-resistance, good bounding properties and low permeability to air while, at the same time, it maintains its high mechanical properties. The random distribution of epoxide groups along rubber chains does not affect the *cis* 1,4 configuration of natural rubber. Two grades have gained commercial importance: ENR 25 (25 mole% epoxidation) and ENR 50 (50 mol% epoxidation).

3.2.2 Properties of raw NR

The average molecular weight of NR varies from 30000 to ten million. The bimodality of MWD (molecular weight distribution) of raw NR has been proved by Subramaniam.[40] The melt viscosity is influenced by the presence of a microgel (7-30%) due to crosslink reactions in the tree latex vessel. The macrogel part is formed during storage and, as previously said, it is due to carbonyl groups (or other chemically active groups) on rubber chains. In mixing stage, mastication is necessary in order to reduce gel content. Long branching chains influence rheological properties of natural rubber, like stress relaxation.[41]

Stiffening is caused by storage at low temperatures: the maximum rate of crystallization happens at -24°C. The T_m and T_g of NR is, respectively, 30°C and -72°C. Processing properties are quite optimal: after 100°C, natural rubber has a workable viscosity. Efficacy of mastication is lower at 100°C and it is temperature dependent.[42]

3.2.3 Properties of vulcanised NR

Several factors influence physical properties of vulcanized natural rubber: among them, presence of plasticizers, filler's type and amount, crosslinking degree and filler dispersion are of primary importance.

Tensile strength of NR vulcanizates are in the order of 30 MPa: this value is ten times higher the SBR one under similar test conditions. Natural rubber TS is temperature dependent: at 100 °C, its value decreases exponentially due to crystallinity suppression. This effect is less pronounced for filler reinforced NR compounds. Tear resistance is another measure of NR

strength: over long structural chains, for compounds like NR, rate and temperature do not affect tearing energy.[43] However, reinforcing filler strongly increases this value. Abrasion in natural rubbers is not as good as some synthetic elastomers like SBR. However, in some surfaces, it can be comparable. Regarding dynamic properties, NR is excellent at high strains compared to non-crystallising elastomeric materials. Frequency of deformation has no or little effect on NR fatigue life. Particle sizes of fillers influence resistance to cut growth because of the presence of branching. Natural rubber has resilience values similar, but higher to those of *cis* 1,4-butadiene, because of the presence of proteins in NR. A good elastic behaviour, which is defined in terms of low value of creep and stress relaxation, is characteristic of natural rubber: it is a direct consequence of high mobility of rubber chains. Creep and stress relaxation can be measured by compression set analysis: the presence of non-rubber constituents made these parameters lower in NR compared to other elastomers like synthetic polyisoprene. Degradation of NR is mainly caused by oxidants (oxygen and ozone), chemicals and heat. The main features associated with degradation reactions are crosslinking, introduction of new functional groups and, mostly, chain scission. Considering oxidant agents, even 1 or 2% of oxygen is able to deeply influence the properties of natural rubber vulcanizates and the oxidation is supposed to have a free radical chain mechanism.[44] Amine and phenolic antioxidants can be added to prevent this phenomenon.

3.3 Synthetic elastomers

The development of synthetic elastomers is a consequence of performance deficiencies of natural rubber:

- low organic solvents resistance;
- poor oxygen resistance;
- low heat resistance.

In most applications up to now, synthetic elastomer compounds have substituted natural rubber because their properties can be adapted and modified according to final use. In this view, four important aspects have to be taken into account:

1. the use of a combination of monomers;
2. the composition of the elastomer;
3. the distribution of different monomers into portions of a chain;

4. microstructure and orientation of the monomers.

For example, resistance to organic solvents can be reached by using strong polar elastomers (nitrile rubber) and oxygen resistance can be tailored by elastomeric compounds with a saturated backbone. Differently from natural rubber, most synthetic polymers are formed by a combination of two or more monomers. SBR, for example, is synthesized starting from styrene and butadiene. This strategy is used for tailoring the properties of the final compound that cannot be made with natural rubber and, generally, with homopolymers.

3.3.1 Processes for the synthesis of polymers

Nowadays there are four main processes for the large production of synthetic polymers:

- Bulk polymerization: in this method, the monomer in liquid state is the reaction medium and the generated heat is dissipated in an evaporative or external colling step.
- Solution polymerization: in this approach, dissolution of the monomer is made in an organic solvent. As soon as the reaction starts, the viscosity of the reaction grows with the polymerization degree: as a consequence, chain growth is limited.
- Suspension polymerization: similarly to the bulk one, monomer in liquid form acts as a solvent. However, the formed polymer precipitates as a suspension state, because it is insoluble in the reaction medium. This method is usually used for the synthesis of high molecular weight polymers due to the slight increase of the reaction medium viscosity.
- Emulsion polymerization: it is usually used in free radical polymerization and it involves water, emulsifiers, water soluble initiators combined with chain modifiers and polymerization stoppers and, obviously, water insoluble monomers. Initially, the emulsifier agent caused the transformation of monomer into droplets, which aggregate into micelles where initiator radicals interact with monomer molecules. At the same time, micelles grow absorbing more monomer and, as a result, a latex is formed. High conversion yields are reached with this method because of the avoiding of terminations reactions. The role water is important because it is an optimal way to dissipate heat. As a final result, polymers with high MW are obtained, because there isn’t a direct correlation of viscosity and molecular weight. It is important to underline that emulsion polymerization can be done in simple reaction vessel.

3.3.2 Styrene Butadiene Rubber (SBR)

As already said, the first commercialised version of SBR was Buna-S in 1937. Nowadays it is the synthetic elastomer mostly produced in terms of volume. SBR usually contains 25% of styrene and 75% of butadiene which usually inserts in 1,2 position (**Fig. 11**):

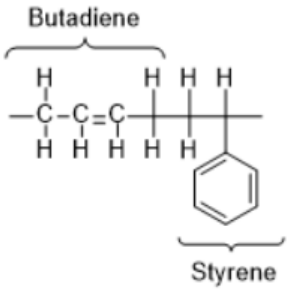

Fig. 11. SBR monomers.

Emulsion and solution SBR-types are available. The former has been proposed for the first time in 1920 from Bayer industries.[45] E-SBR has a high MW and the distribution of styrene and butadiene is governed by the statistics of polymerization process because, as previously said, it a free radical process. This is the main production method for SBR even if S-SBR is an alternative and competitive method. Solution SBR is obtained using Ziegler-Nata transition metal catalysts. Different choice of the anionic/cationic initiator led to the right control of 1,2-butadiene content and of *trans-cis* microstructure. When comparing physical performances, S-SBR values are similar to those of emulsion type; however, it has better flex resistance resilience and lower heat build-up.

3.3.3 Polybutadiene (BR)

Polybutadiene (BR) is second in importance in diene elastomers after SBR. The interesting fact of 1,3-BR is that it can be polymerized to produce a wide range of isomers, but only some of them have the proprieties of elastomers. The differences on the insertion position are the discriminants of the isomers. Commercially, two isomers are important, 1,4- and 1,2-butadiene rubbers (**Fig. 12**):

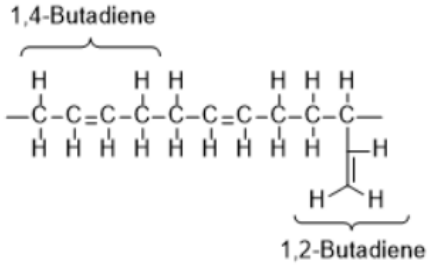

Fig. 12. Butadiene rubbers (1,4 and 1,2 isomers).

Each of these isomers have unique physical, mechanical and elastic behaviours. On the market, it is also available a mixture of the two isomers which also has different elastomeric characteristics. Regarding 1,2-BR, three isomers are possible: syndiotactic, isotactic and atactic. The syndiotactic one is made using cobalt Ziegler Natta and it is a crystalline thermoplastic with a T_m of 220°C. Amorphous 1,2-BR is synthesized using anionic polymerization with a chelating diamine: in this way, the 99% of butadiene is inserted in 1,2-position. Varying the lithium catalyst/chelating modifier ratio and the polymerization temperature, 1,4 insertion, vinyl content and T_g increase.

Considering 1,4-butadiene version, both *cis*- and *trans*-forms are synthesized employing transition metal catalysts. However, due to low T_m, *trans*-1,4-BR is not useful for elastomeric purposes. An attempt to overcome this problem has been the synthesis of an amorphous of 90:10 *cis*-:*trans*-1,4-BR with living anionic catalysts. This compound has shown low hysteresis and good wear proprieties in tyre industry.

In fact, butadiene rubbers are usually used in tyres as replacement of NR and, in sole industry, as a helping compound for lowering abrasion loss.

3.3.4 Polyisoprene (IR)

Polyisoprene is isoprene's homopolymer: natural rubber is 100% formed by *cis*-1,4 IR. Similarly to BR, a variety of isomers can be obtained varying polymerisation parameters. Three insertion position are possible: 1,2-, 1,4- and 3,4-position. Between them, the 1,2- and the 3,4-BR isomers are not commercially important compared to the 1,4- one. Considering the former, the orientation of the substituents on the double bond is the base of the *cis* or *trans* forms.

3.3.5 Butyl/halobutyl rubbers (IIR/CIIR/BIIR)

Butyl and its halogenated-derived compounds (bromo- and chloro-) are examples of saturated elastomers. The main characteristic of these compounds is the presence of a saturated backbone chain with some unsaturations, necessary for vulcanization process, which give more resistance to degradation and environmental ageing. Butyl rubber (IIR) is the result of copolymerization reaction between isoprene (2%) and isobutylene (98%). The main process for its production is slurry polymerization in methyl chloride with Lewis acids (typically aluminium chloride) at very low temperature (about -100°C). By dissolution of IIR in hydrocarbon solution and subsequent treatment with elemental halogen (Br_2 or Cl_2), BIIR or CIIR is obtained (**Scheme 6**):

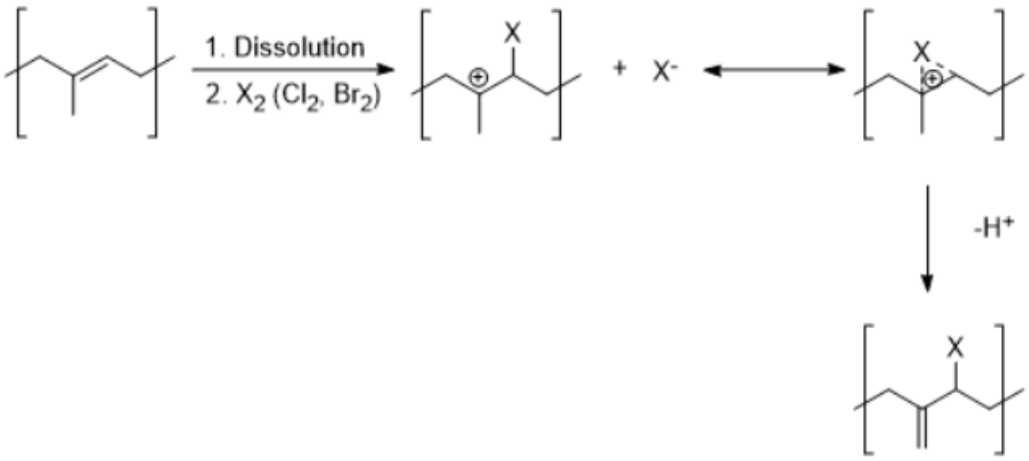

Scheme 6. Synthesis of BIIR or CIIR.

Low air permeability and high loss modulus are the main important features of these compounds. Additionally, the halogenated butyl rubbers have high vulcanization rates and improved co-cure compatibility with other types of unsaturated compounds. Solution properties are similar either in IIR and BIIR/CIIR.

3.3.6 Nitrile rubber (NBR)

Nitrile rubber is a copolymer of 1,3-butadiene and acrylonitrile. It is one of the most important solvent resistant elastomers. Other hydrocarbon-based elastomers vulcanizates (SBR, NR and IR for example), when immersed in organic solvents, swell; as a consequence, there is huge decrease in proprieties such as elongation, tensile strength or abrasion. In this optic, the

development of such elastomers is crucial to create products, which can cover a wide range of applications. The presence of functional groups with strong polarity, like esters or nitriles, has the effect on raising the solubility of the polymer so that it doesn't mix with the solvent. In NBR case, the acrylonitrile polarity is the feature that makes it resistant to common organic solvents (**Fig. 13**):

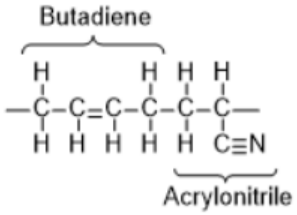

Fig. 13. NBR structure.

Depending on the polymerization parameters, the copolymer structure can show linearity or a high number of branched chains. Generally, a compound with range acrylonitrile units from 8 to 27 wt% is used. Higher presence of ACN led to a more solvent resistance value but the T_g is increased. Emulsion polymerization is the favoured process for industrial production. NBR is used in special applications: in footwear industry, it is used for safety or military soles. NBR can be modified for special applications: hydrogenation is the most important modification. With this process some unsaturations remain and the final result is a better resistance to oxidation and weathering without compromising of other useful properties. The hydrogenated compound is called hydrogenated nitrile rubber (HNBR). Similarly to NBR, several grades are present in the market. A useful consideration has to be made: differently from classic NBR, due to saturated backbone, the ageing and high temperature resistance of HNBR is better and it is the best choice to use in critical applications.

4. Rubber compounding

4.1 Brief introduction

The branch of materials chemistry and science which studies the proper formulation of a rubber or polymer blends for targeting required performances is called compounding. When a compound is formulated, the rubber chemist has to be aware of the aims and requirements of the final product. In order to do this, a proper knowledge of materials chemistry and physics is required. The compounding process has at least three objectives: the first one is the safety of all the actors involved in this operation (environment and workers primarily), while the second and the third ones are, respectively, the cost efficiency and the processability of the compound. The general formula ingredients for a rubber compound are shown in **Table 3**:

Category	Types
Polymer	Natural and synthetic rubber
Filler	Carbon black and silicas
Stabilizer agents	Waxes and antioxidants
Adjuvants	Pigments, oils, resins, processing aids
Vulcanization system	Activators, accelerants, Sulphur

Table 3. General formula ingredients for rubber compounds.

The different types of polymers have been discussed in the previous section; in this chapter, an overview of other components will be made.

4.2 Fillers

Fillers are also known as “reinforcement aids”, because they are added to rubber compounds to enhance several properties like abrasion resistance or tensile strength.

4.2.1 Carbon blacks

Particle size, surface area and activity, particle size distribution and structure are the main qualitative parameters for describing carbon blacks (CBs), while important values for a quantitative characterization are:

1. Iodine number: it describes the weight of iodine absorbed per kilo of CB and it measures the surface area. Higher is this value, smaller is the particle size.
2. CB-DBP value: it stands for Carbon Black DiButylPhtalate value and it describes the volume of DBP (cm^3) absorbed by 100 gr of CB. With this parameter, the size or structure of the filler can be determined. Higher the DBP is, higher the size is.
3. CTAB value: it measures the specific surface area related to micropores effect. Cetyl Trimethylene Ammonium Bromide (CTAB) gives an idea of the portion of a particle surface area in contact with the matrix, because it is excluded from the smaller interstices.
4. Tint: it is the ratio between reflectance of a reference paste and a sample paste constituted of plasticizers, CB and ZnO_2. Tint increases with smaller particles.

Two types are generally used: furnace and thermal carbon blacks. The former is produced by injection of defined grades of petroleum feedstock into combustion gases steams under pre-defined and controlled processing parameters; the latter is the result of thermal decomposition of hydrocarbon-based gases.[46] As carbon black level is increased, hardness and heat build-up of the compound are higher. Other parameters (processability, abrasion resistance and tensile properties) reach a maximum value then decrease considering the same situation. An important consideration has to be made on the surface chemistry of carbon blacks: it has been found that reactive groups (quinones, carboxyls and phenolic groups) react with polymer matrix and they form chemical crosslinks.[47]

4.2.2 Silica

The two fundamental properties of silicas that mostly influence rubber performances are its extent of hydratation and ultimate particle size. Silica particles are characterized by other parameters like pH or chemical composition but, in this context, are of secondary importance. Compared to CBs, the performances of silica are lower: however, this gap disappear when a coupling agent is combined with silica filler.

Silica is amorphous and it is composed of silicon and oxygen which are disposed in a tetrahedral structure forming a three-dimensional lattice. As a consequence, there is no long-range crystal order, but only short-range domains arranged randomly with neighbouring ones. The range of particle size is from 1 to 30 nm to whom a surface area range of 20-300 m^2g^{-1} is associated. The SiO_2 surface chemistry is characterized by silanol functional groups which can be geminal, vicinal or isolated (**Fig. 14**):

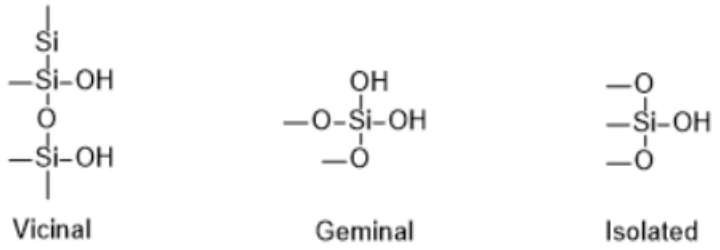

Fig. 14. Silanol groups.

The silanol moieties influence the different degree of surface hydratation. The -OH functionalities on silica surface control the acidity: it has no or little effect on sulphur vulcanization. Due to its high hygroscopicity, silicas must be stored at dry conditions: if hydrated, they can badly affect physical properties. Three class of silicas can be found in the market: standard, semi-highly dispersible (semi-HD) and highly dispersible (HDS) silicas. The difference between them is the concentration of silanol groups, considering that HDS has more geminal groups, while conventional has a greater quantity of isolated silanols.[48] Two advantages are given by using silicas in rubber compounding: improvement in physical performances and reduction in heat build-up if, at least, some CB is substituted. The reinforcement effect is higher in polar elastomers than in non-polar polymers; however, this problem can be overcome if silica filler is used in combination with silane coupling agents.

4.2.2.1 Silane coupling agents

The most important commercial silane is TESPT (bis(triethoxysilylpropyl)tetrasulfane): it is a bifunctional polysulfidic organosilane. The advantages of using silanes as coupling agents are:

1. improving the reinforcing effect of silicas in rubber;

2. lowering heat build-up and hysteresis;
3. improving physical properties of rubber compound;
4. lowering Young's modulus leading to higher hydrophobation reaction.[49,50]

The silica-silane coupling agent mechanism is divided in two steps: the first one involves the hydrophobation reaction between silica and the coupling agent while in the second one new crosslink is formed between polymer and the modified silica of the previous step. The silanization can occur rapidly and *in situ*: high temperatures are necessary because of the presence of bulk substituents in silane coupling agents.

4.3 Stabilizer agents

4.3.1 Rubber degradation

Light, moisture and oxygen are some of the factors involving the degradation of rubber compounds. Usually, oxidation reactions involve the presence of two mechanisms:

1. Chain scission: it causes the breaking of polymer structure and, as a consequence, the compound softens and its abrasion value is higher. The typical example of this type of degradation process is the natural rubber one.
2. Crosslinking reaction: this type of degradation is particularly shown by SBR and NBR. The network formed in the vulcanization step (di- or poly-sulfidic bonds) is broken into monosulfidic one. It can be seen an increase of hardness and stiffness and, at the same time, a decrease of fatigue resistance.

4.3.2 Types of stabilizer agents

The most common stabilizer agents are:

- Staining antioxidants: polymerized dihydroquinolines are one the most used. They find extensive use because they influence long-term durability and migratory properties.
- Non staining antioxidants: four classes are found in this antioxidant type: hydroquinones, phosphites, hindered bisphenol and phenols.
- Waxes: they improve rubber ozone protection under static conditions. In rubber compounding, two types of waxes are used: microcrystalline and paraffin. The former has a T_m in the range from 55 to 100°C and derives from petroleum heavy lube stock; the latter is obtained from the light lube distillate of crude oil and it has a lower T_m

(36-75°C). Waxes act against ozone attack forming a barrier on the surface, which is in equilibrium concentration due to the continuous migration of the wax. Microcrystalline type has a slower migration rate due to higher branching and MW. Paraffin wax serves better at low temperatures.

4.4 Special ingredients

4.4.1 Processing oils

The main purpose of processing oils is as processing aid. They are divided into three categories: aromatic, paraffinic and napthalenic oils. Aromatic type has, as the name suggests, high concentration of unsaturated rings and hydrocarbon chains. Paraffin oils have high levels of napthalenic rings and pendant groups; however, the most important characteristic is the presence of fewer napthalenic groups per molecule. Napthalenic oils are in the middle situation: they contain high levels of unsaturated rings, but a little presence of unsaturation. The choice of the oil is a very important process because, if not chosen well, it tends to discolour, stain and to migrate to surface.[51] The parameters to be taken into consideration are viscosity, MW and molecular composition. A useful value is also aniline point: it represents the point when an oil becomes miscible with aniline.[52] It can be seen as a measure of oil aromaticity. Lower is the aniline point, higher is the aromatic concentration.

4.4.2 Peptizers

The main use of chemical peptizers is their application as oxidation catalysts. In this situation their function is the removing of free radicals which are formed in the initial mixing steps and preventing polymer recombination which can led to a huge decrease of molecular weight and, as a consequence, of viscosity. The use of peptizers also results in incorporation of compound ingredients into the matrix. They are generally used between 0,1 and 0,25 phr, where phr means “part for hundreds of rubber”. In other words, it describes the quantity of a certain material to be added to one hundred of rubber. Its main purpose is to generalize formulas so that, in this way, they can be adapted in all situations.

4.4.3 Resins

Resin compounds are divided into phenolic-, hydrocarbon- and petroleum-based ones. Phenolic resins are divided into reactive and nonreactive. The latter usually are alkyl-phenyl formaldehyde oligomers where the number of carbons in the para-alkyl substituent ranges from 4 to 9. Its main use is as tackifier. Reactive type resins contain free methanol moieties and their main purpose is to create crosslink networks. Reinforcing and promoting adhesion are the main functions of reactive phenolic resins. Hydrocarbon-based resins have high T_g: the first consequence is the fact that, in processing conditions, they melt and, in this way, improve the compound mould viscosity. However, they harden at room temperature and so they enable the maintaining of the hardness and the modulus of the rubber compound. The chemistry at the base of hydrocarbon resins led to different applications: for example, aliphatic resins are used as tackifiers while aromatic one as reinforcing agents. The last type of resins, petroleum resins, are derived from oil refining. Like all other class of resins, several grades are commercially available.

4.5 Vulcanization

The vulcanization process is necessary to produce articles that we use on everyday life, like shoe soles or car tyres. As previously said, un-vulcanized rubber does not possess great properties and it can be very sticky.

Sulphur vulcanization has been the first useful method for producing rubber articles and, nowadays, it comprises for a major part of all vulcanization processes. In this section, a general overview about vulcanization will be made.

4.5.1 Definition and effects on rubber compounds of vulcanization

Vulcanization is generally a proper term for elastomeric compounds. It is a process where new chemically network junctures are produced by the insertion of crosslinks in the structure created by polymer chains (**Fig. 15**). The crosslinks can be composed by different elements or groups.

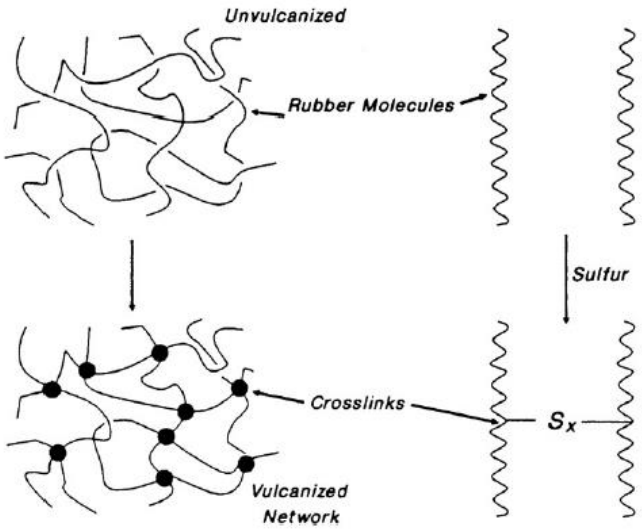

Fig. 15. Vulcanisation process.

Heating is necessary to start vulcanisation process but, in order to give a shape to the final product, the rubber compound has to be put into a mould under pressure. Different and important changes are caused by vulcanization processes. Rubber molecules become linked together in a crosslink network with a characteristic MW in the range of 4000-10000 Da for the average distance between junctures. The formation of a new network is the reason why vulcanised rubber is insoluble in any solvent and why hysteresis is reduced. Other physical-mechanical properties (fatigue life, toughness and tear strength) increase when the number of crosslinks is small. The overcure of a rubber compound led to a significant decrease in elastomeric properties and reversion. Reversion is a phenomenon that refers to the loss of network structure by thermal ageing in nonoxidative conditions.[53]

4.5.2 Accelerators in sulphur vulcanization

The first use of accelerators has been documented in 1906.[54] Since that, numerous compounds have been introduced in the market for accelerating vulcanization.[55,56] Nowadays, for a major part of applications, it is the only effective and rapid crosslinking technique but, in order to perform it, it is necessary to have the moiety shown in **Fig. 16**:

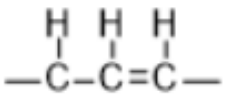

Fig. 16 Necessary moiety for accelerated sulphur vulcanization.

In the compounding formula, also zinc oxide and fatty acid are usually employed: they are known as vulcanization-system activators. The combination between those two ingredients forms a salt that complexes with accelerators and reaction product species, which are formed by the combination of sulphur and accelerators. In major cases, mix of accelerating agents is used to achieve the desired cure of compound. The reaction steps of this type of vulcanization are:

1. accelerator species react with sulphur: the result is the formation of monomeric polysulfides with the Ac-Sx-Ac structure, where Ac is an organic radical derived from the initial species;
2. the monomeric species interact with rubber matrix giving polymeric polysufides (rubber-Sx-Ac);
3. finally, the rubber polysulfides react and crosslinks are formed (rubber-Sx-rubber).

Natural rubber was the first compound to be studied in vulcanization models that has also been applied to other elastomers.[57,58]

4.5.3 Accelerator types

In vulcanization process, sulphur and insoluble sulphur can be used: rhombic one is the most common and it does not need any special procedure for handling and storage. Sulphur can be added up to 2 phr (*parts per hundred rubber*): if more is added, insoluble sulphur is necessary because it prevents the migration of sulphur to surface. Besides, appropriate and careful choice of accelerators must be made. An important factor is the synergism between the combination of accelerator species that enhances the effect of the individual components.
Two classifications are possible:

- according to chemical classifications there are eight groups and accelerators: guanidines, thioureas, sulfenamides, aldehydeamines, dithiocarbamates, xanthates, thiurams and thiazoles;
- according to rate of vulcanization, accelerators are divided into fast, semiultra- and ultra-accelerators.

The type of elastomer/elastomer blends, zinc oxide and fatty acid quantity and final physical properties must be considered in the choice of these ingredients.

4.5.4 Compound preparation

The compounding of elastomers in industries for tyres or shoes production is made into internal mixers and open mill. Internal mixers machines are made by a chamber where the ingredients are added. There are two rotors that, while rotating, create high shear forces: those permit the inclusion and dispersion of fillers and other raw materials inside the polymer matrix and ensure the uniformity of the compound. In the market, different volumes of the chamber are available: the choice is based on the production scale of the plant and on the different versions (black/coloured) of a compound to be realized. After a pre-defined mixing time in the chamber, the compound is convoyed into an open mill where the mixing is completed. These operations can be developed in a range of few minutes. In soles industries, in open mill step, compound is cut into rolls that can be transformed into different final forms:

- Rubber preforms: rubber rolls are inserted into a cutter machine; the compound is pushed into a die cut at a certain velocity and preforms with a determined weight are collected.
- Rubber sheets: rubber from open mill is collected in smaller rolls that are collected into a calender machine. The thickness is controlled before and after the cutting in order to maintain it constant. The sheets are collected at the end of the line and cut into pieces that are charged into the mould.
- Rubber straps for injection moulding: the straps are usually obtained by calendaring process or, sometimes, by a cutter machine. The operations are similar to those of the previous cases except for the fact that rubber straps are collected into large recipients for injection moulding machines.

5. Polyurethane

The first synthesis of polyurethane was made by Bayer in 1937 when he was working in IG Farbenindustrie in Germany.[59,60] The first successful reaction involves the formation of a polyester starting from an ester-based diol with a difunctional isocyanate. However, this wasn't a case of serendipity but the result of several attempts and efforts. In those years, major part of PU literature was based on Bayer's work; however, in the last 75 years, a huge part of development has been made by R&D laboratories of consumer industries, which have

performed and improved processes and formulations that can be suitable for large-scale productions. His importance has been growing since his discovery: nowadays, polyurethanes derivatives have become one of the most versatile class of polymers. In everyday life, we can see objects made from PU: from furniture to car seats, from bedding to shoe soles, it has introduced a new concept of functional chemistry.

5.1 Starting materials and polymerization reactions

The basic structural unit of polyurethanes is reported in **Fig. 17**:

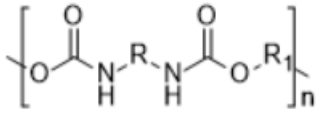

Fig. 17. General structure unit of PU.

As shown in **Fig. 17**, urethane groups are carbamic acid esters derivatives. The most used and important method for the synthesis of urethane moieties is shown in **Scheme 7**:

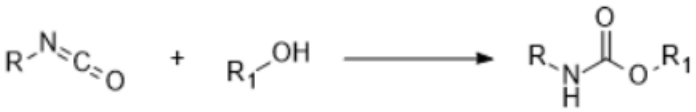

Scheme 7. General PU reaction.

As shown in **Scheme 7**, two classes of compounds are employed as starting materials: isocyanates and compounds having active hydrogens (polyols). The different characteristics and properties influence the final physical performances and polymerization reaction of PU. The combination of isocyanate and polyol is called “system” or “polyurethane system”. Other agents are added in PU formulation in order to control, modify and shape the final compound. Examples of those materials are catalysts, blowing agents, surfactants and cross linkers. The high reactivity of isocyanates towards polyols can be explained considering their resonance structures (**Scheme 8**):

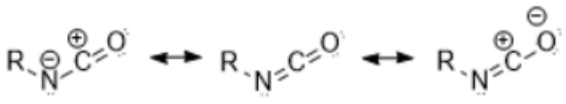

Scheme 8. Resonance structures of isocyanate.

Electron density is shifted towards oxygen atom while carbon has the lowest one. Therefore, carbon atom has a positive charge, the nitrogen an intermediate negative one and, finally, the oxygen a negative one. In fact, the addiction reaction steps are two: the carbon-oxygen double bond attack and the rearrangement to urethane (**Scheme 9**):

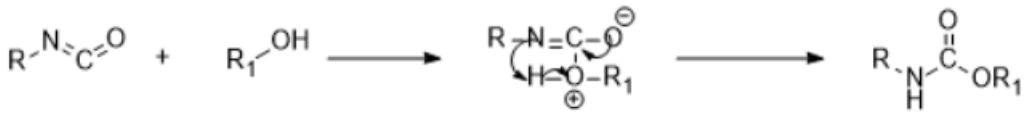

Scheme 9. Reaction steps of PU synthesis.

The oxygen atom (nucleophilic) attacks the carbon (electrophilic) and the nitrogen of the isocyanate group accepts a hydrogen atom. The presence of an electron withdrawing group decreases the reactivity of the NCO moiety; the opposite effect is shown with electron donating substituents. Steric considerations have to be made: if the R groups are too big, reactivity is reduced. Considering the nature of the substituents, aromatic isocyanates are more reactive than aliphatic ones. Elastic PU is synthesized from polyols with a functionality of 2-3 and with a molecular weight in the range from 2 to 12 kDa. In opposite way, rigid PU is obtained from low-MW (0,3-1 kDa) and a higher functionality (3-8). **Fig. 18** shows "hard" and "soft" domains in polyurethane compounds:

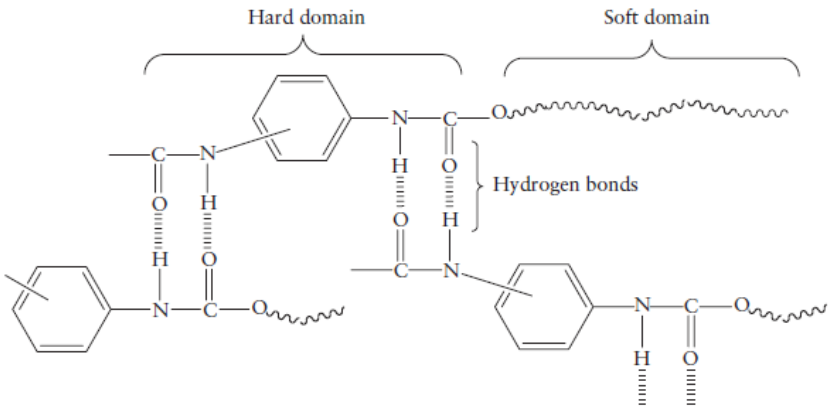

Fig. 18. Hard/soft segments in PU compounds.

Hard segments are connected to the possibility of the presence of H-bonds due to urethane/urea moieties; soft segments derive from high-MW polyol mobility and they give elasticity properties of the final PU.

5.2 Isocyanates: basic concepts and reactions

The general formula for isocyanate compounds is shown in **Fig. 19**:

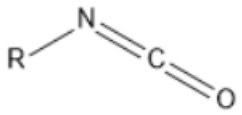

Fig. 19. General structure of isocyanates.

Generally, polyurethane polymers require isocyanates starting materials with two or more functional substitutes. The R groups can be aromatic or aliphatic: the most used in PU production are the first ones for two main reasons:

1. aromatic isocyanates are more reactive than aliphatic ones;
2. aromatic isocyanates are more economical than aliphatic ones.

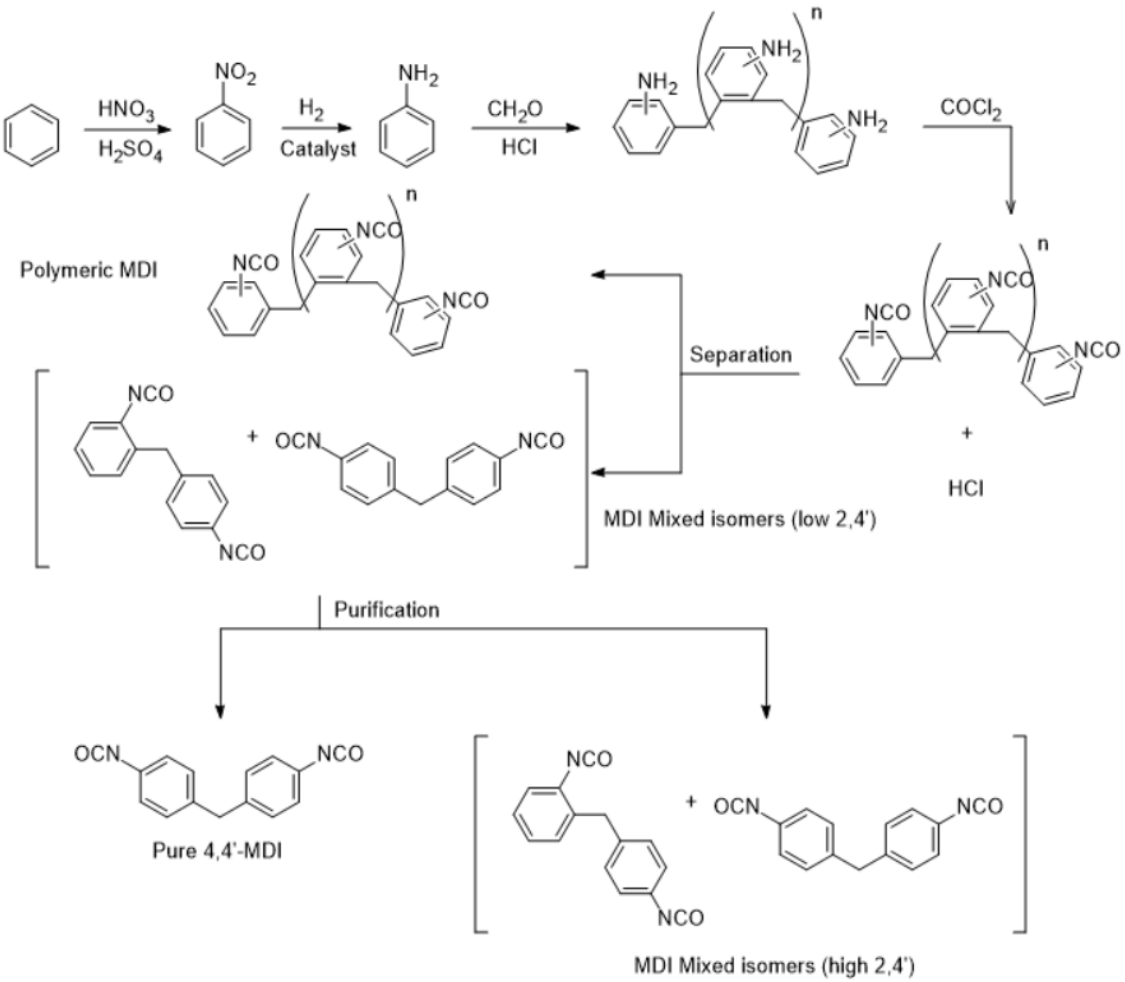

Scheme 10. Synthetic process for MDI production.

The main drawback of isocyanates with aromatic derivatives is the poor stability in the presence of light; for special purposes, aliphatic derivatives are more suitable. The most used aromatic-based isocyanates are MDI (methylene diisocyanate) and TDI (toluene diisocyanate). Their synthetic routes are shown in **Schemes 10** and **11**.

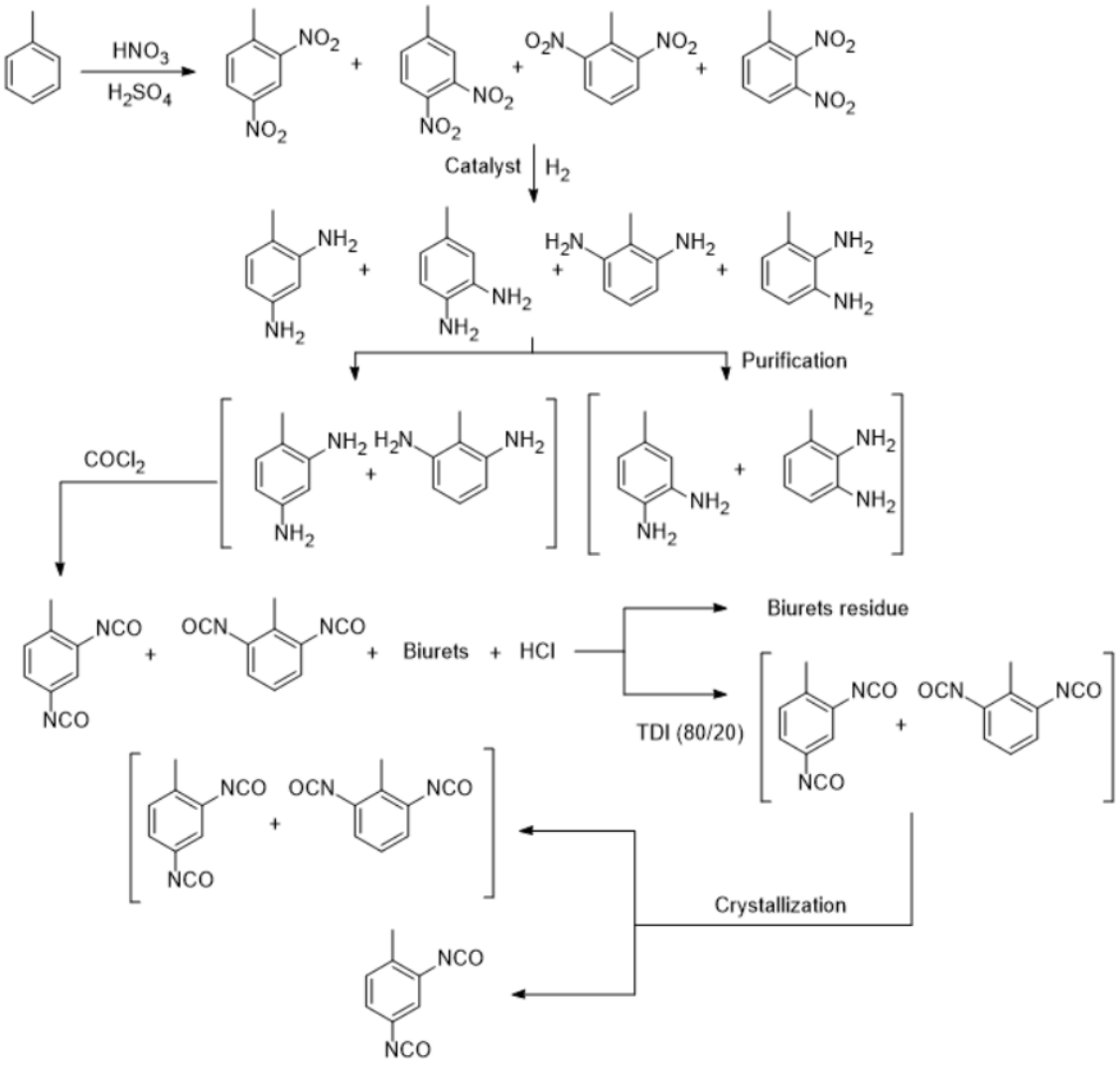

Scheme 11. Synthetic process for TDI production.

The common process for both types of isocyanates is phosgenation of the corresponding amines generated from the reductive hydrogenation of the corresponding nitro compounds. Besides the aromatic-based isocyanates, 1,6-hexamethylene diisocyanate (HDI) is the aliphatic-based one mostly used in polyurethane industry. Its synthetic production is shown in **Scheme 12**:

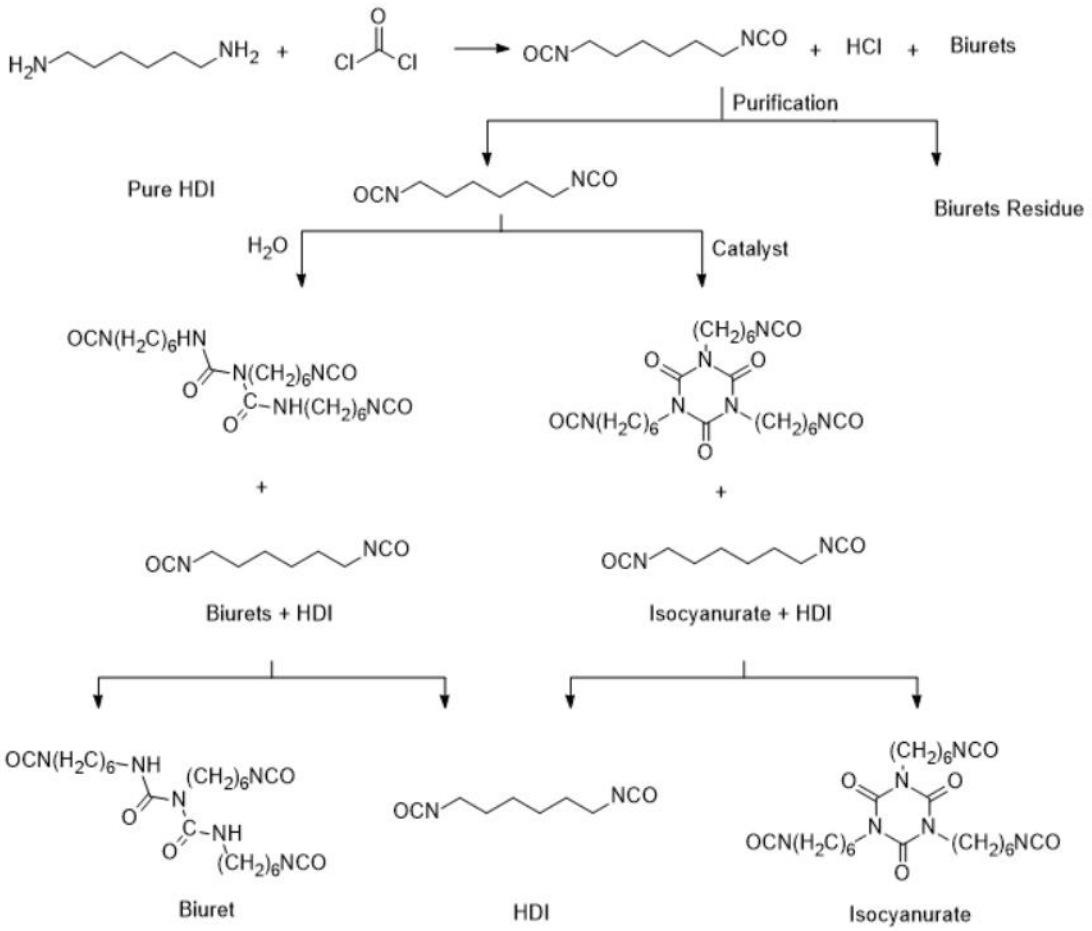

Scheme 12. Synthetic process for HDI.

Besides these three types of isocyanates, several other NCO-derivatives have been developed (**Fig. 20**):

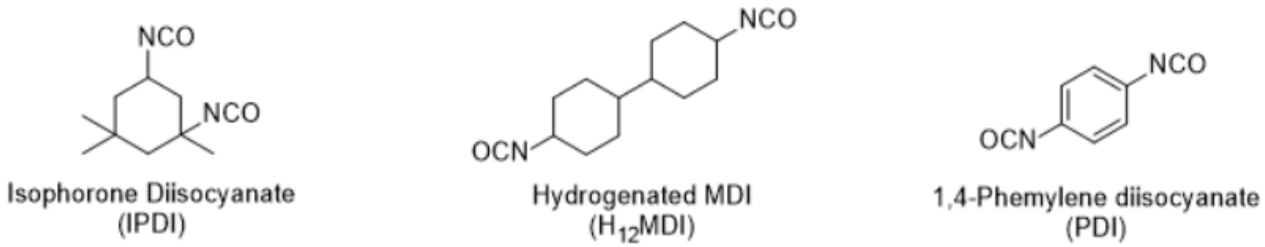

Fig. 20. Other types of isocyanate compounds.

Other that reacting with alcohols to form PUs, there are several other important reactions in isocyanate chemistry:

1. Reaction with water: this is a very important process at the base of the production of PU foams.[61] The product of this reaction is carbon dioxide and an amine which is essential for the cellular structure of PUs (**Scheme 13**):

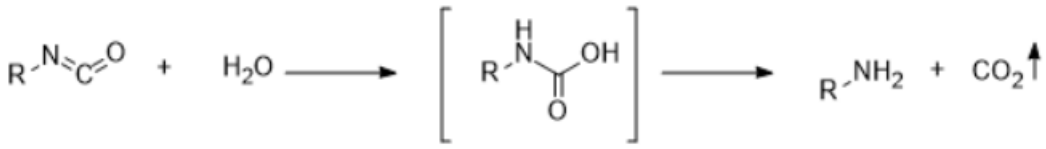

Scheme 13. Reaction of isocyanate with water.

The total heat release per mole of H_2O is 47 kcal/mol.[62] In polyurethane chemistry, water is considered as a blowing agent because a gas (in this case carbon dioxide) is generated in the PU formation. The generated amine from **Scheme 13** further reacts with other isocyanate moieties to produce a symmetrical disubstituted urea. This type of reaction is catalysed by low steric hinderance amines and, in the past, tin and mercury compounds.[63]

2. Reaction with urea/urea groups: the product from this reaction is a biuret (**Scheme 13**):

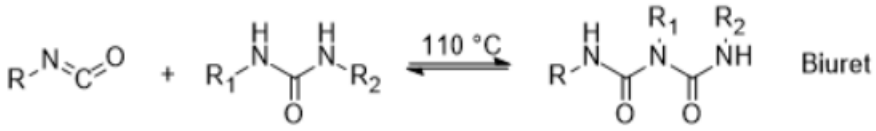

Scheme 13. Reaction of an isocyanate with a urea or urea derivatives.

It is an equilibrium reaction and a minimum temperature of 110°C is required.[64]

3. Reaction with urethane: urethane moieties can be considered "hydrogen active compounds" because of the presence of the hydrogen atom linked to the nitrogen. Allophanate is the product of the reaction urethane group and isocyanate (**Scheme 14**): similarly with the previous one, the formation of allophanate is an equilibrium reaction. The previous conditions are also valid. Biurets and allophanates are important in this type of chemistry because they are a supplementary source of crosslinking.

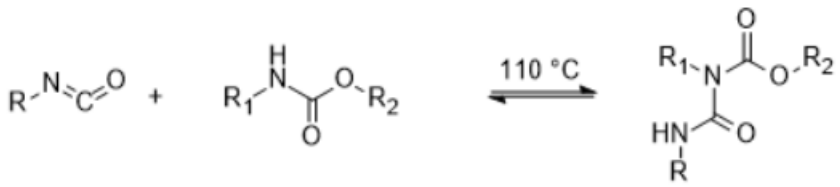

Scheme 14. Reaction of urethane group with isocyanate.

4. Dimerization and trimerization: uretidinediones and carbodiimides are two possible products of dimerization reaction (**Scheme 15**):[65]

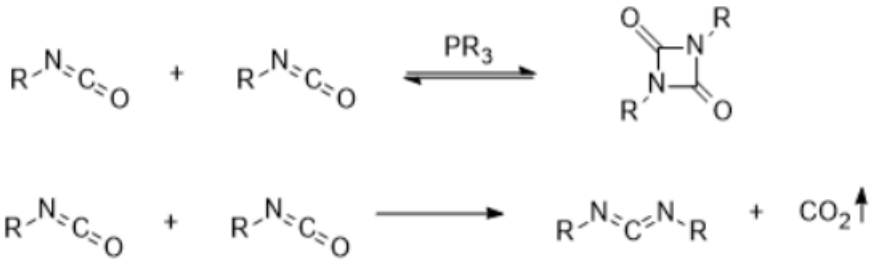

Scheme 15. Dimerization of isocyanates.

In trimerization reactions, highly crosslinked structures are formed: special catalysts like potassium acetate are employed. This type of reactions is used for the manufacture of special products like isocyanuric/urethane isocyanuric foams (**Scheme 16**):[66]

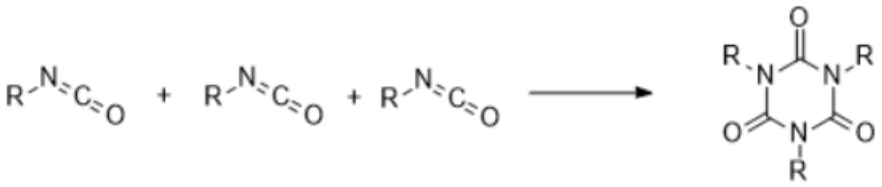

Scheme 16. Trimerization of isocyanates.

5.3 Polyols

Polyols are the second basic component of polyurethane compounds. The number of -OH functionalities defines the name of polyols: diols contain two hydroxyl groups, while triols have three -OHs, etc. Polyols are divided into two categories according to the bond type between the chain and the monomers: polyether and polyester polyols.

5.3.1 Polyether polyols

The first polyether for use in polyurethane production was a poly(oxytetramethylene) glycol derived from tetrahydrofuran, even if in the first experiments for the synthesis of polyether-based PU ethylene or propylene oxide were tried.[67,68] Nowadays, manufacture of polyether for urethane production is mostly based on propylene oxide; before, when prepolymer techniques were the major employed production method for flexible foams, diols like poly(oxypropylene) glycol, PO- and EO-based block copolymers were used as polyethers and as propellants and they still occupy an important role in the market. However, poly(oxyalkylene) derivatives of polyhydric alcohols have taken the lead of the market for two major reasons: firstly, the development of "one-shot" technique for flexible foams, and secondly, the growth of coatings applications and rigid foams production. Nitrogen-containing polyols are commercially available. An example of this type of polyether PUs is poly(oxyethylene)-poly(oxypropylene) block copolymers with ethylendiamine. The tri-substituted nitrogen enhances the polyol reactivity in urethane system compared to the neutral system one. The generic composition of a polyether polyol is shown in **Fig. 21**:

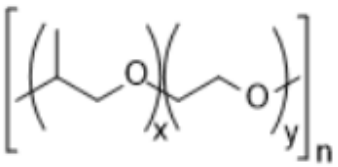

Fig. 21. Generical composition of a polyether polyol.

5.3.2 Polyester polyols

Before the impact of elastomers and urethane foams, the polyesters for plastic fabrication were unsaturated for free radical mechanism cure and often copolymerized with other monomers such as styrene. However, isocyanates easily react with polyesters containing -OH groups: in this optic, the urethane bonds formation is the mechanism for the cure. Saturated polyesters are preferred for urethane applications because the cure mechanism is the urethane bond formation and not the free radical one. An excellent review of many examples of polyester polyols preparation has been written by Müller.[69] The most utilized starting materials for polyesters in urethane application are adipic acid, dimerized linoleic acid,

phthalic anhydride, glycols (ethylene, propylene and 1,3-butylene) and triols (trimethylolpropane, trimethylolethane, glycerine and 1,2,6-hexametriol). The perfect polyester for urethane formation should contain hydroxyl moieties as reactive sites: they should have low acid numbers and very low water content (less than 0,1%). The removal of water in polyester preparation is necessary to speed up the reaction and to obtain a reasonable MW: the classical methods to remove it are made by azeotropic means, sweeping with an inert gas or with high temperatures and vacuum.

6. Rubber treatments (Adhesion)

6.1 Definition of adhesives

Adhesion is the term that refers to the application process of an adhesive. An adhesive substance is a material able to, firstly, be applied on the article surface and, secondly, form bonds between two components. The latter aspect is fundamental if the final product is made by two different materials joined together.[70] Structural and non-structural adhesion are the possible way of bonding: the first refers to the situations where the adherends must be able to support huge number of different stresses up to the characteristic yield point. The bonding has also to be durable throughout the service life of the product. The second way (non-structural) describes a situation where an adhesive bonding does not have to possess durability or to hold substantial weights. The typical example of non-structural bonding is packaging adhesives.

6.2 Properties, functions and classification of adhesives

The fundamental and essential function of an adhesive substance is binding parts togethers: they usually provide structures that show performances equal or superior to conventional assemble process at lower economic costs. Another important adhesive function in bonding is ensuring large areas for stress transfer throughput the adhesion surface, consequently reducing stress concentration in small areas that can be problematic for fractures.[71] Adhesives are useful in joining different materials, like elastomers, plastics, corks or other polymeric compounds: however, surface treatments must be performed. Other properties of adhesive bonding are:

- vibration dampening;
- sealing;
- transfer heat insulating in some cases.

Adhesives are classified according to their origin: natural or synthetic. Natural adhesives examples are natural or protein-based glues. Synthetic adhesives are further divided into industrial (acrylics, silicones, etc.) and special (pressure-sensitive) types.

6.3 Surface treatments

The term "surface treatment" describes the set of operations to do on a sample surface before the application of an adhesive. Some surface treatments don't produce surface chemical modifications (cleaning or removal of loose material) but, in other cases, especially, in polymer bonding, chemical and physical modifications are necessary. In elastomeric case, for example, surface preparation is made for enhancing wettability and creating active sites for adhesion bonding. The general reasons for applying a surface treatment are:

1. modifying surface by creating a microstructure for successive bonding;
2. removing the weak layer on sample surface;
3. improving adhesion forces for the durability of the compound.

The best results are obtained with chemical modifications: in this case, changing the chemistry of the surface means improving surface energy and, as a consequence, adhesion. The change in contact angle values is the main method to evaluate the results of the process.

6.4 Polyurethane adhesives

The first development of polyurethane adhesives is dated in 1940.[72] In the early 50s, PU-adhesives started to be used in elastomeric compounds.[73] Nowadays, they are used in footwear industry for attaching soles or combining two different materials like rubber and PUs. The first competitor of PU adhesives are neoprene-based ones, but they have quickly replaced them.

6.4.1 Raw materials for PU adhesives: Polyols

Polyols for PU-based adhesives are generally classified into three categories:

- polyester polyols;
- polybutadiene polyols;
- polyether polyols.

The main characteristics of polyester-based polyols are their optimal adhesive and cohesive properties. The main disadvantages are low temperature and chemical performances and lack of hydrolytic resistance. However, physical mechanical values are superior to polyether-based ones. They are the product of the reaction between adipic acid and glycols (**Scheme 17**):

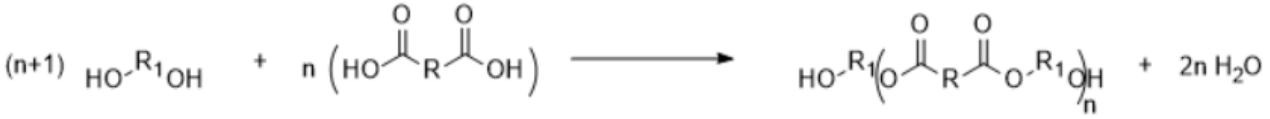

Scheme 17. Synthesis of polyester-based polyols.

The main feature of polybutadiene-based polyols is low temperature properties, because of their low T_g (-70°C), but their economic cost is higher compared to the other two types. Polyether is the most used polyol in adhesive industry. A wide range of product variety has been developed to satisfy all the different applications. The low T_g value (-60°C) is the reason of its good low temperature performances. Other important characteristics are its alkaline hydrolysis and low economic cost. The most employed polyols have a MW in the range from 500 to 2000 for diols.

6.4.2 Raw materials for PU adhesives: Isocyanates

In adhesive industry, two types of isocyanates are usually used: TDI (toluene diisocyanate) and MDI (methylene diisocyanate). TDI is a low-viscosity compound frequently used as raw material for flexible substrates. Typically, it is a 80:20 mixture between 2,4 and 2,6 isomers and two grades of acidity are present in the market: Type I has a low level of acidity, while in Type II it is higher. The latter is generally used because the higher acidity neutralizes the residual polyol base traces and stabilizes the prepolymer. MDI has superior mechanical properties and heat resistance. Its main disadvantage is the fact that it is solid at room temperature. It reacts faster because the isocyanate groups are chemically equivalent compared to TDI. It is normally used in shoe sole adhesives. Numerous efforts have been made using other types of isocyanates. Aliphatic isocyanates are used when UV resistance is

required. However, they have higher production cost and limited use in adhesive application. Block isocyanates have been developed by the reaction of isocyanate moiety with another substance that will prevent the further reaction at room temperature with hydrogen-active compounds, even if it will be the reaction at high temperature. The discovery of these type of isocyanates was made in the early 1940s by Bayer's group.[74] Moisture problem for isocyanate has been solved by blocked isocyanates: commercially there also available water-dispersion blocked isocyanates.

6.5 Surface preparation for PU-based adhesives

In footwear industry, the PU-based adhesives are mainly applied on rubber soles. The presence of dirt, mould release agents and certain compound ingredients (mostly plasticizers and processing oils) will form the so-called "weak boundary layer". In these space regions, the adhesive will probably fail. In all cases, surface treatment is necessary for eliminating this layer and improving bond strength. For this type of adhesives, a chemical surface treatment is the most applied because it modifies rubber surface by inserting new polar functionalities which will react with isocyanate moieties.

6.6 PU adhesive types

6.6.1 One-component adhesives

In sole industry, one of the most used one-component adhesives is based on hydroxypolyurethanes derived from the reaction of MDI with polyester polyols and chain extenders. The NCO/OH ratio is maintained at 1:1 in order to control molecular weight and have a low OH content. In shoe manufacturing, the treated sole is heated at 70°C: after the melt of the polymer, the shoe upper can be fit to the soles. When the product is cooled, the adhesive goes under a recrystallization process and the result is a flexible but resistant bond.[75] Water-borne PU adhesives have slowly taken more importance: they find major applications on shoe soles and texiles.[76] The great advantages of these type of PU-adhesives are:

- good mechanical strength;
- good blending process with almost each other dispersion;
- high hydrophilicity of the building polymers due to the presence of charged groups (anionic or cationic), emulsifiers or long hydrophilic polyols;

- high environmental sustainability.

Finally, blocked isocyanates can be regarded as an example of one-component adhesive type. In this case, at room temperature, the isocyanate moiety doesn't react due to the presence of a blocking agent; however, the reactivity is heat-activated having as a result the formation of bonds.

6.6.2 Two component adhesives

The two-component adhesives are needed in special applications, for example when fast cure is needed or when moisture presence can influence the quality of the final products. Typically, they are starting from a prepolymer or an isocyanate with a low-equivalent-weight, which is cured with polyamines or low-equivalent weight polyols. In the market, they are available in solid or solvent-based form and the two components are mixed together before application process. Just after this step, the two substrates are linked together. The basic and fundamental requirement for having a good bonding is the optimal mixing of the two components.

7. Physical properties

Generally, changing elastomer formulations leads to different performances of the final product. Several elements can be eliminated or substituted in order to have different properties according to the final customer. However, sometimes, even a little change can determine a dramatic difference in physical chemical values. In this section, several parameters and analysis are described.

7.1 Rheometric analysis

As raw materials, rubber compounds don't show any elastomeric properties. In order to achieve them, a crosslink reaction must occur: this process is called vulcanization. Rheometric analysis[77,78] simulates this process and measures the different viscoelastic values. In Delta, it is used an Oscillating Disk Rheometer (ODR): the name derives from the fact that it has an oscillating biconical-shape rotor. During the analysis, a sensor records the resistance values derived from the moving rotor and the rubber. The compound proprieties determine the torque for the oscillation. In **Fig. 22** a photo of the instrument is showed.

Fig. 22. Example of OD Rheometer.

The result of the rheometric analysis is a graph where torque values are in y-axis, while time ones are in the x-axis. Due to the chemical nature of rubbery compounds, the sample shows a viscous and elastomeric behaviour: because of the fact that shear forces are in direct proportion relationship with the degree of vulcanization, the rheometric curve can be seen as a measure of the level of vulcanization process as a function of time at a determined temperature. The first interesting value is the "Moment Lowest" (ML): it represents the drop of viscosity due to the temperature increase. It is lowest torque value and it can be seen as the toughness of the unvulcanized sample at the test temperature. The measuring unit is dNm. The second analytical value is Ts_2. It is measured in unit of time: it represents the time of start of vulcanization process and it is calculated at the time when the torque value rises two 2 dNm units from ML point. In contrast to the ML value there is the "Moment Highest" (MH) one. As the name suggests, it represents the highest torque value and it is expressed in dNm. Correlated to this concept, t_{90} is the time in which MH reaches 90% of its value or, in other words, the 90% of the sample is vulcanized.

7.2 Density

The density[77] value (usually in g cm^{-3}) is strongly influenced by compound composition and it can be used for quality checks. The hydrostatic method is the mostly used. The necessary equipment is:

- electronic densimeter (**Fig. 23**) having a sensibility of 0,001 g;
- beaker with distilled water;
- sample holder (usually a needle);
- moving arm for the beaker.

Equation 3 is used for the calculation of density:

$$Density = \frac{m_1}{m_2}$$

Equation 3. Calculation of density.

Where m_1 is the weight of sample in air and m_2 is the weight of sample when full immersed in distilled water.

Fig. 23. Example of densimeter.

7.3 Abrasion resistance

Compared to other compounds used in soles industry, rubber has a high abrasion resistance[80]. It represents the volume in mm^3 lost by a cylindric sample specimen when it is forced to guide at define contact pressure (usually 5 or 10 N) on a rotating cylinder covered with abrasive test

paper over a distance of 40 m. According to ISO 4649, the abrasion resistance value is calculated from **Equation 4**, here Δm is the difference of the mass value after the analysis and the initial one, d is the density in g/cm^3 and f is the abrasive factor of the paper:

$$Abrasion\ resistance = \frac{\Delta m}{d} \times f \times 100$$

Equation 4. Calculation of Abrasion resistance (mm^3).

The reference limits for abrasion resistance are reported in **Table 4**:

Density (g/cm^3)	**Limits**
< 0,9	⩽ 250 mg
⩾ 0,9	⩽150 mm^3

Table 4. Abrasion resistance limits according to UNI EN ISO 20345[81].

An example of abrasimeter is shown in **Fig. 24**:

Fig. 24. Example of abrasimeter.

7.4 Tensile strength and elongation at break

Tensile strength and elongation at break[82] are two of the most important properties for an elastomeric compound. Tensile strength is measured in MPa and it represents the maximum applicable force before the breaking of the sample. Elongation at break is the maximum elongation over a constant load before the breaking of the sample. A dynamometer (**Fig. 25**) is necessary for these tests.

Fig. 25. Example of a dynamometer.

The rate used in the analysis is usually 500 mm/m: the final result is a graph of force in function of elongation. The samples have dumb-bell shape and they are cut from rubber plates or soles: the general rule says that, in order to have a correct representation of the sample, the samples have to be cut in horizontal and vertical way. **Equations 5** and **6** describe how to find the two values, where F_r is force at break, A is the transversal section, l is the useful length on the elongated sample and l_0 is the useful initial length:

$$Tensile\ Strength = \frac{F_r}{A}$$

Equation 5. Equation for tensile strength.

$$Elongation\ at\ break = \frac{l - l_0}{l_0} \times 100$$

Equation 6. Equation for elongation at break.

Stress at 100% and at 300% are also useful values. It is important to say that these values are directly calculated from the instrument by an internal program.

7.5 Tear strength

Tear Strength[83] (TS) is defined according to **Equation 7**, where F_m is the maximum force applied in N and d is the medium thickness (mm) of the specimen:

$$Tear\ Strength = \frac{F_m}{d}$$

Equation 7. Equation for tear strength.

In other words, tear strength is the sample resistance to tear propagation. The instrument is the same used for tensile strength and elongation. The rate of analysis is constant (100 mm/m): the sample has trouser-like shape and they are cut from rubber plates or soles.

7.6 Hardness

The common measuring unit for hardness[84] in rubber compounds is Shore A. The values range from 0 to 100: hardness is higher if its value is near the upper limit. It represents the resistance of the sample to the penetration of a needle under a certain spring force. It is necessary to measure it at least three times in different regions of the sample in order to have a more accurate analysis. **Fig. 26** shows an example of durometer.

Fig. 26. Example of durometer instrument.

7.7 Peeling

The common test for verifying adhesion between different materials is peel test[85]. The procedure requires (at least) a 25 mm strip-like sample. The sample must be long enough in order to see separation over 100 nm. Each grip of a tensile testing machine takes one end of the specimen: the moving rate is 100 mm/min (**Fig. 27**):

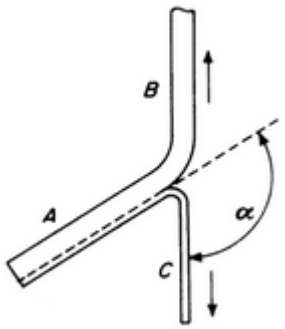

Fig. 27. Peel test.

The reference limits for peeling are reported in **Table 5**.

Density (g/cm^3)	Limits (N/mm)
< 0,9	⩾ 1,7
⩾ 0,9	⩾ 3,0

Table 5. Peeling resistance limits according to UNI EN ISO 20345.

7.8 Fuel-oil resistance

The term “swelling” described a common phaenomenon in rubber chemistry: it stands for change in volume due to liquid absorption of a rubbery sample. The swelling can have a profound influence on physical properties (for example, decrease of hardness). The choice of a representative liquid is also important: the common solvent for this test is 2,2,4-triethylpentane, also known as 1-octane (**Fig. 28**):

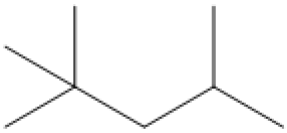

Fig. 28. 2,2,4-trimethyl pentane (1-octane).

The time of immersion is 22 ± 0,25 h and the formula for the recovering the change in mass is **Equation 8**, where m_i is the initial mass in air and m_f is mass of the piece after immersion:

$$Fuel\ oil\ resistance = \frac{m_f - m_i}{m_i} \times 100$$

Equation 8. Fuel oil resistance[86].

According to the UNI ISO EN 20344:2012 reference limit, the change of mass should be less than 12% in order to have an anti-oil compound.

7.9 Electric resistance

Many applications require the reduction of electric discharge in rubber articles. Rubber soles can be considered as properly dispersion paths. According to the different use, there are:

- conductive articles: the electric resistance is below 10^5 Ω;
- antistatic articles: the electric resistance is between 10^5 and 10^9 Ω; in this region there is a particular range called ESD (ElectroStatic Discharge) between 10^5 and $35*10^6$ Ω;
- dielectric (insulating) articles: the electric resistance is over 10^9 Ω.

Electric resistance[87] values are also influenced by the additives for the formulation (for example, carbon black). An Ohmmeter is preferred for this analysis: it must have an open-circuit nominal tension of 500 VDC and it must not lose more than 3 W in the test sample.

8. Experimental section

8.1 Brief introduction

As said in preface, this is not a classical PhD work in the sense that the candidate studied a specific research topic. This work is based on practical approach to problem solving: industrially speaking, production is everyday life and, without it, it would be impossible to grant new researches or activities. All the data reported is the result of a lot of efforts but, due to industrial secret, not all the work can be described; however, this can be a good insight into industrial research.

8.2 Definition of a range time for treatments for rubber/polyurethane soles

Soles for shoes can be made, obviously, with different materials: rubber, polyurethane, ethylene vinyl acetate, etc. Physical performances, costs and final product applications are the main differences that soles industry should consider when a project starts. For example, polyurethane soles have low cost but also low mechanical performances, while rubber ones guarantee superior performances but at higher price. In the 80s, an idea was born: coupling rubber soles with PU. Delta Spa was one of the first companies applying this technology. However, if the rubber surface is not treated, the two materials simply do not join because of the chemical and physical differences between them. Surface treatments involve cleaning of the surface, application of a primer and, successively, of the polyurethane adhesive. While cleaning of the surface can be avoided because it takes time at industrial scale and lowers production, the primer application step is essential. The general process for production of a rubber-PU sole is shown in **Fig. 29**:

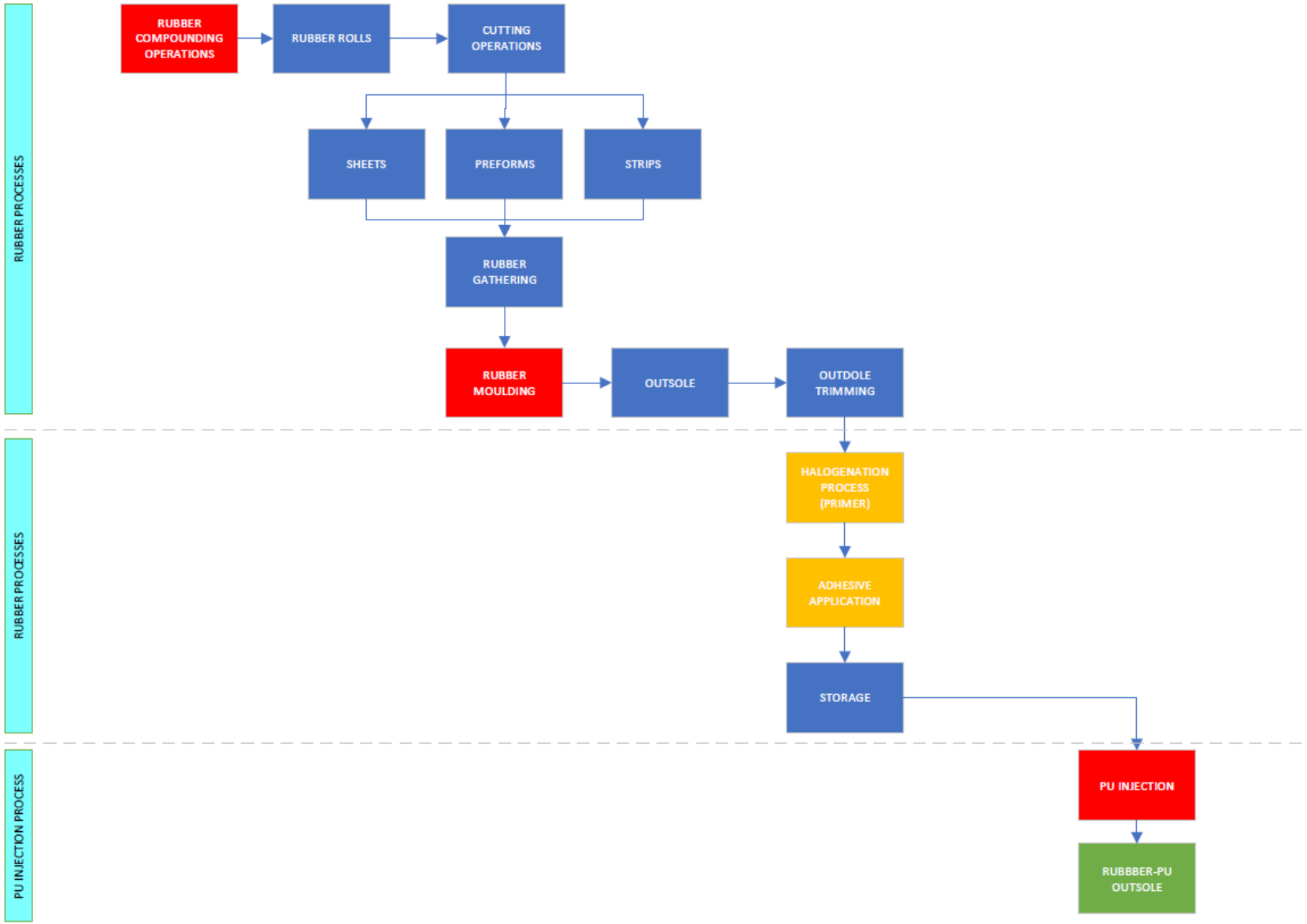

Fig. 29. Rubber/PU outsoles production processes.

Each step must be made with attention. As already said, the essential steps are halogenation and adhesives application. If they are not made in the correct way, adhesion failures are common. This fact has two important consequences:

1. Economic loss: the product cannot be delivered to the final customer because it cannot make a shoe with a defected sole. The articles need to be reprinted: it means an additional consume of raw materials and machines;
2. Environmental concerns: if the product is defected and can't be repaired, it goes into dump and, as a consequence, accumulation issue can be created.

It is necessary to define time ranges for the two rubber treatment steps. In this section, every step of a rubber/PU outsole is described and the main aim is the definition of range times where these operations can be made without successive failures in the final product.

8.2.1 Rubber compounding and moulding

The compound formula used for sample soles is shown in **Table 6**:

Ingredients	Quantity (phr)
Rubber	100%
Silica fillers	45
Silane coupling agents	2
Antioxidant	1.1
Activators	3.3
Vulcanization retarder	0.7
Primary accelerator	0.5
Secondary accelerator	0.6
Sulphur	1.2

Table 6. Compound formula.

Due to industrial secret, the quantity of each type of rubber cannot be revealed: however, due to surface treatment's purpose, it is a mixer of diene-based elastomers. The steps of compounding are the following:

1. insertion of rubber into the internal mixer (rubber mastication);
2. addition of silica and silane;
3. addition of additive agents, accelerators and sulphur;
4. mixing of ingredients (ca 5 min);
5. dumping into open mill and successive mixing (ca 3 min);
6. making of rubber roll and cutting into preforms.

The first analysis on the rubber compound is the rheometric curve determination (see **Section 7**) (**Fig. 30**, **Tab. 7**):

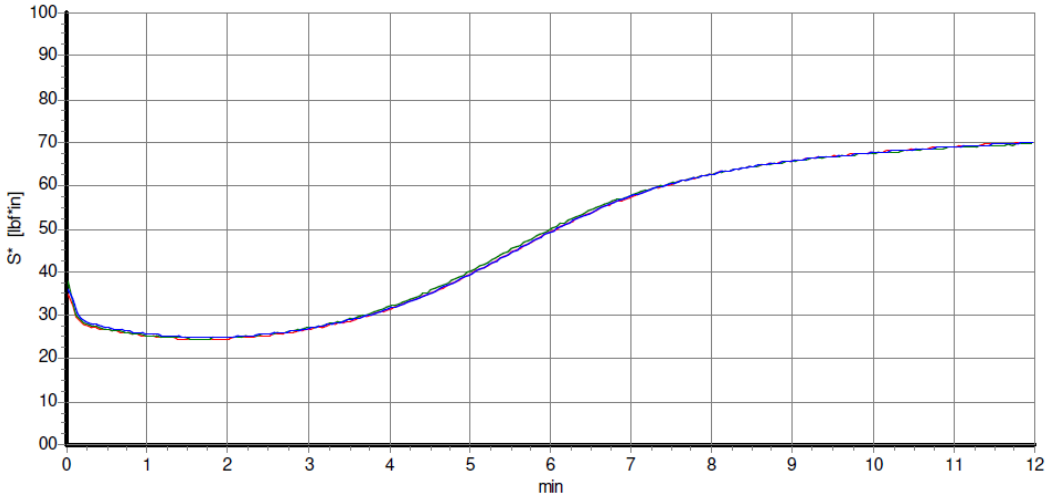

Fig. 30. Samples rheometric curves.

Samples	ML	Ts1	Ts2	t90	MH
1	24.54	2.34	2.57	8.52	69.99
2	24.68	2.31	2.53	8.49	69.76
3	24.84	2.34	2.58	8.53	69.96

Tab. 7. Rheometric values for samples 1, 2 and 3.

Three samples were taken randomly from the rubber preforms. With the found values and the relative samples, rubber plates were moulding. The parameters of this operation were 168 °C for mould temperature, 510 seconds for cure time and 100 bar for compression force. Also in

this case, the physical mechanical parameters of three plates (relative to each vulcanization curve) were analysed and the results are reported (**Table 8**, **Fig. 31**, **Fig. 32** and **Fig. 33**):

Physical property	M. U.	Limit	Sample 1	Sample 2	Sample 3
Hardness	Shore A	71±3	69	70	68
Density	g/cm^3	1.130±0.030	1.124	1.125	1.128
Abrasion resistance	mm^3	<100	75.3	77.7	70.8
Tensile strength	N/mm^2	>14	21.4	22.5	22.3
Elongation at break	%	>450	703	708	705
Tear strength	N/mm	>13	14.8	13.4	14.3

Table 8. Physical mechanical analysis for samples 1, 2 and 3 (abrasive factor: 0.94).

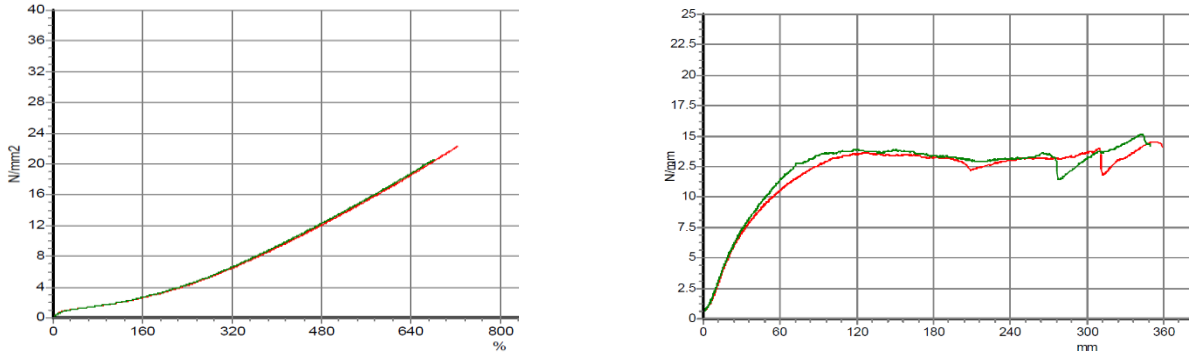

(a) **(b)**

Fig. 31. Physical mechanical tests of Sample 1: (a): elongation and tensile strength, (b): tear strength (red: horizontal sample; green: vertical sample).

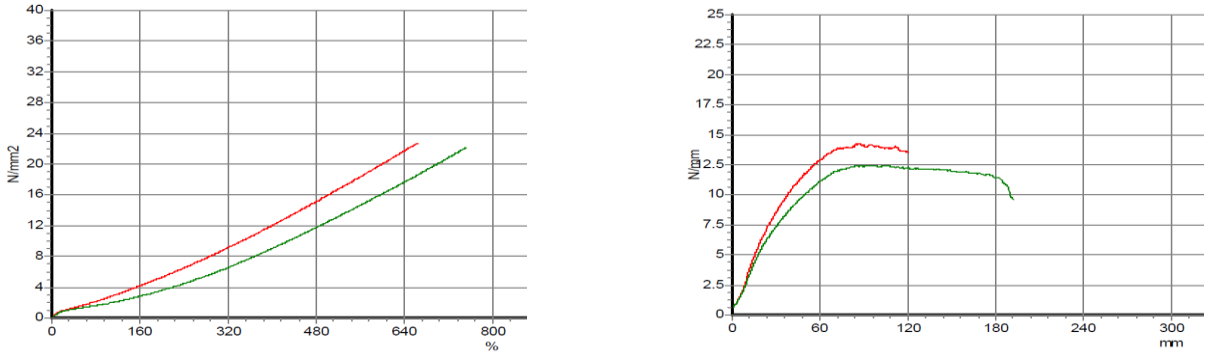

(a) **(b)**

Fig. 32. Physical mechanical tests of Sample 2: (a): elongation and tensile strength, (b): tear strength (red: horizontal sample; green: vertical sample).

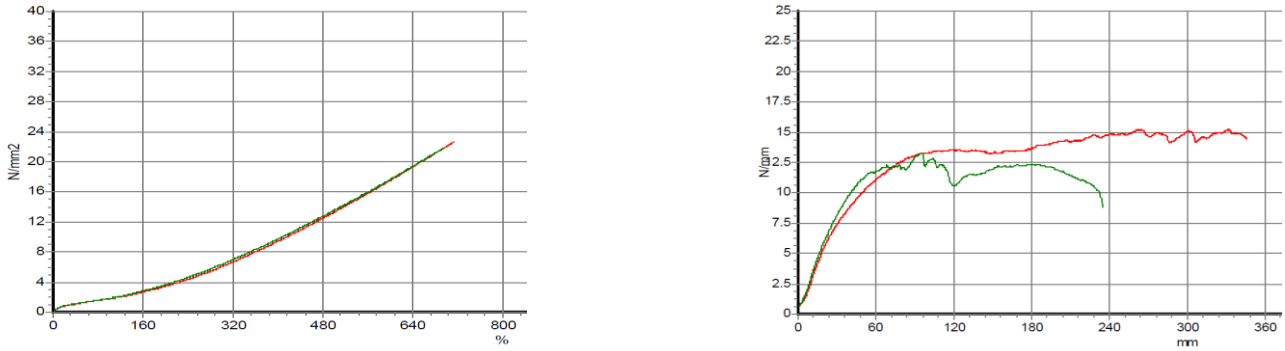

(a) **(b)**

Fig. 33. Physical mechanical tests of Sample 3: (a): elongation and tensile strength, (b): tear strength (red: horizontal sample; green: vertical sample).

All the values are in the desired value range. The uniformity of the compound is mostly shown by ODR analysis: the three curves are almost overlapped, with little differences between them. Also, physical performances are quite similar: these facts show an optimal mixing of the ingredients during compounding processes. The successive step is the production of the soles. The preform is inserted into a heated mould (usually 180 °C) which closes after a defined time. The amount of time in which the mould is closed is the vulcanization time and it is necessary to shape the final product (**Fig. 34**):

Fig. 34. Sample rubber soles.

The excess of rubber is eliminated with trimming processes. After this operation, the outsole will be halogenated and the adhesive will be applied.

8.2.2 Rubber treatments

Halogenation process is made by spraying a solution of organic solvent and a chlorinating agent. The solution is inserted into a reservoir which is under inert atmosphere. The outsole is charged into a line and it is heated into oven at 90 °C; the successive operation is the chlorination. The quality of the process is controlled by an UV-lamp. Adhesive application is made at least 45 minutes after halogenation. The adhesive solution is composed by a PU-based adhesive and hardener and it is applied by robot spraying. A reservoir of adhesive solution is directly linked to the robot which can read the shape of the sole and, consequently, apply the solution efficiently. The spectra of the species after the processes are reported (**Figures 35** and **36**):

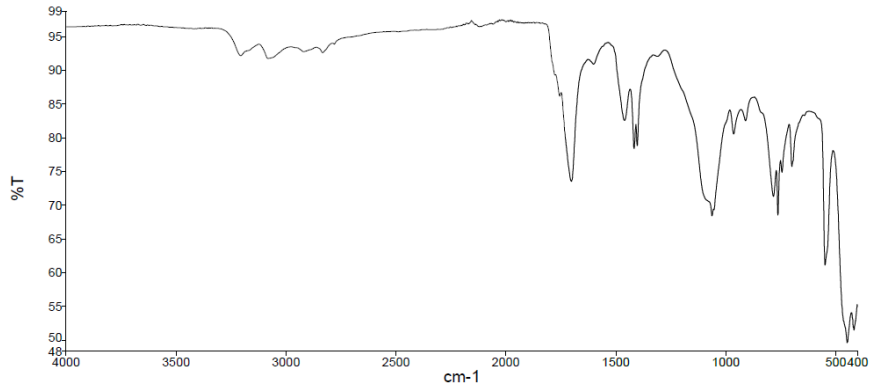

Fig. 35. IR spectrum of chlorinated sample.

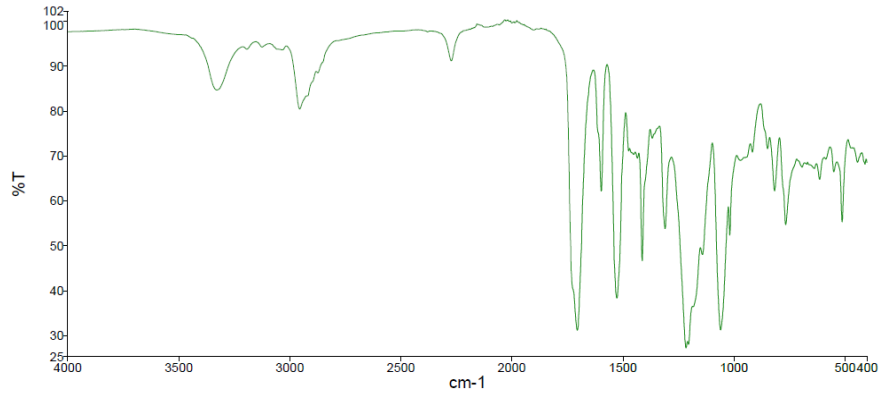

Fig. 36. IR spectrum of sample with PU adhesive.

IR spectra are recorded in order to show that treatments modify rubber surfaces. These new functionalities are clearly shown by the presence of a new intense band at 1701 cm^{-1} (C=O) in the chlorination spectrum and by the new bands at 3330 cm^{-1} (N-H) and 2273 cm^{-1} (N=C=O) in the spectrum of sample with PU adhesive. **Fig. 37** shows the comparison of the three spectra:

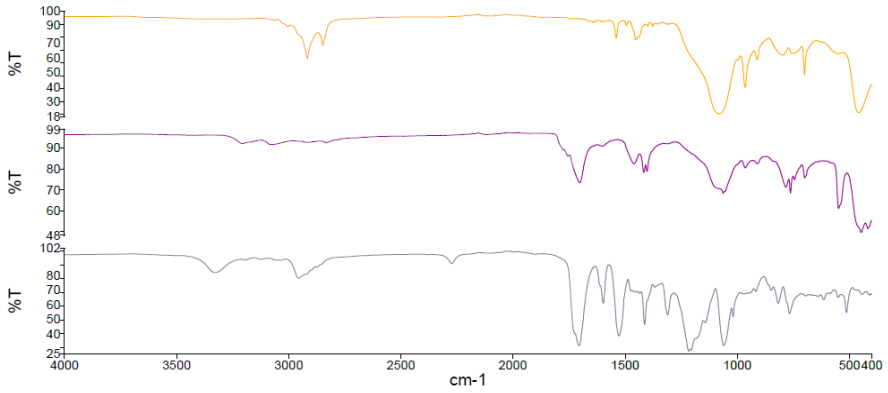

Fig. 37. IR spectra comparison.

The yellow, purple and grey graphs in **Fig. 37** represent, respectively, the IR analysis of non-treated, chlorinated and adhesive-applicated samples.

8.2.3 Polyurethane

The injection of polyurethane is an essential step for the quality of the final product. A machine is dedicated for this operation and it is composed by three different reservoirs: the first one contains the isocyanate in prepolymer form, the second one the polyol material and the last one the colour paste which is used for creating different versions for the rubber/PU soles. This kind of polyurethane is a midsole one, so on one hand it loses some physical performances but, on the other one, softness and flexibility are improved. The procedure is:

1. The rubber sole is put on the heated mould (60-70 °C).
2. The adhesive film is activated by using a series of infrared lamps.
3. The PU material is injected over the sole. The mixing of the three materials is made on the head of the machine: according to specific parameters previously set to the machine, the mixture is injected in the mould. After this process, the upper part is closed.
4. After a predetermined time, which is necessary for the expansion and the crosslinking of the material, the mould opens and the rubber/polyurethane sole is obtained.

A general formulation for midsole PU is shown in **Table 9**:

Ingredients	%
Isocyanate	Prepolymer form
Polyol resin	88
Chain extender	10
Catalyst	1.5
Surfactant	0.25
Blowing agent	0.25

Table 9. General formula for midsole PU.

Physical-mechanical analyses were also performed on polyurethane plates (**Table 10**, **Figures 38** and **39**):

Physical properties	M.U.	Limit	1	2
Hardness	Shore A	45±5	49	50
Density	g/cm^3	0.50±0,03	0.51	0.53
Abrasion resistance	mm^3	<250	138	143
Tensile strength	N/mm^2	>4	5.8	5.8
Elongation at break	%	>300	350	326
Tear strength	N/mm	>5	8.3	7.3

Table 10. Physical mechanical analysis for PU plates 1 and 2.

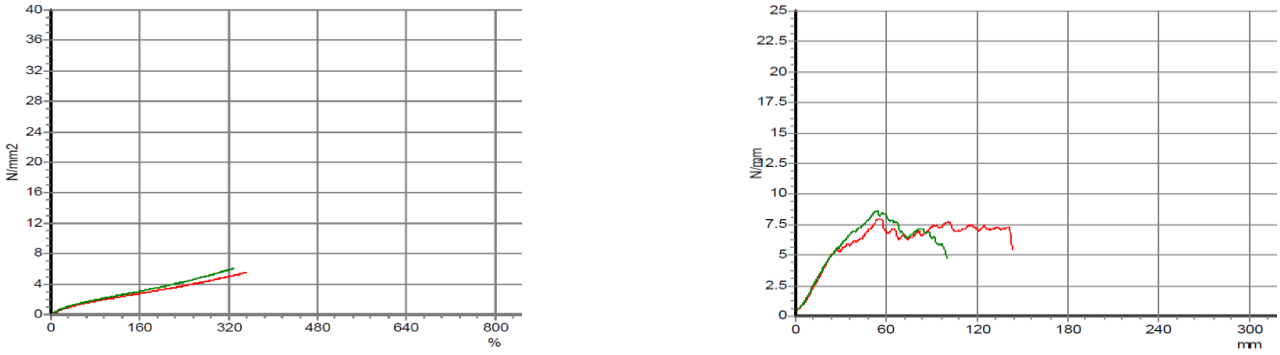

(a) **(b)**

Fig. 38. Physical mechanical tests of PU plate 1: (a): elongation and tensile strength, (b): tear strength (red: horizontal sample; green: vertical sample).

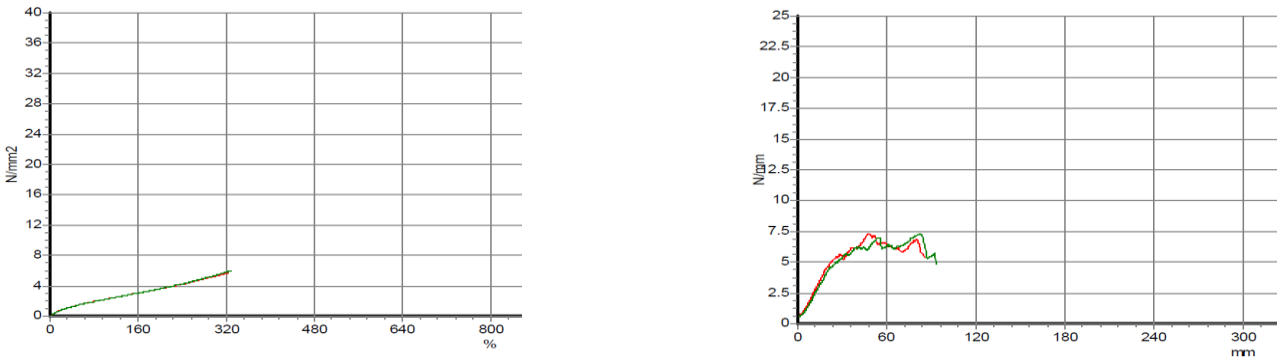

(a) **(b)**

Fig. 39. Physical mechanical tests of PU plate 2: (a): elongation and tensile strength, (b): tear strength (red: horizontal sample; green: vertical sample).

8.2.4 Determination of time ranges for chlorination

The determination of time range was firstly evaluated for chlorination for a dual reason: firstly, according to **Fig. 29**, it is the immediate operation after the printing of the soles and secondly, it is an essential step for an adequate bonding between the two materials. The procedure was applying the halogenating solution on all samples and then, at a fixed time, spraying the adhesive solution and injecting the PU. The time range was evaluated over a period of 34 days, starting the tests after one week because, due to company experience and process time, this is the estimated period between moulding from rubber department and injection of PU. The strength of the adhesion between rubber and PU was evaluated by peeling test (see **Section 7**) following the specification of ISO 36 at 500 mm min^{-1} as test speed. The acceptable limits must be above 4 N/mm. In **Table 11** test results are reported:

Time from primer application (days)	Peeling value (N/mm)
7	4.8
12	5.7
15	5.3
19	5.7
22	5.9
26	4.5
30	4.4
34	3.4

Table 11. Chlorination peeling test results.

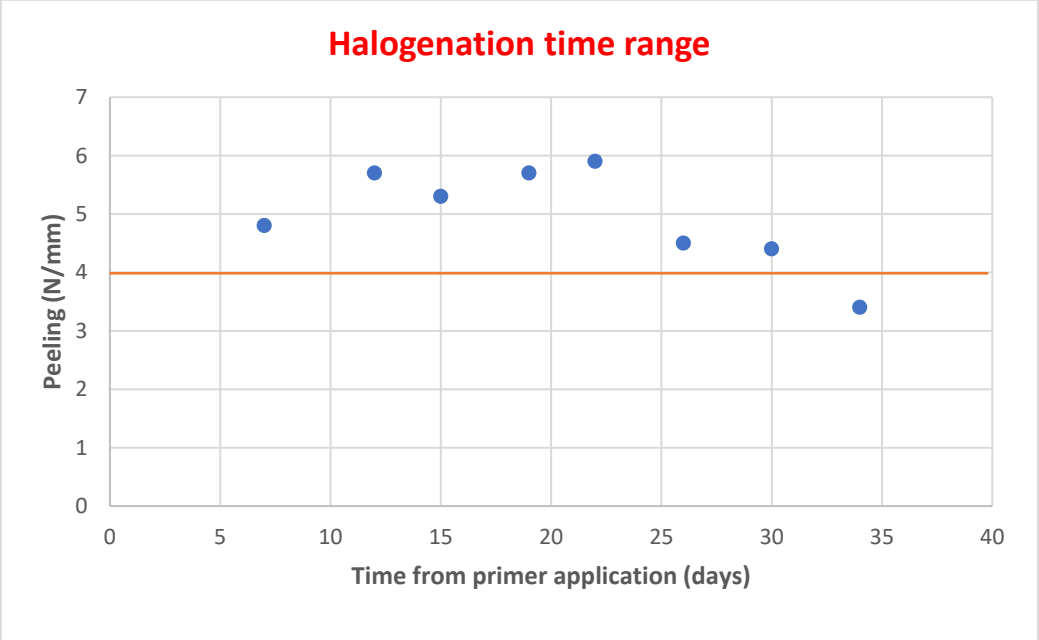

Fig. 40. Evaluation of chlorination peeling test time range.

Almost all the founded values (**Fig. 40**) are above the acceptable limit, except for the value at 34 days (3.4 N/mm). The higher value is found at 19 days (5.9 N/mm). From this experimental data, the ideal time range for chlorination is not over 19 days: the decrease after this time is probably due to the presence of white crystals of triisocyanuric acid which does not allow the correct adhesion of PU material.

8.2.5 Determination of time ranges for adhesive application

The time range determination of adhesive application follows a similar methodology regarding testing (ISO 36, speed test: 500 mmmin^{-1}) and acceptable values (> 4 N/mm) but, in this case, all the samples were initially halogenated and then, at a fixed time, adhesive solution was applied and PU injected. The same times were also applied in this situation. In **Table 12** test results are reported:

Time from adhesive application (days)	Peeling value (N/mm)
7	5.1
12	5.9
15	5.7
19	6.1
22	4.8
26	5.1
30	4.9
34	3.8

Table 12. Adhesion process peeling test results.

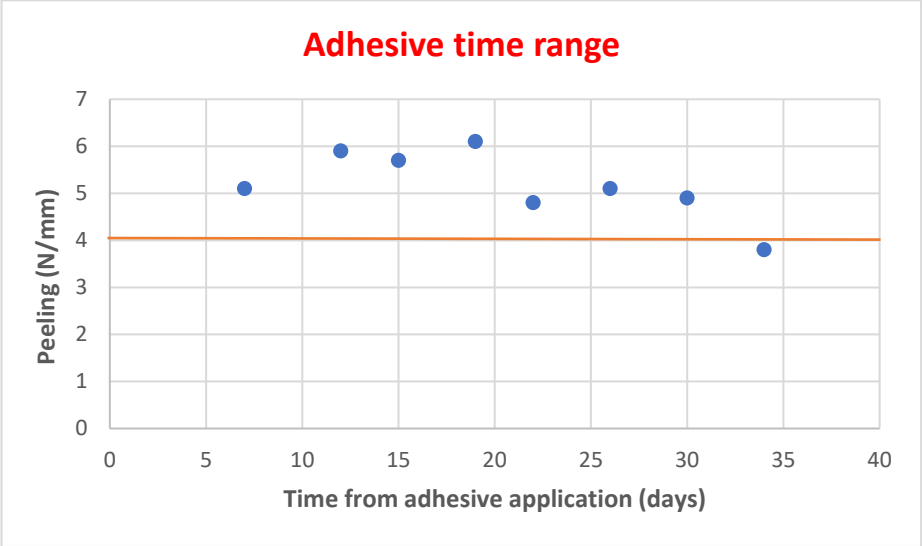

Fig. 41. Evaluation of adhesion peeling test time range.

Also in this case, almost all the values (**Fig. 41**) are above the acceptable limit, except for the value at 34 days (3.8 N/mm). The higher value is found at 22 days (5.9 N/mm). From the evaluation of this experimental data, the ideal time range for chlorination is not over 19 days: the decrease after this time is probably due to the crystallization process over PU adhesive film that probably influences the reactivation process and, as a consequence, PU adhesion on rubber surface.

8.2.6 Conclusion

The determination of time ranges for chlorination and adhesive application processes has been

made. For the halogenation process, the best value is obtained at 19 days, while for the other step, adhesive application, the bond strength reaches its maximum at 22 days. These time ranges have been applied in production and recent data shows a reduction on waste production and an increase in quality by 5%. Moreover, no complaints have been received from customers since the application of these parameters.

8.3 Ice slip resistance of soles for safety applications

In recent years, work safety has become one of the most important aspects to be taken into consideration. According to INAIL recent data, in 2021, more than 3 people died every day during working activities in Italy. Working casualties reports show a +0,2% compared to 2020 (555.236 reports) and, among them, 1221 with fatal results (death) and 55288 with associated working pathologies.[88] A good safety practice is choosing safety shoes with the right specifications for the final use. The outsole of this kind of product is the most important part because on one hand, it ensures all the desired characteristics and on the other hand, it is the first part in contact with ground so, as a consequence, it must have a specific design. One of the most challenging issues is ice slip resistance. Due to the recent climatic changes, the probability of falling over an icy surface is increased. The first solution proposed by Delta is Fibregrip®, which essentially consists in a combination of polymers, resins and vegetable fibres and it gives an excellent slip resistance value on ice. The added fibres are of natural origin. The nature of their high performances on icy surfaces is due to their freeze process, which happens at low temperature, and consequently the frozen fibres create friction with the ground. The aim of this work is improving this approach using different compounds and evaluating slip resistance value for these samples.

8.3.1 Testing procedures

The requirements for safety shoes are contained in UNI EN 20344:2012. More specifically, the testing procedures for slip resistance analysis are enclosed in ISO EN 13287:2019 (last update) (**Figures 42** and **43**) or, more generally, SATRA TM 144.

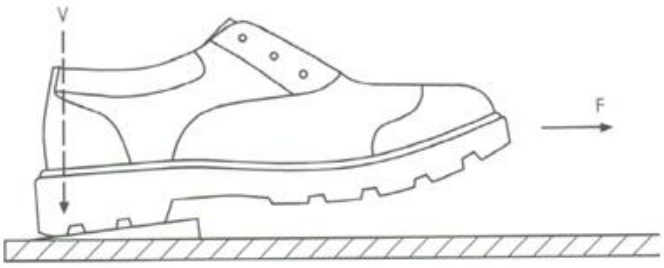

Fig. 42. Forward heel slip resistance.

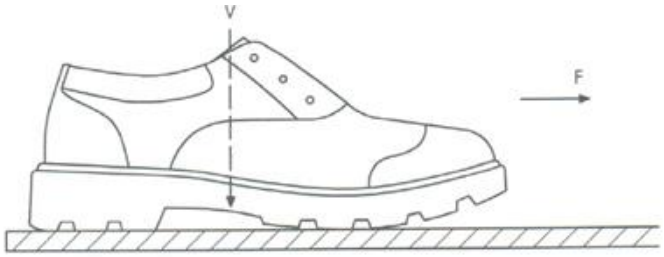

Fig. 43. Forward flat slip resistance.

As shown in **Figures 42** and **43**, two values are determined: the forward heel one and forward flat one. The normative test also specifies the minimum results for a good slip resistant sole. For forward hell part, the result (CoF: Friction Coefficient) must be higher than 0.28 while, for forward flat slip, it must be higher than 0.32. The test surface was ice with water at room temperature. A tex-bond film is applied on the surface of the outsole to simulate the upper part of the shoe.

8.3.2 Glass spheres

Glass spheres were firstly employed in combination with natural fibres to improve the performances of the formulation (**Table 13**):

Components	Quantity (phr)
Rubber	100%
Silica and silane	42
Compounding agents	4.7
Resin	3.2
Accelerator	0.7
Sulphur	1.4
Glass spheres	15
Natural fibres	5

Table 13. Rubber formulation with natural fibres and glass spheres.

Some plates were moulded with this rubber compound (T: 166 °C; time: 10 min) and cut in small pieces that were inserted for the moulding of sample sole shown in **Figure 44**:

Fig. 44. Sample sole having white inserts with formulation shown in **Table 13**.

IR spectrum of the white rubber pieces was also recorded (**Figure 45**).

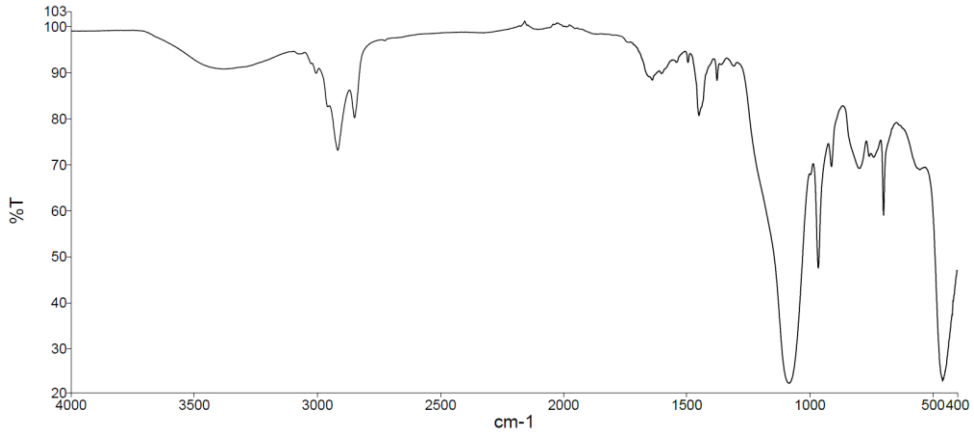

Fig. 45. IR spectrum of white inserts with formulation shown in **Table 13**.

The great quantity of glass spheres is indicated by the large peak at about 1080 cm^{-1}. The slip resistance test was performed with the method described in the past sections and the values are reported in **Table 14**.

Part of the sole analysed	Limit	Result
Forward heel	> 0.28	0.02
Forward flat	> 0.32	0.13

Table 14. Slip resistance values of sole in **Fig. 44**.

Surprisingly, negative results were obtained. In order to understand the reason of this outcome, SEM analysis were performed (**Fig. 46**):

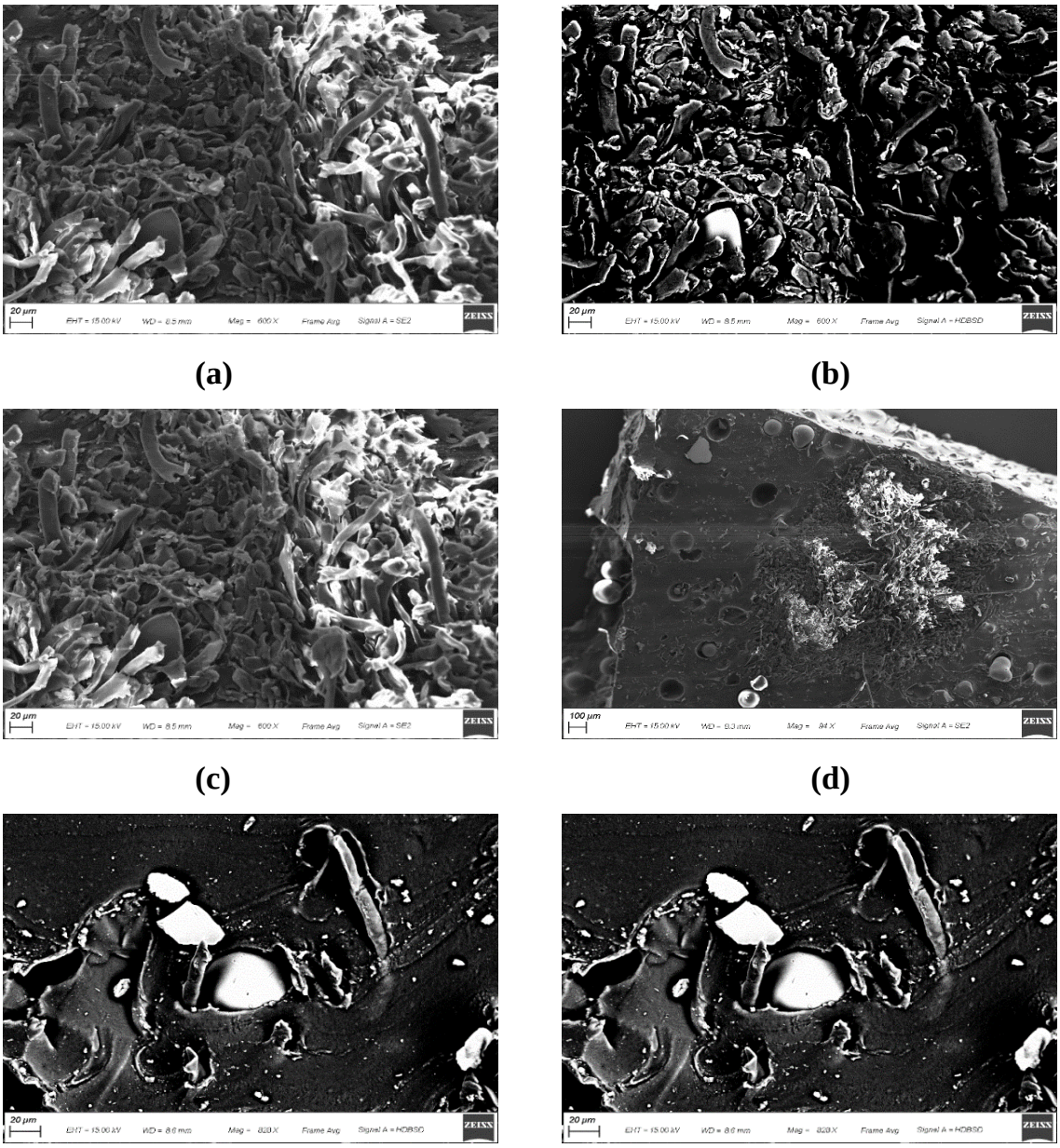

Fig. 46. SEM images recorded at different magnification: (a) 600x, (b) 600x, (c) 600x, (d) 600x, (e) 828x, (f) 828x.

The SEM images show a lack of distribution of glass spheres in rubber matrix maybe due to a not optimal distribution in compounding step. The presence of natural fibres in combination with glass spheres clearly does not improve the slip resistance properties of rubber sole because of the lack of synergistic effect of the two ingredients.

8.3.3 Glass fibres

Glass fibres were employed to overcome the problems seen with glass spheres and natural

fibres. The methodology was the same and the formulation of rubber compound with glass fibres is shown in **Table 15**.

Components	Quantity (phr)
Rubber	100%
Silica and silane	42
Compounding agents	4.7
Resin	3.2
Accelerator	0.7
Sulphur	1.4
Glass fibres	10

Table 15. Rubber formulation with glass fibres.

Also in this case, the plates were printed with the same parameters and cut. The sample sole was moulded (**Fig. 47**).

Fig. 47. Sample sole having white inserts with formulation shown in **Table 15**.

IR spectrum was also performed in this case (**Fig. 48**).

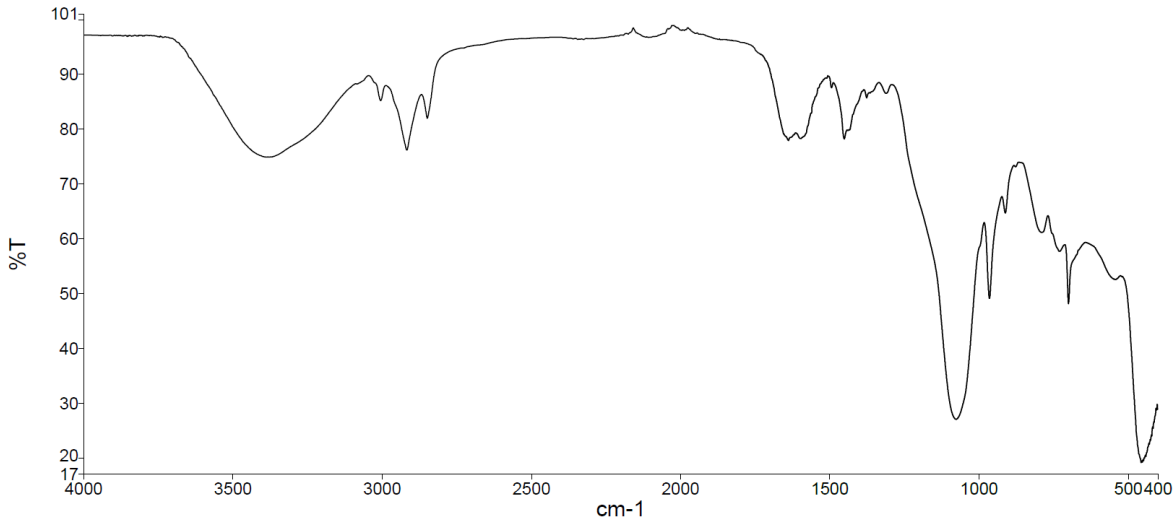

Fig. 48. IR spectrum of white inserts with formulation shown in **Table 15**.

The typical band due to the Si-O moiety can be observed at 1080 cm^{-1}, but it is not as large as in the previous case. The slip resistance test was performed with the method described in the past sections and the values are reported in **Table 16**.

Part of the sole analysed	Limit	Result
Forward heel	> 0,28	0,40
Forward flat	> 0,32	0,45

Table 16. Slip resistance values of sole in **Fig. 47**.

Slip resistant test shows the bounty of the fibre glass system. In order to study deeply the surface of the sole and the inserts, also in this case SEM images were recorded (**Fig. 49**). SEM images show a more uniform distribution of glass fibres in the rubber matrix. The absence of natural fibres led to a better compounding situation. In addition, the breaking of the fibres while touching the ground increases friction and, consequently, slip resistance, which is much higher with respect to glass spheres.

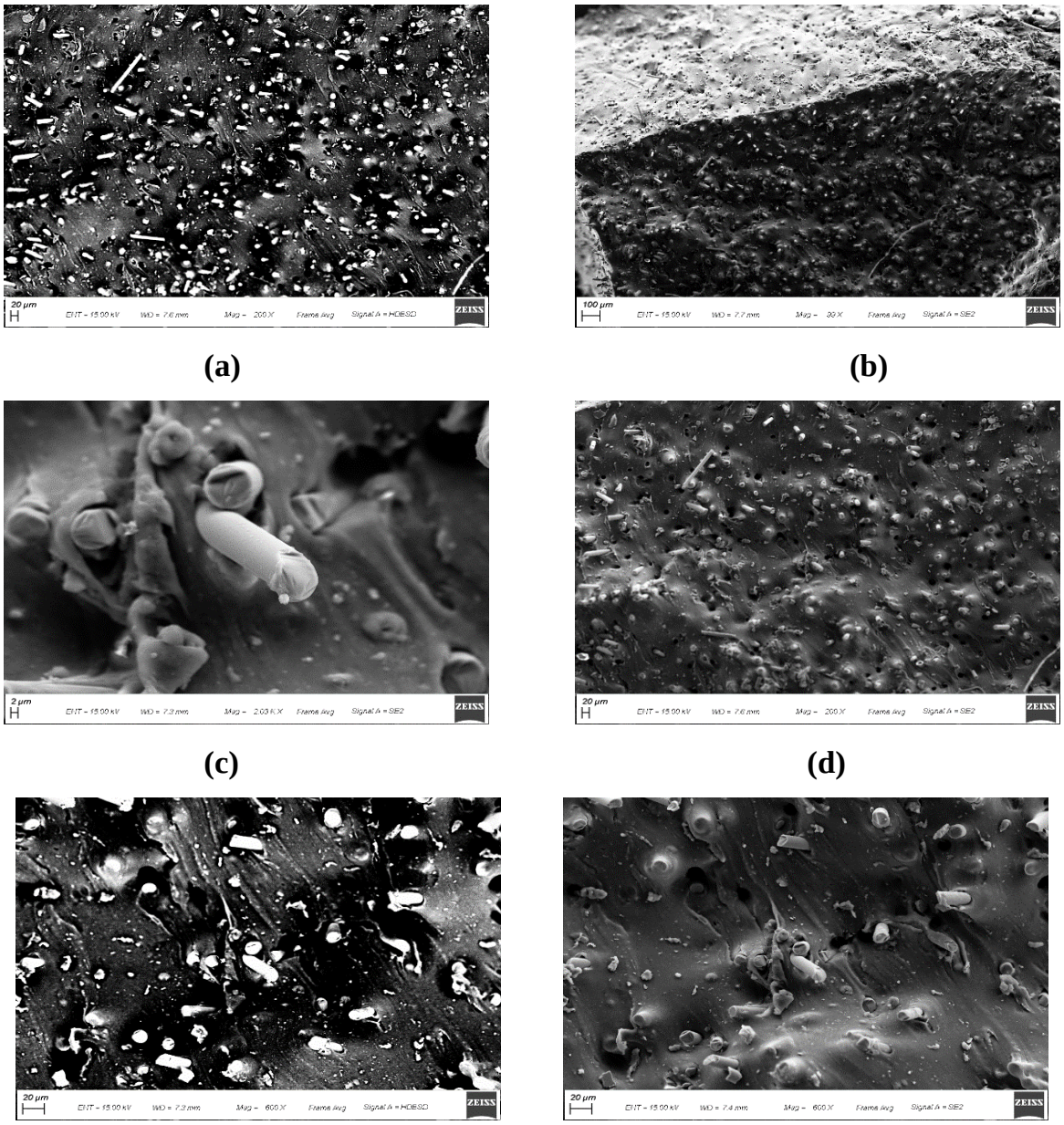

(a) **(b)**

(c) **(d)**

(e) **(f)**

Fig. 49. SEM images recorded at different magnification: (a) 30x, (b) 200x, (c) 200x, (d) 2.03kx, (e) 600x, (f) 600x.

8.3.4 Conclusion

The improvement of Fibregrip® system has been done by substituting, in the first trial, part of natural fibres with glass spheres and, in the second one, by using only glass fibres. With the second approach higher slip resistance values have been obtained: the better distribution of fibre glass is one of the main reasons for this result. This concept can be applied to safety shoes, as seen in **Figures 44** and **47**. The next step is trying to avoid the use of any external reinforcing agent (except silica and silane) to obtain slip resistant values comparable to the

fibre glass system. This can be obtained by studying different combination of polymer compounds. The development of this new formulation could be suitable for other applications (sport or fashion).

8.4 Oil-resistant rubber formulation for military outsoles

Military outsoles require very specific and performing rubber compound. The development of these elastomeric material must consider several aspects like electronic parameters (electronic resistance) and oil resistance (resistance to common solvents and oils) in addition to all the other physical-mechanical properties. The common specifications are reported in **Table 17**.

Properties	Normative	U.M.	Values
Density	ISO 2781	g/cm^3	1.150-1.250
Abrasion Resistance	ISO 4649	mm^3	< 120
Hardness	ISO 868	ShA	64-68
Elongation at break	ISO 37-1	%	> 450
Breaking Strength	ISO 37-1	N/mm^2	> 14
Electric Resistance	ISO 2878	MOhm	0.1-100
Tear Resistance	ISO 34-1	N/mm	> 12
Oil Resistance	EN 20344 p. 8.6.1	%	< 2

Table 17. Common specifications for military soles.

Oil resistance is the most important parameter and the most difficult to reach in this context. The aim of the work described in this section was formulating a compound with properties described in **Table 17** starting from a standard oil-resistant formulation.

8.4.1 Properties of a standard anti-oil compound

The standard anti-oil formulation is reported in **Table 18**.

The physical mechanical values related to this material are reported in **Table 19**.

Ingredients	Quantity (phr)
Standard-grade NBR	87%
NR	10%
Master	3%
Silica and silane	38
Compounding agents	10.3
Accelerants	1.1
Sulphur	2

Table 18. Formulation of a standard oil-resistant rubber compound.

Properties	U.M.	Values	Results
Density	g/cm^3	1.150-1.250	1.155
Abrasion Resistance	mm^3	< 120	100
Hardness	ShA	64-68	67
Elongation at break	%	> 450	550
Breaking Strength	N/mm^2	> 14	15.2
Electric Resistance	MOhm	0.1-100	55
Tear Resistance	N/mm	> 12	13
Oil Resistance	%	< 2	**5.1**

Table 19. Physical-mechanical values for standard anti-oil compound.

Considering **Table 19**, the standard-grade NBR is not sufficient to guarantee an adequate oil resistance value, which is almost two times higher than the specification limit. The other parameters show the bounty of the compound but, considering the results, it could be suitable for other types of products like safety soles. Starting from this point, a new formulation was developed maintaining the physical properties of the standard compound but improving the oil resistance parameter.

8.4.2 New oil-resistant rubber compound

Modifications were made on the combination of the starting polymers: firstly, NBR was considered. The standard nitrile rubber, as previously said, is not sufficient for the oil

resistance parameter. The critical factor on NBR material is acrylonitrile content: it is one of the most important values that influence mechanical and tribological properties of NBR-based formulation.[89,90] The NBR acrylonitrile content for the rubber used in standard formulation is 30%: this type of elastomeric compound is known as “Medium-nitrile”. Considering the oil resistant values, nitrile rubber having a high AN content is ideal for formulations because there is a direct relationship between AN content and solubility in organic solvent: higher is the acrylonitrile content, lower is the solubility and, as a consequence, the increase in volume is lower. In this case, the standard NBR was substituted by a NBR compound with a 43% AN content. Secondly, the natural rubber was substituted by epoxidized natural rubber. NR has a low oil resistance: the insertion of epoxide functionalities has a dual effect: it increases the oil resistance of the compound and other important physical values. The third modification was made on the colours ingredients. Rubber formulations may have different colours, depending on the colour used in compounding step. Usually, colour can be added to formulation in different ways (powder, EVA-supported pigment or colour master).

Ingredients	**Quantity (phr)**
NBR (40% AN)	90%
Epoxidized NR	10%
Pure colour	3
Silica and silane	38
Compounding agents	10.3
Accelerants	11
Sulphur	2

Table 20. New oil-resistant formulation.

Each of the possibilities has disadvantages: colour powder can be lost in the internal chamber of the mixer, EVA supported colours may not be fully dissolved in rubber matrix and colour master, which is formed in a pre-defined ratio of rubber: colour may contain some ingredients that can lower the performance of the compound. In the standard NBR-formulation, a black master colour was used: the main problem associated with it could be the presence of processing oils used as ingredients of the material or present in the rubber starting material

(for example: oil-extended SBR). In this case, pure colour is used. The formulation of the new compound is shown in **Table 20**.

The elastomeric material was masticated in the internal mixer for two mins because the high AN content makes it harder. The other ingredients were added after the mastication step. The pure colour was distributed uniformly over the rubber compound. Physical-mechanical analyses were performed and the results are shown in **Table 21**.

Properties	**U.M.**	**Values**	**Results**
Density	g/cm^3	1.150-1.250	1.167
Abrasion Resistance	mm^3	< 120	84
Hardness	ShA	64-68	68
Elongation at break	%	> 450	510
Breaking Strength	N/mm^2	> 14	15.4
Electric Resistance	MOhm	0,1-100	40
Tear Resistance	N/mm	> 12	16
Oil Resistance	%	< 2	**0.48**

Table 21. Physical-mechanical values for new anti-oil compound.

Oil resistance values, in this case, are ten time lower than standard NBR formulation one and it is optimal for military application. Hardness and density are higher due to the presence of high-content NBR rubber. The use of epoxidized NR increases abrasion resistance but the compound loses something in elongation value. A production scale test was made starting from these good values. Two types of colours with the new formulation were made. The soles were moulded by compression with the presence of a textile called felt. The characteristic of this textile material is reported on **Table 22**.

Properties	M.U.	Values
Composition	%	60 polyester 40 Polyamide
Area Weight	gm^{-2}	400±10
Thickness	mm	2.3±0.3
Density	gcm^{-3}	0.17
Max change of dimensions at 110°C	/	<1
Temperature resistance (Continuous)	°C	110
Temperature resistance (Peaks)	°C	115

Table 22. Felt characteristics.

The textile is applied for two reasons: firstly, it is necessary for producing shoes with upper PU injection method and, secondly, it is used in order to avoid the combination of halogenation/adhesive application processes, which, as previously said, can be problematic if the soles are not use in a short time. **Fig. 50** shows the sample soles.

(a) **(b)**

Fig. 50. Sample soles with new anti-oil formulation: (a) black and sand version, (b) upper surface with felt.

Oil and abrasion resistance are the main interesting parameters. The main differences in performing test between plates and soles are the different design of the surfaces (linear for

plates, discontinuous for soles) and the different thickness of the samples. In **Table 23** test results are reported.

Sample	Limit	Abrasion resistance (mm^3)	Limit	Oil resistance (%)
Black (42)	<100 mm^3	95.1	< 2%	-0.44
Sand (42)	<100 mm^3	93.2	< 2%	0.94

Table 23. Soles test results.

The presence of felt does not influence in a significant way the oil resistance value: for sand version, which is also made using TiO_2 as colouring agent, the volume of the sample increases 0.94 % which is under the specification. However, the negative value for black version highlights the shrinkage of the volume of the sample. Considering abrasion resistance, the testing results are under the specification indicating that the design surface is not a critical factor in this situation.

8.4.3 Conclusion

A more performing oil-resisting compound has been developed and its physical-mechanical characteristics have been evaluated. The use of a 43% AN-content NBR, pure colour and epoxidized-NR are useful for improving and obtaining interesting oil-resistance values. A production scale test was also performed with the use of an external textile (felt). Black and sand soles with the improved formulation were printed. The abrasion and oil resistance were evaluated: the results showed the quality of the compound and the fact that this type of soles is suitable for military applications.

9. Synthesis of new imidalozium trihydridoborate and triphenylborate species

The second part of this PhD thesis describes the work on the synthesis of new imidalozium trihydridoborate and triphenylborate species made in Prof. Santini and Pellei's research group. They are NHC-derivatives (N-Heterocyclic Carbenes) and have gained growing attention in numerous chemistry applications, such as catalysis and medicinal chemistry.[91-100] Another important feature of this class of compounds is their use in material chemistry as polymerization catalysts and, mainly, as ionic liquids.[101]

9.1 N-Heterocyclic Carbenes

N-Heterocyclic carbenes (NHCs) have attracted growing attention in the past two decades and their chemistry have been increasingly studied and understood. The main advantages are their applicability and versability. The first applications were introduced almost in the beginning of XX century by the work of Tschugajeff's research group.[102] Only three decades ago, NHCs have been characterised as a class of compounds by, firstly, Arduengo's work and, secondly, by the huge research effort in their activity as promising ligands for homogeneous catalysis.[103,104] Most NHCs are based on five-membered heterocyclic moieties such as are imidazole and imidazoline derivatives. Nowadays, a correct and standard representation is not fully recognized and thus, different versions are found in literature: however, the most accurate one displays the charges.[105] According to Molecular Orbitals theory, NHCs are σ-basic/π*-acids ligands: they have a lone electron pair in a high σ orbital which gives them a higher σ-donicity (basicity) compared to the one of phosphines.[106,107] The presence of an empty low-energetic π*orbital is fundamental for this property because it gives NHCs the electron-acceptor character. This is important because it can accept the electrons from filled d orbitals of the metals in d→ π* back donation process.[108] In the presence of an electron-deficient metal, this class of compounds can also show π→d donation.[109] In recent years, two important features must be added in addition to the previous facts: the first one is the NHCs capability of accepting electron density from the metals into π* orbitals, while the second one is the π-donor behaviour towards electron poor metals.[110,111] The electronic properties of N-heterocyclic carbenes can be tailored by different means:

1. changing N-substituent groups;
2. considering NHC skeleton;
3. changing the substituents on C atoms of the NHC skeleton.

The steric effect on NHCs is one of critical aspects to be considered: however, differently from phosphines, they present a local C2 symmetry axis. As a consequence, the Tolman cone angle cannot be employed for NHC ligands.[112] An useful value has been introduced to solve the problem: it is called "percent buried volume" (%VBur) and it describes the fraction of the volume of the first coordination sphere around the metal occupied by a certain ligand.[113]

9.2 NHCs synthetic routes

The synthetic procedures shown in **Scheme 18** can be generally applied for NHC-based derivatives:

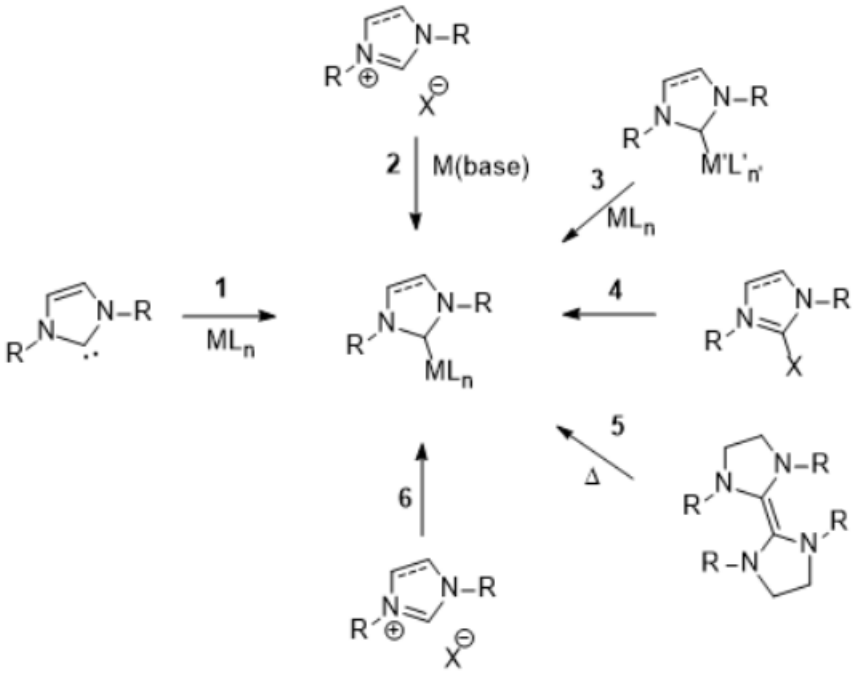

Scheme 18. NHCs synthetic routes.

Reaction 1 is based on the generation of a free carbene by different means from the respective NHC precursor and on the successive coordination to a metal centre while, in **reaction 2**, the base deprotonates the imidazole(idin)ium salt and, as a result, the counter-anion of the salt and NHC are coordinated. In **reaction 3**, a carbene transfer regent is the responsible for the delivering of the NHC to the second metal by transmetallation process. **Route 5** describes the

formation of NHCs by imidazolidinylidene complexes formed by C=C bond activation of the dimerised imidazolidiylidene. The last two reactions, **4** and **6**, are less common and they represent C-X or C-H bond activation through an oxidative addition.[24,25]

9.3 N-Heterocyclic Carbenes Borate anions

As previously said, NHCs based on imidazole-2-ylidene and imidazoline-2-ylidene have been synthesized and reported in literature.[116] These NHCs derivatives are characterized by the presence of only organic substituents attached to nitrogen. Substitution of one of these nitrogen substituents by borane led to generation of carbene borate anions NHC-BR_3^- which are anionic analogues of neutral imidazole-2-ylidenes (**Fig. 51**):

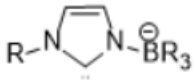

Fig. 51. Carbene Borate anions NHC-BR_3^-.

In **Fig. 51** R can be an aryl or an alkyl functional group. The deprotonation reaction of imidazolium-borate or imidazole-borane with butyllithium forms carbene-borate anions NHC-BH_3^-, as reported by Siebert's research group (**Fig. 52**): [117]

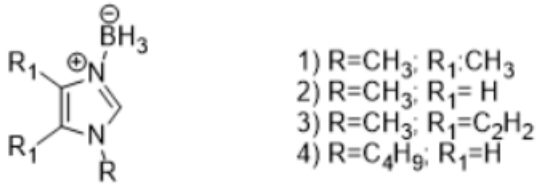

Fig. 52. Imidazolium tryhydroborate species.

The nucleophilicity of the compound is necessary for the synthesis of anionic iron derivatives using as starting material $Fe(CO)_5$: the same considerations can be made using as reagent $BrMn(CO)_5$ but, in this case, a neutral manganese complex is obtained.[118] In literature, dianinionic chelating dicarbene-diborane ligands syntheses have also been reported: they are based on the reaction of borane and triethylborane-based bis(imidazoyl) compounds and BuLi.[119] Considering deprotonation reactions, some processes like isomerization to the 2-borate imidazole forms by 1,2-BR_3 migration, dimerization or intramolecular addition/elimination don't have the same probability to happen.[120-122] The formation of

isomers is the main result derived from the various efforts of deprotonation reactions of different imidazoles and benzimidazoles because of the ring closure caused by rapid intramolecular nucleophilic aromatic substitution.[123] Additionally, Contreas's work describes the imidazoboles synthesis by H_2 elimination from (N-alkylimidazolium)borate species with iodine at high temperature.[124] Other examples of imidazoboles are reported by Liu.[120] A special attention is given to functionalized imidazole-based NHCs due to their versatility in tuning properties and environment at coordinated metal. The employment of anionic NHC-borates is still not relevant compared to the use of examples showing coordination of chelate and pincer NHC ligands.[125] Fehlhammer's work primarily described the synthesis of tris(3-methylimidazolin-2-ylidene-1-yl)borate with the topology of Trofimenko's scorpionates, where BH groups connect the carbene unitis.[126] In the last decade, Santini and Pellei's research group developed new several complexes of coinage metals NHCs from different precursors, like $[HB(RImH)_3]Br_2$ (being R Benzyl, Mesityl and t-Butyl), $[H_2N(HTz^{Bn})_2]Br$, $H_2C(Him^R)2$ and $H_2C(HTz^R)_2$ (being Him: imidazole, HTz: 1,2,4-triazole, R= $(CH_2)_2COO^-$ or $(CH_2)_3SO_2^-$).[127-129] It's important to point out that mono(azoyl)borate compounds have not been studied in the same manner of the respective parent poly(azoyl)borates.[130,131]

9.4 Characterization and experimental data

9.4.1 Materials and general methods

All syntheses and handling were carried out under an atmosphere of dry oxygen-free dinitrogen, using standard Schlenk techniques or a glove box. Glassware was dried with a heat-gun under high vacuum. Solvents were purchased from commercial sources and purified by conventional methods prior to use. Elemental analyses (C, H, N, and S) were performed with a Fisons Instruments EA-1108 CHNS-O Elemental Analyzer (Thermo Fisher Scientific Inc., Waltham, MA, USA). Melting points were taken on an SMP3 Stuart Scientific Instrument (Bibby Sterilin Ltd., London, UK). IR spectra were recorded from 4000 to 400 cm^{-1} on a PerkinElmer Frontier FT-IR instrument (Perkin Elmer Inc., Waltham, MA, USA), equipped with single reflection universal diamond ATR top-plate. IR annotations used were as follows: br = broad, m = medium, mbr = medium broad, s = strong, sbr = strong broad, sh = shoulder, vs = very strong, w = weak, wbr = weak broad. ^{1}H-, ^{13}C-, and ^{11}B-NMR spectra were recorded with an Oxford AS400 Varian spectrometer (400.4 MHz for ^{1}H, 100.1 MHz

for ^{13}C, and 128.4 MHz for ^{11}B) (Oxford Instruments, MA, USA) or with a 500 Bruker Ascend (500.1 MHz for 1H, 125 MHz for ^{13}C, and 160.5 MHz for ^{11}B) (Bruker BioSpin Corporation, 15 Fortune Drive, Billerica, MA, USA). Referencing was relative to tetramethylsilane (TMS) (^{1}H and ^{13}C) and BF_3•Et_2O (^{11}B). NMR annotations used were as follows: br = broad; d = doublet, m = multiplet, s = singlet. Syntheses under microwave irradiation were performed by means of a Flexible Microwave Platform FlexSynth Milestone apparatus (Milestone Srl, Via Fatebenefratelli, Sorisole (BG), Italy). The reactions were performed in a 100-mL PTFE vessel, sealed using a Teflon crimp top. Electrospray mass spectra (ESI-MS) were obtained in positive- (ESI(+)MS) or negative-ion (ESI(-)MS) mode on an Agilent Technologies Series 1100 LC/MSD Mass Spectrometer (Agilent Technologies Inc, Santa Clara, CA, USA), using a methanol or acetonitrile mobile phase. The compounds were added to reagent grade methanol to give approximately 0.1 mM solutions, injected (1 µL) into the spectrometer via a Hewlett Packard 1090 Series II UV-Visible HPLC system (Agilent Technologies Inc, Santa Clara, CA, USA) fitted with an autosampler. The pump delivered the solutions to the mass spectrometer source at a flow rate of 300 mL min^{-1}, and nitrogen was employed both as a drying and nebulizing gas. Capillary voltages were typically 4000 and 3500 V for the ESI(+)MS and ESI(-)MS modes, respectively. Confirmation of all major species in this ESI-MS study was supported by comparison of the observed and predicted isotope distribution patterns, the latter calculated using the IsoPro 3.1 computer program (T-Tech Inc., Norcross, GA, USA). 1-Benzylimidazole, 1-methylimidazole, BH_3•THF complex, ammonium tetraphenylborate and silver oxide were purchased from Sigma-Aldrich (Merck Life Science S.r.l., Via Monte Rosa, Milano, Italy). The 1-mesitylimidazole was synthesized in accordance with the literature method.[132]

9.4.2 Synthesis of (HIm^{Bn})BH_3 (1)

1-Benzylimidazole (1.840 g, 11.631 mmol) was dissolved in dry THF (50 mL) under N_2 atmosphere and BH_3•THF complex (12.0 mL, 1M) was added drop by drop. The reaction mixture was stirred at room temperature for 24 h. Then, the volatiles were removed under reduced pressure to give a colourless oil. It was re-crystallized by $CHCl_3$/diethyl ether/n-hexane (1/3/3) solution to obtain a white precipitate; it was filtered, washed with diethyl ether, and dried under reduced pressure to give **1** in 80% yield (1.601 g). Single crystals of **1** suitable

for X-ray analysis were obtained by slow evaporation of a $CHCl_3$ solution of **1**. Melting point: 92-94 °C. IR (cm^{-1}): 3159w, 3135m, 3061w, 3038w (C-H); 2352m, 2297m, 2255m (B-H); 1540m, 1533m (C=C/C=N). ^{1}H-NMR ($CDCl_3$, 293 K): δ 2.2 (br, 3H, BH_3), 5.13 (s, 2H, CH_2Ph), 6.91 (s, 1H, 4-CH or 5-CH), 7.14 (s, 1H, 4-CH or 5-CH), 7.23–7.44 (m, 5H, C_6H_5), 7.79 (s, 1H, 2-CH). ^{1}H-NMR (CD_3OD, 293 K): δ 2.2 (qbr, 3H, BH_3), 5.24 (s, 2H, CH_2Ph), 7,03 (s, 1H, 4-CH or 5-CH), 7.19 (s, 1H, 4-CH or 5-CH), 7.26-7.43 (m, 5H, C_6H5), 8.13 (s, 1H, 2-CH). ^{13}C{^{1}H}-NMR ($CDCl_3$, 293 K): δ 52.35 (CH_2Ph), 119.94, 127.98, 128.21, 129.33, 129.47, 133.46 (CH), 136.33 (2-CH). ^{11}B{^{1}H}-NMR ($CDCl_3$, 293 K): δ - 19.38 (s, BH_3). ^{11}B-NMR ($CDCl_3$, 293 K): δ - 19.38 (q, BH_3, J_{B-H} = 96 Hz). ESI-MS(+) (major positive-ions, CH_3OH), *m/z* (%): 159 (40) $[HIm^{Bn} + H]^+$, 181 (40) $[HIm^{Bn} + Na]^+$, 195 (90) $[(HIm^{Bn})BH_3 + Na]^+$, 329 (100) $[(HIm^{Bn})_2BH_2]^+$. Anal. Calcd. for $C_{10}H_{13}BN_2$: C 69.82, H 7.62, N 16.28%. Found: C 69.52, H 7.30, N 15.91%.

9.4.3 Synthesis of $(HIm^{Mes})BH_3$ (2)

1-mesityl-imidazole (0.930 g, 5.000 mmol) was dissolved in dry THF (30 mL) under N_2 atmosphere and BH_3•THF complex (5.2 mL, 1M) was added drop by drop. The reaction mixture was stirred at room temperature for 24 h. Then, the volatiles were removed under reduced pressure to give a brown oil. It was re-crystallized by $CHCl_3$/diethyl ether/n-hexane (1/3/3) solution to obtain a brown precipitate; it was filtered, washed with diethyl ether, and dried under reduced pressure to give **2** in 68% yield (0.680 g). Single crystals of **2** suitable for X-ray analysis were obtained by slow evaporation of a $CHCl_3$/THF solution of **2**. Melting point: 109-111 °C. FT-IR (cm^{-1}): 3177w, 3155w, 3132w, 3061w, 3028w (C-H); 2374m, 2338m, 2323m, 2300m, 2259m (B-H); 1526s (C=C/C=N). ^{1}H-NMR ($CDCl_3$, 293 K): δ 2.03 (s, 6H, CH_3^{Mes}), 2.3 (br, 3H, BH3), 2.37 (s, 3H, CH_3^{Mes}), 6.90 (s, 1H, 4-CH or 5-CH), 7.02 (s, 2H, CH^{Mes}), 7.31 (s, 1H, 4-CH or 5-CH), 7.75 (s, 1H, 2-CH). ^{1}H-NMR (CD_3OD, 293 K): δ 2.04 (s, 6H, CH_3^{Mes}), 2.1 (br, 3H, BH_3), 2.35 (s, 3H, CH_3^{Mes}), 7.08 (s, 2H, CH^{Mes}), 7.23 (s, 1H, 4-CH or 5-CH), 7.25 (s, 1H, 4-CH or 5-CH), 8.14 (s, 1H, 2-CH). ^{13}C{^{1}H}-NMR ($CDCl_3$, 293 K): δ 17.33, 21.06 (CH_3^{Mes}), 121.25, 128.12, 129.49, 131.71, 134.86, 136.85 (CH), 140.34 (2-CH). ^{11}B-NMR (CDCl3, 293 K): δ - 19.21 (dbr, BH_3). ESI-MS(+) (major positive-ions, CH_3OH), *m/z* (%): 187 (15) $[HIm^{Mes} + H]^+$, 223 (55) $[(HIm^{Mes})BH_3 + Na]^+$, 385 (100)

$[(HIm^{Mes})_2BH_2]^+$. Anal. Calcd. for $C_{12}H_{17}BN_2$: C 72.03, H 8.56, N 14.00%; found: C 71.81, H 8.25, N 13.60%.

9.4.4 Synthesis of $(HIm^{CH3})BPh_3$ (3)

A large excess of 1-methylimidazole (0.603 g, 7.344 mmol) was dissolved in acetonitrile (CH_3CN, 60 mL). Then, ammonium tetraphenylborate (NH_4BPh_4, 1.770 g, 5.248 mmol) was added to the solution. A white precipitate was formed, but the solution became limpid after 1 h. The reaction proceeded for 70 h at reflux under magnetic stirring. At the end, the solution was dried at reduced pressure, obtaining a white solid. Et_2O was added to the round-bottom flask to purify the residue from the starting materials that did not react. The resulting suspension was filtered, dried under reduced pressure, and further purified with $CHCl_3$ to precipitate the excess of NH_4BPh_4. The mixture was filtered and the mother liquors were dried at reduced pressure to give the white ligand $(HIm^{CH3})BPh_3$ (**3**) in 76% yield (1.293 g). Melting point: 209-212 °C. FT-IR (cm^{-1}): 3158w, 3133m, 3085w, 3064m, 3054mbr, 3010mbr (C-H); 1546m, 1531m, 1483mbr (C=C/C=N). ^{1}H-NMR (DMSO-*d*$_6$, 293 K): δ 3.79 (s, 3H, NCH_3), 6.90 (d, 1H, 4-CH or 5-CH), 7.03–7.15 (m, 15H, CH), 7.44 (d, 1H, 4-CH or 5-CH), 8.09 (s, 1H, 2-CH). ^{13}C{^{1}H}-NMR (DMSO-*d*$_6$, 293 K): δ 35.13 (NCH_3), 122.34, 124.85, 126.42, 127.02, 134.49, 138.58 (CH). ^{11}B-NMR (Acetone-*d*$_6$, 293 K): δ - 6.52 (s, BPh_3). ESI-MS(+) (major positive ions, CH_3CN), *m/z* (%): 83 (100) $[HIm^{CH3} + H]+$, 247 (25) $[(HIm^{CH3})BPh_2]^+$. Anal. Calcd. for $C_{22}H_{21}BN_2$: C 81.50, H 6.53, N 8.64; found: C 81.14, H 6.56, N 8.38%.

9.4.5 Synthesis of $(HIm^{Bn})BPh_3$ (4)

A large excess of 1-benzylimidazole (0.633 g, 4.000 mmol) was dissolved in CH_3CN (60 mL). Then, NH_4BPh_4 (0.961 g, 2.850 mmol) was added to the solution. A white precipitate was formed, but the solution became limpid after 1 h. The reaction proceeded for 70 h at reflux under magnetic stirring. At the end, the solution was dried at reduced pressure, obtaining a white solid. EtOH was added to the round-bottom flask to purify the residue from the starting materials that did not react. The resulting suspension was filtered and dried at reduced pressure to give the white ligand $(HIm^{Bn})BPh_3$ (**4**) in 50% yield (0.570 g). Melting point: 175-178 °C. FT-IR (cm^{-1}): 3163m, 3140m, 3125m, 3064mbr, 3023m (C-H); 1531mbr, 1506m, 1489mbr (C=C/C=N). ^{1}H-NMR (DMSO-*d*$_6$, 293 K): δ 5.39 (s, 2H, CH_2Ph), 6.91 (s,

1H, 4-CH or 5-CH), 7.04-7.43 (m, 20H, C_6H_5), 7.49 (s, 1H, 4-CH or 5-CH), 8.37 (s, 1H, 2-CH). $^{13}C\{^1H\}$-NMR (DMSO-d_6, 293 K): δ 51.24 (CH_2Ph), 121.25, 124.90, 127.23, 128.21, 129.33, 129.47, 133.46 (CH), 136.33 (2-CH). ^{11}B-NMR ($CDCl_3$, 293 K): δ - 6.37 (s, BPh_3). ESI-MS(+) (major positive ions, CH_3CN), *m/z* (%): 91 (80) $[C_7H_7]^+$, 159 (100) $[HIm^{Bn} + H]^+$, 242 (50) $[BPh_3 + H]^+$, 481 (45) $[(Im^{Bn})_2BPh_2]^+$. Anal. Calcd. for $C_{28}H_{25}BN_2$: C 84.01, H 6.29, N 7.00; found: C 83.72, H 6.03, N 7.06%.

9.4.6 Synthesis of $(Im^{Bn}BPh_2)_2$ (5)

In a 100-mL PTFE vessel equipped with a magnetic stir bar, Compound **4** (0.360 g, 0.900 mmol), silver oxide (Ag_2O, 0.104 g, 0.450 mmol), and CH_3CN (25 mL) were added. The reaction mixture was heated in the microwave reactor following a pre-set heating ramp, up to 80 °C. Once the temperature was reached, the reaction proceeded for 1 h and then it was cooled following a pre-set cooling ramp, to room temperature. All the steps were performed always under magnetic stirring. At the end, the mixture was filtered and the obtained mother liquors were dried at reduced pressure to give the oily brownish residue $(Im^{Bn}BPh_2)_2$ (**5**) in 54% yield (0.157 g). FT-IR (cm^{-1}): 3161m, 3143m, 3113sh, 3087m, 3064m, 3038m, 3024m, 3010m, 2999m, 2972m, 2938wbr (C-H); 1600m, 1587m, 1571m, 1534s, 1509s, 1496sbr (C=C/C=N). ^1H-NMR (DMSO-d_6, 293 K): δ 5.18 (s, 2H, CH_2), 6.91 (s, 1H, 4-CH or 5-CH), 7.18–7.36 (m, 15H, ArH), 7.77 (s, 1H, 4-CH or 5-CH). ^1H-NMR ($CDCl_3$, 293 K): δ 5.13 (s, 2H, CH_2), 6.92 (s, 1H, 4-CH or 5-CH), 7.11-7.44 (m, 15H, ArH), 7.67 (s, 1H, 4-CH or 5-CH). $^{13}C\{^1H\}$-NMR (DMSO-d_6, 293 K): δ 50.04 (CH_2Ph), 120.14, 127.98, 128.28, 128.79, 128.94, 129.17, 130.56, 134.47 (CH), 159.18 (2-C). ^{11}B-NMR (DMSO-d_6, 293 K): δ 1.43 (s). ESI-MS(+) (major positive ions, CH_3CN), *m/z* (%): 91 (95) $[C_7H_7]^+$, 159 (100) $[HIm^{Bn} + H]^+$. Elemental analysis for $C_{44}H_{38}B_2N_4$ (%): calculated: H 5.94, C 82.01, N 8.69; found: H 6.04, C 81.27, N 8.89%.

9.4.7 Crystallographic Data Collection and Refinement

A suitable crystal covered with a layer of hydrocarbon/Paratone-N oil was selected and mounted on a Cryo-loop and immediately placed in the low temperature nitrogen stream. X-ray intensity data were measured at 100(2) K on a Bruker SMART APEX II CCD area detector system equipped with an Oxford Cryosystems 700 series cooler, a graphite

monochromator, and a Mo Kα fine-focus sealed tube (λ = 0.71073 Å). Intensity data were processed using the Bruker ApexII program suite. Absorption corrections were applied by using SADABS. Initial atomic positions were located by direct methods using XS, and the structures of the compounds were refined by the least-squares method using SHELXL.[133] All the non-hydrogen atoms were refined anisotropically. The hydrogen atoms attached to boron (B-H) were located in difference Fourier maps, included and refined freely with isotropic displacement parameters. All the other hydrogen atoms were placed at calculated positions and refined using a riding model. X-ray structural figures were generated using Olex2.[134] The CCDC 2010217-2010218 contain the supplementary crystallographic data. These data can be obtained free of charge via http://www.ccdc.cam.ac.uk/conts/retrieving.html or from the Cambridge Crystallographic Data Centre (CCDC), 12 Union Road, Cambridge, CB2 1EZ, UK).

9.5 Synthesis of N-(alkyl/aryl)imidazolium)borate-based systems

The aim of the research work described in this section is the synthesis of (N-(alkyl/aryl)imidazolium)borate-based systems and the study of their function as carbene precursors for the synthesis of N-heterocyclic carbenes-silver(I) complexes. **Schemes 19** and **20** show the two different one step synthesis of N-(alkyl/aryl) imidazolium borate adducts **1-4**:

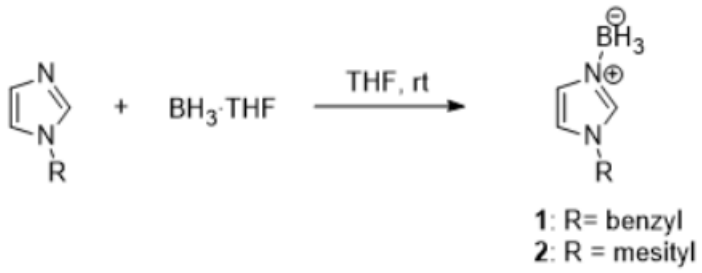

Scheme 19. Synthesis of precursors 1-2.

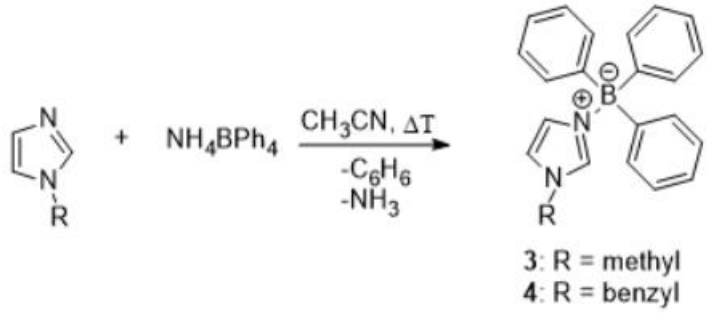

Scheme 20. Synthesis of precursors 3-4.

The colourless imidazolium-borate derivatives **1** and **2** have been synthesized by the reaction of one equivalent of BH_3•THF and a solution of N-benzyl- or N-mesitylimidazole in nearly quantitative yields. Imidazolium trihydridoborates **1** and **2** are, respectively, white and brown solids and soluble in common organic solvents (CH_3OH, $CHCl_3$, CH_2Cl_2, THF, DMSO and acetone). Adducts **3** and **4** are prepared by reaction of an acetonitrile solution of N-methyl- or N-benzylimidazole and ammonium tetraphenylborate under reflux conditions. In these conditions, it is commonly known that triphenylboranes are produced by the instability of the tetraphenylborate anion; additionally, if heating with alkylammonium salts, they can lose a phenyl ring and successively form a nitrogen-borum bond with the ammonium compound.[130,131] In this study, a similar situation happens: the by-products of reaction in **Scheme 20** are volatile benzene and ammonia and the formation of adduct **4** is achieved in good yield. Derivatives **3** and **4** are white solids and they are soluble in THF, CH_2Cl_2, $CHCl_3$, CH_3CN, DMSO and acetone. Several analytical techniques (CHN analysis, ^{1}H-NMR, ^{13}C-NMR, ^{11}B-NMR, FT-IR spectroscopy and ESI-MS) confirmed the authenticity of the four precursors. By dissolution of the crude compounds **1** and **2** in chloroform, single crystals suitable for X-rays diffraction analysis were obtained. **Fig. 53** and **Fig. 54** show crystalline structures for adducts **1** and **2**, respectively.

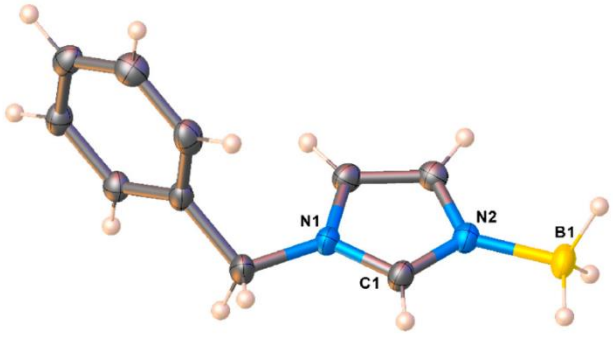

Fig. 53. Molecular structure of $(HIm^{Bn})BH_3$ (**1**).

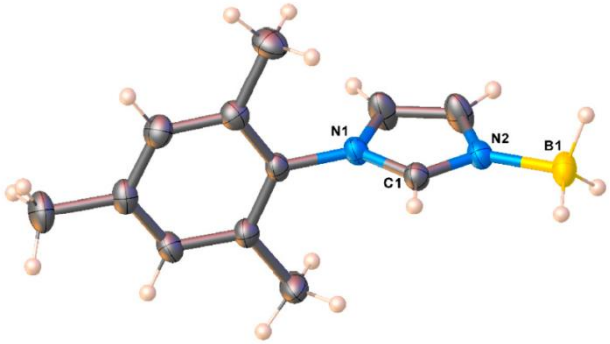

Fig. 54. Molecular structure of (Him^{Mes})BH_3 (**2**).

Precursor **1**, (HIm^{Bn})BH_3 (**Fig. 53**), crystallizes in the Orthorhombic $P2_12_12_1$ space group; it is monomeric at solid state and C1-N1 distance is slightly higher than C1-N2 one (1.343 Å compared to 1.323 Å). Interesting selected bond distances (Å) and angles (°) are: N1-C1 1.343(2), N2-C1 1.323(2), N2-B1 1.587(2), N1-C4 1.474(2), N1-C1-N2 110.29(14), C1-N2-B1 126.58(14)

Precursor **2**, (Him^{Mes})BH_3 (**Fig. 54**), crystallizes in the Monoclinic $P2_1/n$ space group with two chemically similar but crystallographically different molecules in the asymmetric unit. Interesting selected bond distances (Å) and angles (°) are: N1-C1 1.3442(14), N2-C1 1.3207(14), N2-B1 1.5836(16), N1-C4 1.4465(14), N1-C1-N2 110.36(10), C1-N2-B1 127.91(10).

There is also a similarity between structural features of **1** and **2**.

The FT-IR spectra of the four adducts show characteristic peaks. The presence of azolyl rings C-H stretchings is present for compounds **1-4** in the range 3010-3177 cm^{-1} while, in compounds **1** and **2**, intense absorptions in the 2255-2374 cm^{-1} region are due to the BH_3 moieties. The ^1H- and ^{13}C-NMR spectra of the four precursors are recorded in different solvents: $CDCl_3$ and CD_3OD for **1** and **2** and DMSO for **3** and **4**. All derivatives show a single set of resonances for imidazolium rings; additionally, considering ^1H-NMR spectra of **1** and **2**, after two days in CD_3OD at room temperature, the signal at the 2-CH position does not show any sign of a reduction in intensity. This fact suggests that there is an absence of fast H-D exchange phenomenon and, as a consequence, lack of deuteration at this position.

For compounds **1** and **2**, the ^{11}B-NMR spectrum, recorded in $CDCl_3$, shows a quartet at δ -19.38 (**1**) and δ -19.21 (**2**): these groups of signals indicate coordination of imidazole rings at

the BH_3 moiety.[135] In compounds **3** and **4**, the presence of the four-coordinated boron center is demonstrated by single broad resonances observed at δ - 6.52 ppm for **3** in $(CD_3)_2CO$ and at δ - 6.37 for **4** in $CDCl_3$. Those data are in according with literature.[136]

Considering the ESI(+)-MS spectra of **1** and **2**, peaks at *m/z* 195 and 223 are ascribed at the molecular species $[(HIm^{Bn})BH_3 + Na]^+$ and $[(HIm^{Mes})BH_3 + Na]^+$, respectively. Additionally, these spectra display the presence of other peaks due to the fragmentation species $[Him^R + H]^+$ and to the aggregates $[(Him^R)BH_2]^+$, being R a benzyl or mesityl group. In a similar manner, the spectra of adducts **3** and **4** show peaks at *m/z* 83 and 159 related to the presence of $[Him^{CH3} + H]^+$ and $[Him^{Bn} + H]^+$ respectively, along with a fragment peak at *m/z* 247 ($[(Him^{CH3})BPh_2]^+$, 25%) and an aggregate peak at *m/z* 481 ($[(Im^{Bn})_2BPh_2]^+$, 45%) in **3** and **4** respectively.

9.6 Reactivity of compounds 1-4 as carbene precursors for NHCs-silver(I) complexes

In order to evaluate the reactivity of adducts **1-4** as carbene precursors, reaction with n-BuLi was performed. However, the result of this reaction with **1-4** always led to decomposition species and not to the desired product (imidazole-2-ylidines). Further reactions with silver oxide using different conditions (temperature: room temperature or reflux; reaction times: 5, 24, 48 and 120 h; solvent: THF, CH_2Cl_2, CH_3OH and CH_3CN) or with silver acetate in CH_3OH or acetonitrile were performed trying to obtain silver carbene complexes: however, all the reactions gave unsatisfactory results, because only mixtures of unreacted or decomposition products were detected. Surprisingly, imidazabole species **5** (**Fig. 55**) was the only partially isolable product of the reaction of **4** with Ag_2O in acetonitrile.

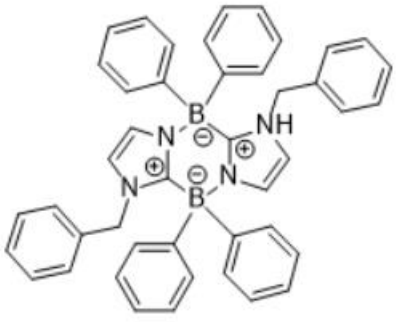

Fig. 55. Imidazabole species **5**, $(Im^{Bn}BPh_2)_2$.

The direct synthesis of imidazaboles can be achieved by using microwave-assisted methods, according to literature.[137] The parameters of this MW method are a pre-set heating ramp of 1 h up to 80°C in technical-grade acetonitrile using silver oxide (**Scheme 21**):

Scheme 21. Microwave-assisted synthesis of **5**.

The formation of the imidazabole $(Im^{Bn}BPh_2)_2$ (**5**) could be ascribed by the abstraction of proton at 2-position of the imidazolium-triphenylborate and the successive bimolecular condensation of the corresponding anions with elimination of two benzene molecules. Taking a deeper look into the structure of **5**, it contains a framework of 1,4-diazonia-2,5-diboratacycklohexa-3,6-diene, which can be also a result of intramolecular a carbene-borate reaction. It is an oil soluble in CH_3OH, acetonitrile and DMSO. The differences between starting material **4** and imidazabole **5** are clear in spectroscopic analyses. In ^{1}H-NMR spectrum of **5** in deuterated DMSO, the diagnostic 2-CH imidazolium signal of **4** at 8,37 ppm disappears upon cyclization. Analogously, in the ^{13}C-NMR spectrum, the 2-*C*H imidazolium signal of **4** at 136.33 ppm was no longer observed in the spectrum of **5** that instead showed a new, albeit poorly intense, 2-C signal at 159.18 ppm indicative of the carbene-borate formation.[138] The ^{11}B-NMR spectrum contains a singlet at δ 1.43. The decreased ^{11}B- NMR nuclear shielding in **5** as compared to 4 (δ^{11}B -6.37) points towards lower delocalization of the positive charge in the imidazabole system.[139] Isomerization to the 2-borate imidazole forms by 1,2-BR_3 migration, intramolecular addition/elimination or dimerization reactions may occur on deprotonation, involving intermediates such as in **Scheme 22**:

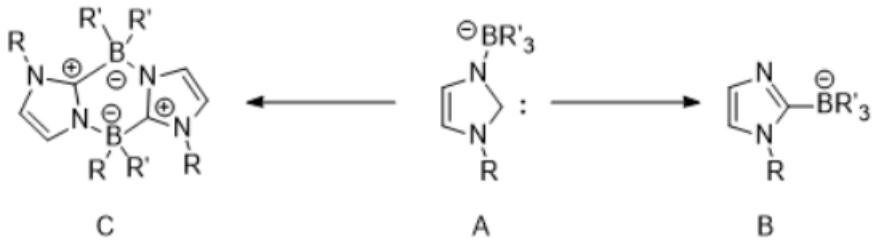

Scheme 22. Rearrangement species (**B** and **C**) by isomerization or dimerization of the NHC-borate form (**A**).

Rearrangement species **B** and **C** may come from isomerization or dimerization of the NHC-borate form **A**. Vagedes's research work suggests that the direct interconversion of such anions by 1,2-migration is rare.[123] In more probably situation, the Lewis acidic borane compensates the negative charge in a more efficient manner when it is bound to the carbon atom instead of the nitrogen atom; however, their interconversion was precluded by a very high barrier of the respective 1,2-BR_3 shift.[123] In particular, for compound **5**, the probably initially generated "anionic Arduengo carbene" product **A** is proved unstable under the reaction conditions and it must be assumed that the rearrangement, experimentally observed to yield species **C**, is likely to have proceeded intermolecularly by two successive nucleophilic substitutions or by radical pathway.[120] As demonstrated in the BR_3-functionalized NHC, the incorporation of anionic borate functionality enhances the donating ability of NHC. However, we must conclude that the N- borato carbene anion A could exhibit its characteristic NHC chemistry when prepared or generated under conditions precluding intermolecular rearrangement pathways to their thermodynamically favored C(2)-borated imidazole isomers or head-to-tail imidazabole dimers.

10. Catalytic studies of Cu(II) complexes in allylic oxidation

This part of the thesis describes catalytic studies of copper(II) catalysts in allylic oxidation, which has high potential for synthetic applications. Kharasch-Sosnovsky reaction is an interesting reaction by which allyl esters can be obtained in high yields, regio- and stereo-selectivity. However, this reaction has some limitations that will be described in the next sections. The aim of this work is the synthesis of new copper(II) complexes, their study as catalysts in Kharasch-Sosnovsky reaction and improvement of reaction parameters for a more sustainable method.

10.1 Introduction

In recent years, research efforts on innovative and catalytic metal complexes for devising functionalized intermediates have been growing. One of the most studied reaction is the allylic oxidation of alkenes.[140-142] This type of reactions allows the synthesis of highly functionalized products, such as carboxylic acids, alcohols, aldehydes, ketones and epoxides, which are useful and important starting materials for industrial applications.[143] The most applied synthetic method for this aim is Kharasch-Sosnovsky reaction, which consists in an allylic oxidation with Cu catalysts and peroxyester oxidant and generates final products with the olefin left intact. The Kharasch-Sosnovsky reaction was firstly introduced in 1958 with increasing research interest (**Scheme 23**):[144-148]

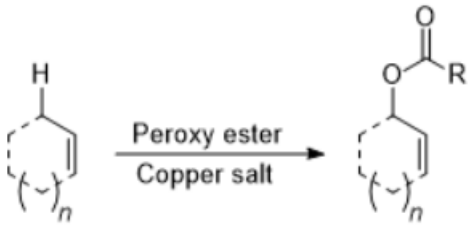

Scheme 23. Kharasch-Sosnovsky reaction.

The main disadvantage of Kharasch-Sosnovsky reaction is the lack of a general approach due to issues like overoxidation, long reaction time, poor compatibility with other functional moieties, superstoichiometric amounts of olefins, regio- and stereo-selectivity. The chemistry of Se, Cr, Pd, Rh and Cu has also been employed in this reaction.[149-152] Copper sources may

be of a different origin, from Cu(I) (CuBr, CuCl, Cu_2O) or Cu(II) salts (CuO, $Cu(OAc)_2$) to more substituted copper complexes. The precise mechanism of the reaction is quite complex because no direct relationship between copper salt and ligand has been discovered.[149,153,154] Copper(II) salts, due to their stability and handling safety, are suitable catalysts for the reaction: however, performing Kharasch-Sosnovsky reaction with Cu(I) complexes gives higher and more reproducible yields than using Cu(II) species, which also need the presence of an external reducing agent, usually phenylhydrazine ($PhNHNH_2$).[155,156]

"Scorpionates" or poly(pyrazoyl)borates ligands were discovered almost sixty years ago by the Trofimenko's pioneering work.[157] Among scorpionates ligands, bis(azol-1-yl)acetate heteroscorpionate ligands, having the general formula $[HC(CO_2H)(az)_2]$ (where az is N-heretocyclic ring),[158,159] have, in recent years, attracted the research interest: a particular aspect is their coordination chemistry towards main group and transition metals which has been deeply studied.[160,161] Among them, the coordination behaviour of complexes containing κ^3N,N,O-scorpionate ligands is interesting because it finds application as metalloenzyme models and in organometallic chemistry.[149,141,162] Additionally, in recent years, the attention and interest in the catalytic activity of these complexes has increased exponentially.[163] Even if few catalytic studies have been carried out, some of them are active catalysts in C-H bond functionalization/activation,[164] ring-closing metathesis,[165] olefin oxidation[166] and polymerization[167,168]. Bis(pyrazol-1-yl)acetates can be also used as starting material in material chemistry, for example in the development of hybrid organic-inorganic materials[169] and for the preparation of solid-phase-grafted ligands[170,171].

The interest and application of copper-catalysed organic reactions have recently increased because copper is an earth-abundant metal and, as a consequence, the main advantages of its use are the cost effectiveness and sustainability.[172,173] In Kharasch-Sosnovsky reaction oxaline-based Cu(I) or Cu(II) complexes are mostly employed; according to literature, studies on catalytic activity of bis(pyrazoyl)acetates Cu(II) complexes are unknown despite the huge research work based on poly(azoyl)acetates. During the last few decades, Santini and Pellei's research work has been focused on the synthesis of new bis (azol-1-yl)carboxylate heteroscorpionate ligands with different moieties.[174-178] Several structurally characterized copper(II) complexes have been synthetized starting from facially coordinating bis(pyrazol-1-yl) acetates, substituted in 3- and 5-position of the pyrazolyl moiety.[179]

10.2 Characterization and experimental data

10.2.1 Materials and general methods

All syntheses and handling were carried out under a dry and oxygen-free atmosphere, using standard Schlenk techniques. All solvents were dried, degassed, and distilled prior to use. Elemental analyses (C,H,N,S) were performed with a Fisons Instruments EA-1108 CHNS-O Elemental Analyzer (Thermo Fisher Scientific Inc., Waltham, MA, USA). Melting points were taken on an SMP3 Stuart Scientific Instrument (Bibby Sterilin Ltd., London, UK). IR spectra were recorded from 4000 to 700 cm^{-1} on a PerkinElmer Frontier FT-IR instrument (PerkinElmer Inc., Waltham, MA, USA), equipped with a single-reflection universal diamond ATR top-plate. IR annotations used: m = medium, s = strong, sh = shoulder, vs = very strong, vw = very weak, w = weak. ^{1}H- and ^{13}C-NMR spectra were recorded with an Oxford AS400 Varian Spectrometer (400.4 MHz for ^{1}H and 100.1 MHz for ^{13}C) (Agilent Technologies Inc, Santa Clara, CA, USA) or with a 500Bruker Ascend (500.1 MHz for ^{1}H and 125 MHz for ^{13}C) (Bruker BioSpin Corporation, 15 Fortune Drive, Billerica, MA, USA). Referencing was relative to tetramethylsilane (TMS) (^{1}H and ^{13}C). NMR annotations used were as follows: d = doublet, m = multiplet, s = singlet, t = triplet. Electrospray ionization mass spectra (ESI-MS) were obtained in positive- (ESI-MS(+)) or negative-ion (ESI-MS(−)) mode on an Agilent Technologies Series 1100 LC/MSD Mass Spectrometer (Agilent Technologies Inc., Santa Clara, CA, USA), using a water or acetonitrile mobile phase. The compounds were added to reagent grade water or acetonitrile to give approximately 0.1 mM solutions, injected (1 μL) into the spectrometer via a Hewlett Packard 1090 Series II UV-Visible HPLC system (Agilent Technologies Inc., Santa Clara, CA, USA) fitted with an autosampler. The pump delivered the solutions to the mass spectrometer source at a flow rate of 300 mL/min, and nitrogen was employed both as a drying and nebulizing gas. Capillary voltages were typically 4000 V and 3500 V for the ESI-MS(+) and ESI-MS(−) mode, respectively. Confirmation of all major species in this ESI-MS study was supported by a comparison of the observed and predicted isotope distribution patterns, the latter calculated using the IsoPro 3.1 computer program (T-Tech Inc., Norcross, GA, USA). Gas chromatography-mass spectra (GC-MS) analyses were obtained on an Agilent GC(6850N)/MS(5973N) (Stevens Creek Blvd, Santa Clara, CA, USA); electronic impact technique (70 eV); GC/MSD software; HP-5MS column (30 m, Id 0.25 μm, film thickness 0.25 μm).

10.2.2 Synthesis of $(Pz)_2CH(COOH)$ - (L^{1H}) (6)

In a round-bottom flask, dichloroacetic acid (3.143 g, 24.375 mmol) was dissolved in tetrahydrofuran (THF, 250 mL). Then, KOH (5.470 g, 97.500 mmol,), K_2CO_3 (13.475 g, 97.500 mmol), pyrazole (Pz, 3.319 g, 48.750 mmol) and tetra-*n*-butylammonium bromide (TBAB, 0.484 g, 1.500 mmol) were added, giving an opalescent mixture with a white suspension. TBAB was added as phase-transfer catalyst. The reaction was carried out under magnetic stirring at reflux for 24 hours and the reaction color changed from white to yellow to slightly pink. At the end, the solvent was dried at reduced pressure and the obtained brown-orange residue was solubilized in water (about 50 mL). The brown solution was acidified to neutral pH (about 7-7.5) by addition of hydrochloric acid (6 M, about 20 mL) and it was extracted with diethyl ether (3 x 50 mL). The yellowish aqueous phase was further acidified to acid pH (about 2) by addition of HCl (6 M, about 20 mL) and it was vigorously stirred at room temperature for 10-15 minutes, observing the formation of a white precipitate. The obtained precipitate was recovered by filtration, poured into a separatory funnel and dissolved in THF (50 mL). Et_2O (150 mL) was also added into the separatory funnel, in order to improve the separation between organic and aqueous phase. Extractions with H_2O (3 x 25 mL) were performed, to purify the product from potassium chloride (KCl). The organic phase was collected into a flask and anhydrous sodium sulfate (Na_2SO_4) was added to remove moisture. The mixture was filtered and the organic phase was dried at reduced pressure to give the white solid ligand $(Pz)_2CH(COOH)$ (L^{1H}, **6**) in 82% yield. Melting point: 164-167 °C. FT-IR (cm^{-1}): 3177w, 3149w, 3131w, 3108w, 2977w (C-H); 2457wbr (O-H); 1824wbr; 1722m (ν_{asym} C=O); 1518m (C=C/C=N); 1446w, 1435w, 1403m, 1392s, 1352m, 1318w, 1291m, 1260vs, 1232s, 1223s, 1186m, 1171s, 1092s, 1059s, 1049s, 986m, 966mbr, 918m, 887w, 863m, 850m, 821s, 763vs, 752vs, 715vs. ^{1}H-NMR ($(CD_3)_2CO$, 293 K): δ 6.35 (t, 2H, 4-C*H*), 7.46 (s, 1H, C*H*CO), 7.57 (d, 2H, 5-C*H*), 7.99 (d, 2H, 3-C*H*), 12.01 (br, 1H, COO*H*). $^{13}C\{^1H\}$-NMR ($(CD_3)_2CO$, 293 K): δ 74.13 (*C*HCO), 106.43 (4-C_{Pz}), 130.50 (5-C_{Pz}), 140.10 (3-C_{Pz}), 165.21 (*C*O). ESI-MS(+) (major positive ions, MeCN), *m/z* (%): 231 (100) $[L^{1H} + K]^+$. ESI-MS(-) (major negative ions, MeCN), *m/z* (%): 147 (25) $[(Pz)_2CH]^-$, 191 (100) $[L^1]^-$. Anal. Calcd. for $C_8H_8N_4O_2$: N 29.15, C 50.00, H 4.20; found: N 29.31, C 50.25, H 4.23.

10.2.3 Synthesis of $(Pz^{3,5\text{-}Me})_2CH(COOH)$ - (L^{2H}) (7)

In a round-bottom flask, dichloroacetic acid (3.143 g, 24.375 mmol) was dissolved in THF (250 mL). Then, KOH (5.470 g, 97.500 mmol,), K_2CO_3 (138.206 g/mol, 97.500 mmol, 13.475 g), 3,5-dimethylpyrazole ($Pz^{3,5\text{-}Me}$, 4.686 g, 48.750 mmol) and TBAB (0.484 g, 1.500 mmol) were added, giving an opalescent mixture with a white suspension. TBAB was added as phase-transfer catalyst. The reaction was carried out under magnetic stirring at reflux for 24 hours and the reaction color changed from white to yellow. At the end, the solvent was dried at reduced pressure and the obtained yellowish residue was solubilized in H_2O (about 50 mL). The orange-yellow solution was acidified to neutral pH (about 7-7.5) by addition of HCl (6 M, about 20 mL) and it was extracted with Et_2O (3 x 50 mL). The yellowish aqueous phase was further acidified to acid pH (about 2) by addition of HCl (6 M, about 20 mL) and it was vigorously stirred at room temperature for 10-15 minutes, observing the formation of a white precipitate. The obtained precipitate was recovered by filtration, poured into a separatory funnel and dissolved in THF (50 mL). Et_2O (150 mL) was also added into the separatory funnel, to improve the separation between organic and aqueous phase. Extractions with H_2O (3 x 25 mL) were performed, to purify the product from KCl. The organic phase was collected into a flask and anhydrous Na_2SO_4 was added to remove moisture. The mixture was filtered and the organic phase was dried at reduced pressure to give the white solid ligand $(Pz^{3,5\text{-}Me})_2CH(COOH)$ (L^{2H}, **7**) in 78% yield. Melting point: 174-177 °C. FT-IR (cm^{-1}): 2967w, 2926w, 2856wbr (C-H); 2446wbr (O-H); 1739m (ν_{asym} C=O); 1562m (C=C/C=N); 1443w, 1415m, 1378m, 1367m, 1345m, 1319m, 1266m, 1229s, 1161m, 1148m, 1116m, 1041m, 1030sh, 975m, 946m, 890m, 828m, 814m, 808m, 788m, 766m, 725m, 706vs. ^{1}H-NMR ($CDCl_3$, 293 K): δ 2.21 (s, 6H, 3- or 5-CH_3), 2.27 (s, 6H, 3- or 5-CH_3), 5.92 (s, 2H, 4-C*H*), 6.92 (s, 1H, C*H*CO), 9.32 (br, 1H, COO*H*). ^{13}C{^{1}H}-NMR ($CDCl_3$, 293 K): δ 11.22 (5-C*C*H_3), 13.03 (3-C*C*H_3), 70.78 (*C*HCO), 107.91 (4-C_{Pz}), 142.59 (5-C_{Pz}), 148.71 (3-C_{Pz}), 164.92 (*C*O). ESI-MS(+) (major positive ions, MeCN), *m/z* (%): 249 (30) $[L^{2H} + H]^+$, 271 (100) $[L^{2H} + Na]^+$. ESI-MS(-) (major negative ions, MeCN), *m/z* (%): 203 (70) $[(Pz^{3,5\text{-}Me})_2CH]^-$, 247 (100) $[L^2]^-$. Anal. Calcd. for $C_{12}H_{16}N_4O_2$: N 22.57, C 58.05, H 6.50; found: N 22.56, C 58.00, H 6.46.

10.2.4 Synthesis of $(Pz)_2CH(COOHex)$ - (L^{1Hex}) (8)

In a round-bottom flask, ligand L^{1H} (**6**; 192.175 g/mol, 4.000 mmol, 0.769 g) was added to a solution of dry THF (30 mL) and 1-hexanol (HexOH; 102.175 g/mol, 4.000 mmol, 0.409 g). The obtained mixture was cooled to 0 °C and left under magnetic stirring for 30 minutes. Subsequently, a solution of *N*,*N'*-dicyclohexylcarbodiimide (DCC; 206.333 g/mol, 8.000 mmol, 1.651 g) in dry THF (70 mL) was added drop by drop. The resulting mixture was left under magnetic stirring, at room temperature, for 24 hours. After that, THF was dried at reduced pressure, EtOAc was poured into the round-bottom flask and the obtained mixture was filtered. The mother liquors were washed with a dilute aqueous solution of citric acid (pH ≈ 4, 2 x 50 mL) and, subsequently, with a saturated aqueous solution of $NaHCO_3$ (2 x 50 mL). The organic phase was collected into a flask, anhydrous Na_2SO_4 was added to remove moisture, the obtained mixture was filtered and the organic phase was dried at reduced pressure. The crude residue was purified by chromatographic column (packed with SiO_2; elution with cyclohexane:EtOAc 90:10 and then with cyclohexane:EtOAc 80:20). The final product was recovered and dried under reduced pressure. The pale-yellow oily ligand $(Pz)_2CH(COOHex)$ (L^{1Hex}, **8**) was obtained in 80% yield. FT-IR (cm^{-1}): 3322vw, 3139w, 3109w, 2956m, 2923s, 2871m, 2851m (C-H); 1754vs (ν_{asym} C=O); 1626w, 1574w, 1517m (C=C/C=N); 1465m, 1451m, 1436m, 1393vs, 1385vs, 1354m, 1329m, 1292vs, 1253vs, 1223vs, 1213vs, 1187m, 1161vs, 1088vs, 1053vs, 1022m, 993m, 972s, 957vs, 938sh, 912s, 905vs, 892m, 858m, 845m, 827m, 806vs, 777vs, 762vs, 725s. ^{1}H-NMR ($CDCl_3$, 293 K): δ 0.88 (t, 3H, $O(CH_2)_5CH_3$), 1.25-1.31 (m, 6H, $O(CH_2)_2(CH_2)_3CH_3$), 1.61-1.68 (m, 2H, $OCH_2CH_2(CH_2)_3CH_3$), 4.29 (t, 2H, $OCH_2(CH_2)_4CH_3$), 6.36 (t, 2H, 4-C*H*), 7.09 (s, 1H, C*H*CO), 7.61 (d, 2H, 5-C*H*), 7.77 (d, 2H, 3-C*H*). ^{1}H-NMR (CD_3CN, 293 K): δ 0.89 (t, 3H, $O(CH_2)_5CH_3$), 1.24-1.31 (m, 6H, $O(CH_2)_2(CH_2)_3CH_3$), 1.55-1.60 (m, 2H, $OCH_2CH_2(CH_2)_3CH_3$), 4.23 (t, 2H, $OCH_2(CH_2)_4CH_3$), 6.36 (t, 2H, 4-C*H*), 7.28 (s, 1H, C*H*CO), 7.57 (d, 2H, 5-C*H*), 7.84 (d, 2H, 3-C*H*). ^{1}H-NMR (DMSO-d_6, 293 K): δ 0.81 (t, 3H, $O(CH_2)_5CH_3$), 1.13-1.19 (m, 6H, $O(CH_2)_2(CH_2)_3CH_3$), 1.47 (mbr, 2H, $OCH_2CH_2(CH_2)_3CH_3$), 4.14 (t, 2H, $OCH_2(CH_2)_4CH_3$), 6.33 (t, 2H, 4-C*H*), 7.56 (d, 2H, 5-C*H*), 7.71 (s, 1H, C*H*CO), 7.94 (d, 2H, 3-C*H*). ^{13}C{^{1}H}-NMR ($CDCl_3$, 293 K): δ 13.91 ($O(CH_2)_5CH_3$); 22.43, 25.21, 28.21, 31.19 ($OCH_2(CH_2)_4CH_3$); 67.23 ($OCH_2(CH_2)_4CH_3$); 74.63 (*C*HCO); 107.28 (4-C_{Pz}); 130.12 (5-C_{Pz}); 140.90 (3-C_{Pz}); 164.40 (*C*O). ESI-MS(+) (major positive ions, MeCN), *m/z*

(%): 209 (10) [(Pz)CH(COOHex)]$^+$, 277 (15) [L^{1Hex} + H]$^+$, 299 (100) [L^{1Hex} + Na]$^+$, 315 (5) [L^{1Hex} + K]$^+$. ESI-MS(-) (major negative ions, MeCN), *m/z* (%): 147 (100) [$(Pz)_2CH]^-$. Anal. Calcd. for $C_{14}H_{20}N_4O_2$: N 20.28, C 60.85, H 7.30; found: N 19.85, C 61.38, H 7.43.

10.2.5 Synthesis of $(Pz^{3,5\text{-}Me})_2CH(COOHex)$ - (L^{2Hex}) (9)

In a round-bottom flask, ligand L^{2H} (**7**; 248.281 g/mol, 3.000 mmol, 0.745 g) and cerium trichloride heptahydrate ($CeCl_3 \cdot 7H_2O$; 372.571 g/mol, 0.600 mmol, 0.224 g) were added to dry THF (15 mL), obtaining a mixture which was cooled to 0 °C and left under magnetic stirring for 30 minutes. Subsequently, a mixture of DCC (206.333 g/mol, 6.000 mmol, 1.238 g) and DMAP (122.168 g/mol, 1.000 mmol, 0.122 g) in dry THF (15 mL) was added drop by drop. HexOH (102.175 g/mol, 3.000 mmol, 0.307 g) was then added and the mixture was left under magnetic stirring, at room temperature, for 24 hours. After that, THF was dried at reduced pressure, EtOAc (60 mL) was poured into the round-bottom flask and the crude product was extracted from the residue, obtaining a mixture which was filtered. The obtained mother liquors were washed with a dilute aqueous solution of citric acid (pH ≈ 4, 2 x 40 mL) and with a saturated aqueous solution of $NaHCO_3$ (2 x 40 mL). The organic phase was collected into a flask, anhydrous Na_2SO_4 was added to remove moisture, the obtained mixture was filtered and the organic phase was dried at reduced pressure. The crude residue was purified by chromatographic column (packed with SiO_2; elution with *n*-hexane:EtOAc 90:10 and then with *n*-hexane:EtOAc 80:20). The final product was recovered and dried under reduced pressure. The white solid ligand $(Pz^{3,5\text{-}Me})_2CH(COOHex)$ (L^{2Hex}, **9**) was obtained in 75% yield. Melting point: 43-45 °C. FT-IR (cm^{-1}): 3100vw, 2935m, 2871m (C-H); 1755s (ν_{asym} C=O); 564m (C=C/C=N); 1454m, 1440m, 1416m, 1402m, 1380m, 1349m, 1334s, 1327m, 1297w, 1266s, 1227s, 1211s, 1157m, 1123m, 1075m, 1035m, 1010m, 978s, 937m, 911m, 897m, 823m, 804s, 789s, 754s, 723m. ^{1}H-NMR ($CDCl_3$, 293 K): δ 0.90 (t, 3H, $O(CH_2)_5CH_3$), 1.32 (sbr, 6H, $O(CH_2)_2(CH_2)_3CH_3$), 1.68 (m, 2H, $OCH_2CH_2(CH_2)_3CH_3$), 2.16 (s, 6H, 3-CH_3), 2.22 (s, 6H, 5-CH_3), 4.31 (t, 2H, $OCH_2(CH_2)_4CH_3$), 5.88 (s, 2H, 4-CH), 7.02 (s, 1H, CHCO). $^{13}C\{^1H\}$-NMR ($CDCl_3$, 293 K): δ 11.36, 13.17, 13.97 ($O(CH_2)_5CH_3$, 3- and 5-CCH3); 22.51, 25.36, 28.27, 31.29 ($OCH_2(CH_2)_4CH_3$); 67.20 ($OCH_2(CH_2)_4CH_3$); 72.35 (CHCO); 107.73 (4-C_{Pz}); 142.59, 148.25 (3-C_{Pz} and 5-C_{Pz}); 164.31 (CO). ESI-MS(+) (major

positive ions, MeCN), *m/z* (%): 333 (90) $[L^{2Hex} + H]^+$, 333 (90) $[L^{2Hex} + Na]^+$. Anal. Calcd. for $C_{18}H_{28}N_4O_2$: N 16.85, C 65.03, H 8.49; found: N 16.46, C 65.21, H 8.49.

10.2.6 Synthesis of $[Cu(L^{1Hex})]Cl_2$ (10)

The ligand L^{1Hex} (**8**; 276.334 g/mol, 1.086 mmol, 0.300 g) and the acceptor $CuCl_2 \cdot 2H_2O$ (170.476 g/mol, 1.086 mmol, 0.185 g) were solubilized in MeCN (50 mL). The reaction was left under magnetic stirring at room temperature for 6 hours. After that, the mixture was filtered and the precipitate was dried at reduced pressure. The light green complex $[Cu(L^{1Hex})]Cl_2$ (**10**) was obtained in 51% yield. Melting point: 175-181 °C. FT-IR (cm^{-1}): 3142w, 3122w, 3101m, 2993w, 2930m, 2867m (C-H); 1742vs (ν_{asym} C=O); 1517w, 1455m (C=C/C=N); 1403m, 1356w, 1287vs, 1256m, 1229m, 1196m, 1103m, 1093w, 1069m, 1059s, 990m, 978w, 953w, 924w, 914m, 880w, 865w, 823w, 803w, 763vs, 726w. ESI-MS(+) (major positive ions, MeCN), *m/z* (%): 277 (20) $[L^{1Hex} + H]^+$, 339 (50) $[Cu(L^{1Hex} - H)]^+$, 374 (60) $[(L^{1Hex})CuCl]^+$, 615 (100) $[(L^{1Hex})Cu(L^{1Hex} - H)]^+$, 650 (40) $[(L^{1Hex})_2CuCl]^+$. ESI-MS(-) (major negative ions, MeCN), *m/z* (%): 170 (100) $[CuCl_3]^-$. Anal. Calcd. for $C_{14}H_{20}Cl_2CuN_4O_2$: N 13.64, C 40.93, H 4.91; found: N 12.81, C 42.90, H 5.01.

10.2.7 Synthesis of $\{[Cu(L^{1Hex})]Br(\mu\text{-}Br)\}_2$ (11)

This compound was prepared following the procedure described for **10** but employing the acceptor $CuBr_2$ (223.354 g/mol, 0.750 mmol, 0.168 g). The brown-violet complex $\{[Cu(L^{1Hex})]Br(\mu\text{-}Br)\}_2$ (**11**) was obtained in 96% yield. Crystals of the complex **11**, suitable for X-ray analysis, were obtained by slow evaporation of an Me_2CO solution of **11**. Melting point: 163-166 °C. FT-IR (cm^{-1}): 3146w, 3134w, 3122w, 3101m, 2983w, 2952m, 2929m, 2908sh, 2865m (C-H); 1740vs (ν_{asym} C=O); 1525sh, 1515m, 1463sh, 1455m (C=C/C=N); 1402s, 1373w, 1356w, 1345w, 1286vs, 1255s, 1227vs, 1195s, 1179m, 1102m, 1094m, 1068m, 1058vs, 1019w, 989m, 976m, 951m, 922m, 911m, 878w, 864m, 823m, 803m, 762vs, 723m. ESI-MS(+) (major positive ions, MeCN), *m/z* (%): 145 (100) $[CuBr]^+$, 299 (10) $[L^{1Hex} + Na]^+$, 339 (20) $[Cu(L^{1Hex} - H)]^+$. Anal. Calcd. for $C_{14}H_{20}Br_2CuN_4O_2$: N 11.21, C 33.65, H 4.03; found: N 10.48, C 33.98, H 3.98.

10.2.8 Synthesis of $[Cu(L^{2Hex})]Cl_2$ (12)

The ligand L^{2Hex} (**9**; 332.448 g/mol, 1.000 mmol, 0.332 g) was solubilized in MeCN (50 mL) and stirred at room temperature for 15 minutes. Subsequently, the acceptor $CuCl_2 \cdot 2H_2O$ (170.476 g/mol, 1.000 mmol, 0.170 g) was added, obtaining a green solution. The reaction was carried out under magnetic stirring at room temperature for 24 hours. After that, the reaction was dried at reduced pressure obtaining a green oil, Et_2O (30 mL) was poured into the round-bottom flask and the mixture was left under magnetic stirring at room temperature for 15 minutes. The mixture was filtered and the precipitate was dried at reduced pressure, to give the dark yellow complex $[Cu(L^{2Hex})]Cl_2$ (**12**) in 91% yield. Melting point: 156-166 °C. FT-IR (cm^{-1}): 3137w, 3100w, 2958m, 2933m, 2860w (C-H); 1761s (ν_{asym} C=O); 1559m (C=C/C=N); 1463s, 1418m, 1382s, 1316s, 1299m, 1282m, 1264s, 1230s, 1216m, 1166w, 1139w, 1118w, 1049m, 988m, 905m, 868m, 842m, 807m, 784m, 718m, 708m. ESI-MS(+) (major positive ions, MeCN), *m/z* (%): 333 (70) $[L^{2Hex} + H]^+$, 395 (10) $[Cu(L^{2Hex} - H)]^+$, 430 (75) $[(L^{2Hex})CuCl]^+$, 642 (60) $[(L^{2Hex})Cu(L^{2})]^+$, 727 (100) $[(L^{2Hex})Cu(L^{2Hex} - H)]^+$, 762 (20) $[(L^{2Hex})_2CuCl]^+$. ESI-MS(-) (major negative ions, MeCN), *m/z* (%): 170 (100) $[CuCl_3]^-$. Anal. Calcd. for $C_{18}H_{28}Cl_2CuN_4O_2$: N 12.00, C 46.30, H 6.04; found: N 11.65, C 45.96, H 5.76.

10.2.9 Synthesis of $[Cu(L^{2Hex})]Br_2$ (13)

The ligand L^{2Hex} (**9**; 332.448 g/mol, 1.000 mmol, 0.332 g) was solubilized in MeCN (50 mL) and stirred at room temperature for 15 minutes. Subsequently, the acceptor $CuBr_2$ (223.354 g/mol, 1.000 mmol, 0.223 g) was added, obtaining a green solution. The reaction was carried out under magnetic stirring at room temperature for 24 hours. After that, the mixture was filtered and the precipitate was dried at reduced pressure. The brown complex $[Cu(L^{2Hex})]Br_2$ (**13**) was obtained in 90% yield. Melting point: 132-135 °C. FT-IR (cm^{-1}): 3136w, 3102w, 2957m, 2928m, 2859wbr (C-H); 1756vs (ν_{asym} C=O); 1563s (C=C/C=N), 1465s, 1421m, 1385s, 1377sh, 1315s, 1298m, 1271s, 1230s, 1163w, 1134w, 1119m, 1050m, 990m, 953m, 910m, 877m, 826m, 790m, 724m, 707m. ESI-MS(+) (major positive ions, MeCN), *m/z* (%): 395 (20) $[Cu(L^{2Hex} - H)]^+$, 476 (70) $[(L^{2Hex})CuBr]^+$, 727 (100) $[(L^{2Hex})Cu(L^{2Hex} - H)]^+$, 808 (25) $[(L^{2Hex})_2CuBr]^+$. ESI-MS(-) (major negative ions, MeCN), *m/z* (%): 304 (100) $[CuBr_3]^-$, 636 (5) $[(L^{2Hex})CuBr_2 + Br]^-$. EA (%) calculated for $C_{18}H_{28}Br_2CuN_4O_2$: N 10.08, C 38.90, H 5.08; found: N 9.84, C 39.19, H 5.09.

10.3 Results and discussion

The aims of this work are two: firstly, the synthesis of esterified bis(pyrazol-1-yl) acetate ligands and the related copper(II) complexes and relative characterization and secondly, the study of their catalytic activity in Kharasch-Sosnovsky reaction.

10.3.1 Synthesis of esterified ligands

Ligands L^{1Hex} (**8**) and L^{2Hex} (**9**) were prepared using precursors **6** and **7**, respectively, and HexOH as starting materials, according to the procedure reported in **Scheme 24**. The ^{1}H- and ^{13}C-NMR spectra of **8** and **9**, recorded in $CDCl_3$ solution, showed all the expected signals for the ligands and only one set of resonances for the pyrazole rings, indicating that the pyrazoles are equivalents. The FT-IR spectra showed all the expected bands for the ligands; in particular, weak and medium absorptions due to the C-H stretching were observed in the range 2851-3322 cm^{-1}. The asymmetric stretching of the C=O groups are detected as strong peaks at 1754 and 1755 cm^{-1}, respectively, in the range of the ester groups. The ESI-MS study was performed solubilizing ligands **8** and **9** in MeCN: the ESI-MS(+) spectra showed the molecular peaks at *m/z* 277 and 333, attributable to the species $[L^{1Hex} + H]^+$ and $[L^{2Hex} + H]^+$, respectively.

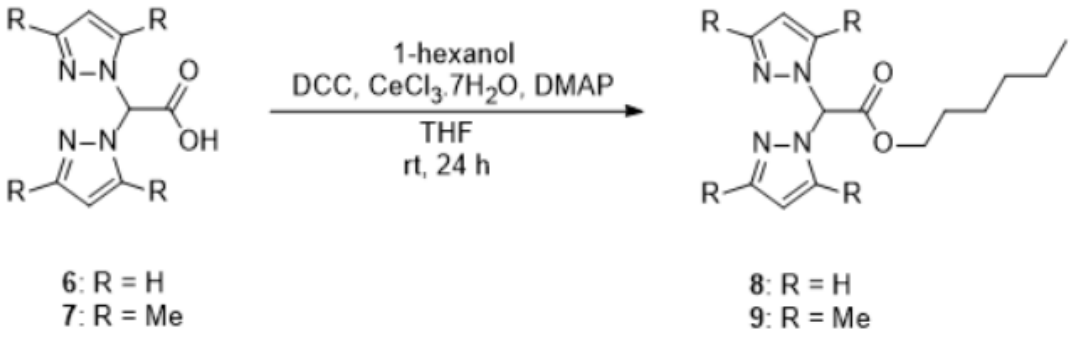

Scheme 24. Reaction for the synthesis of ligands **8** and **9**.

10.3.2 Synthesis of complexes

Complex $[Cu(L^{1Hex})]Cl_2$ (**10**) was prepared using ligand **8** and $CuCl_2 \cdot 2H_2O$ as starting materials, according to the procedure reported in **Scheme 25**.

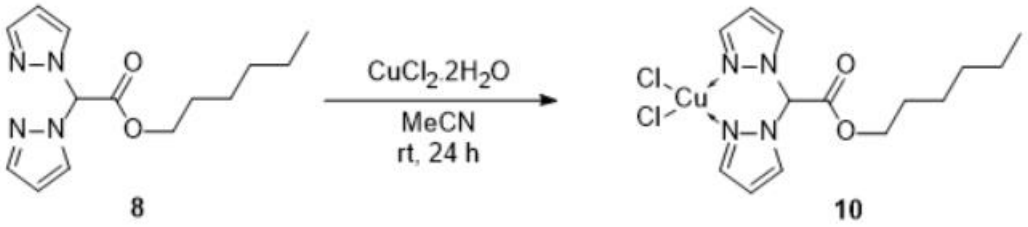

Scheme 25. Reaction for the synthesis of complex **10**.

The FT-IR spectrum showed all the expected bands for the complex; in particular, weak and medium absorptions due to the C-H stretching were observed in the range 2867-3142 cm^{-1}. The asymmetric stretching of the C=O group is detected as a strong peak at 1742 cm^{-1}, without a significant variation with respect to the absorption detectable in the spectrum of the free ligand (ν_{asym} C=O 1754 cm^{-1}), indicating that in the solid state the carbonyl group is not involved in the coordination of the metal. The ESI-MS study was performed solubilizing complex **10** in MeCN: the ESI-MS(+) spectrum showed a peak at *m/z* 374, attributable to the species $[(L^{1Hex})CuCl]^+$ that confirms the complex formation, while the ESI-MS(-) spectrum showed the main peak at *m/z* 170, assignable to the species $[CuCl_3]^-$.

Complex $\{[Cu(L^{1Hex})]Br(\mu\text{-}Br)\}_2$ (**11**) was prepared using ligand **8** and $CuBr_2$ as starting materials, according to the procedure reported in **Scheme 26**.

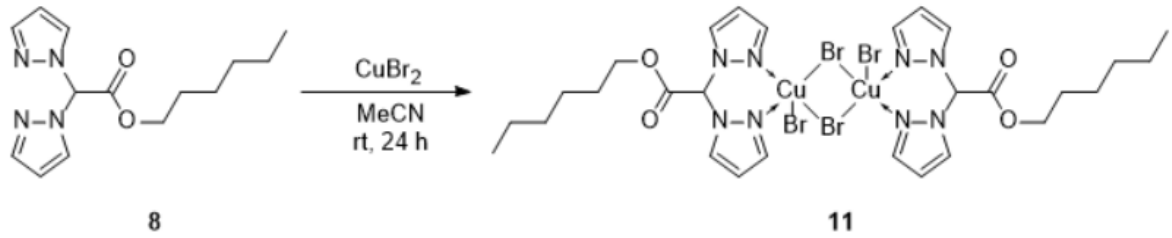

Scheme 26. Reaction for the synthesis of complex **11**.

The FT-IR spectrum showed all the expected bands for the complex; in particular, weak and medium absorptions due to the C-H stretching were observed in the range 2865-3146 cm^{-1}. The asymmetric stretching of the C=O group is detected as a strong peak at 1740 cm^{-1}, without a significant variation with respect to the absorption detectable in the spectrum of the free ligand (ν_{asym} C=O 1754 cm^{-1}), indicating that the carbonyl group is not involved in the coordination of the metal, in accordance with X-ray crystal structure with the ligands

chelating in a κ^2-N,N bidentate fashion. The ESI-MS study was performed solubilizing complex **11** in MeCN: the ESI-MS(+) spectrum showed peaks at *m/z* 339 and 615, attributable to the species $[Cu(L^{1Hex} - H)]^+$ and $[(L^{1Hex})Cu(L^{1Hex} - H)]^+$, respectively.

Crystals of complex **11** were obtained by slow evaporation of an Me_2CO solution of **11**.

Empirical formula	**$C_{14}H_{20}N_4O_2CuBr_2$**
Formula weight	**499.70**
Temperature / K	296.9(9)
Crystal system	Monoclinic
Space group	$P2_1/c$
a / Å	13.0171(4)
b / Å	9.8111(2)
c / Å	15.8632(4)
α / °	90
β / °	110.248(3)
γ / °	90
Volume / Å^3	1900.73(9)
Z	4
ρ_{calc} g/cm^3	1.746
μ / mm^{-1}	5.366
F(000)	988.0
Crystal size / mm^3	0.6 × 0.4 × 0.01
Radiation	Mo Kα (λ = 0.71073)
Index ranges	$-15 \leq h \leq 17$, $-13 \leq k \leq 12$, $-19 \leq l \leq 20$
Reflections collected	22513
Independent reflections / R_{int}	4228 / 0.0437
Data / Restraints / Parameters	4228 / 78 / 293
Goodness-of-fit on F^2	1.058
Final R indexes [$I \geq 2\sigma(I)$]	R_1 = 0.0351, wR_2 = 0.0666
Largest diff. peak / hole / e Å^{-3}	0.50 / −0.46

Table 24. Summary of crystal data and structure refinement for complex **11**.

A summary of the crystal/structure refinement data is given in **Table 24**, selected bond lengths and angles were reported in **Table 25** and **Table 26**, an ORTEP-like[180] representation of the complex is given in **Figure 56** and the distorted square pyramidal polyhedra about the two Cu centres were highlighted in **Figure 57.**

Br(1)-Cu(1)	2.4302(4)	Br(2)-Cu(1)	2.3687(6)
Br(1)-Cu(1)^{I}	2.7600(5)	Cu(1)-N(1)	2.017(2)
Cu(1)-N(3)	2.042(3)	N(1)-N(2)	1.357(3)
N(3)-N(4)	1.369(3)	N(1)-C(3)	1.330(4)
N(2)-C(1)	1.342(4)	N(3)-C(6)	1.305(4)
N(4)-C(4)	1.338(4)	N(2)-C(7)	1.445(3)
N(4)-C(7)	1.434(4)	C(1)-C(2)	1.344(5)
C(2)-C(3)	1.384(5)	C(4)-C(5)	1.355(5)
C(5)-C(6)	1.399(5)	C(7)-C(8)	1.533(4)
O(1)-C(8)	1.198(3)	O(2)-C(8)	1.310(4)

Table 25. Bond lengths (Å) of **11**.

Cu(1)-Br(1)-Cu(1)^{I}	93.544(13)	Br(1)-Cu(1)-Br(1)^{I}	86.456(13)
N(1)-Cu(1)-Br(1)^{I}	93.87(7)	N(3)-Cu(1)-Br(1)^{I}	97.29(7)
Br(2)-Cu(1)-Br(1)	93.260(18)	N(1)-Cu(1)-Br(1)	176.35(7)
N(3)-Cu(1)-Br(2)	157.34(7)	N(1)-Cu(1)-N(3)	85.69(10)
N(1)-Cu(1)-Br(2)	90.16(8)	N(3)-Cu(1)-Br(1)	90.67(7)
N(2)-N(1)-Cu(1)	122.68(17)	N(4)-N(3)-Cu(1)	121.3(2)
N(1)-N(2)-C(7)	118.8(2)	N(3)-N(4)-C(7)	119.4(2)
N(1)-C(3)-C(2)	110.6(3)	N(3)-C(6)-C(5)	111.5(3)
C(1)-N(2)-N(1)	111.2(2)	C(4)-N(4)-N(3)	110.6(3)
N(2)-C(1)-C(2)	107.3(3)	N(4)-C(4)-C(5)	107.9(3)
N(4)-C(7)-N(2)	110.1(2)	C(1)-C(2)-C(3)	106.2(3)
C(4)-C(5)-C(6)	104.8(4)	O(2)-C(8)-C(7)	108.8(2)

Table 26. Bond angles (deg) of **11**.

The crystal structure investigation has revealed that in the solid state the compound exists as a dimer of formula $\{[Cu(L^{1Hex})]Br(\mu\text{-}Br)\}_2$, with the Br(1) ions binding two symmetry-related units to each other. This complex is one of the few mono- or di-nuclear bis(pyrazolyl)acetate copper complexes[181,182] with uncoordinating acetate moieties and also one of the relatively not-so-abundant copper complexes showing μ-bridging bromide ions coupled with two pentacyclic N-based ligands.[183-188]

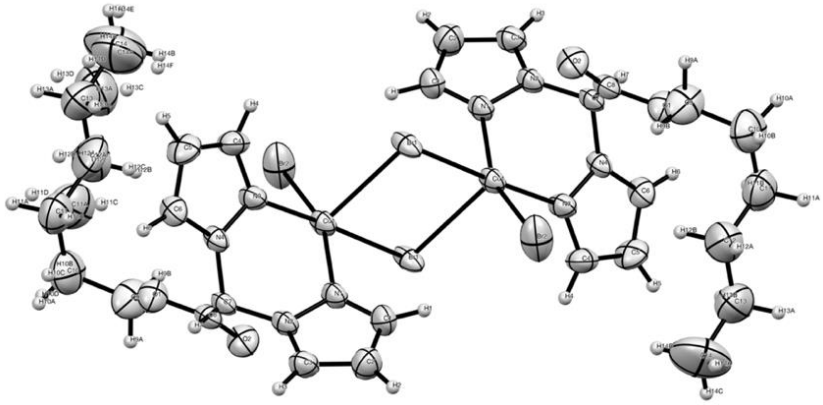

Fig. 56. ORTEP-like molecular structure of **11** with thermal ellipsoids drawn at the 30% probability level.

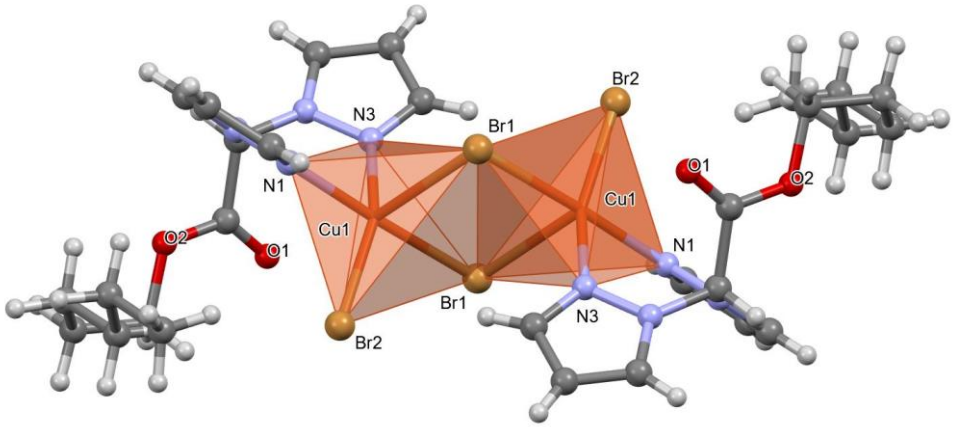

Fig. 57. *Mercury*[189] ball-and-stick representation of the dimeric complex highlighting the square pyramidal environment of the copper atoms. Only one of the hexyloxy chain arrangement has been shown for clarity. Monomeric units on the left and on the right show, respectively, apical bromide or basal square plane towards the observer.

In the dimer, two μ-bridging Br(1) and two Cu atoms define a Cu_2Br_2 tetracycle. The Cu atom is penta-coordinated and the environment has a distorted square planar shape; the latter seems to be the preferred one in similar compounds. In the pyramid basal plane sit the N(1) and N(3) atoms of the two pyrazolyl rings, that are in *trans* position with the Br(1) and Br(2) atoms, respectively. As for metal-involving bonds, the Cu(1)-Br(2) length of the terminal bromide

ion (see **Tables 25** and **26**) is about 0.06 Å shorter than the Cu(1)-Br(1) distance (2.3687(6) *vs* 2.4302(4) Å); the Cu(1)−Br(1)^{I} bond length of the μ-bridging Br ion is instead appreciably longer at 2.7600(5), about 0.33 Å longer than the terminal Cu-Br bond. This value is higher than the reported average for similar compounds (2.59 Å), but fits within the reported range (2.37-3.06 Å). Similar considerations can apply to Cu-N(1) and Cu-N(3) distances, respectively, 2.017(2) and 2.042(3) Å (mean: 2.00, range: 1.97-2.09 Å). The situation closely matches that found in the two known compounds showing also a bis-pyrazolyl moiety.[182,183] The N-N and C-N bond distances in the pyrazole residues and the C-C bonds in the hexyl chain appear in line with known data and do not deserve further comment. It is instead worth noting that the O(1) oxygen of the carboxylic moiety is roughly in *trans* position with respect to the symmetry related bridging Br(1) atom (angle O(1)-Cu(1)-Br(1)^{I} of 162.6°), in a virtual sixth Cu coordination position, however, the Cu(1)-O(1) distance is 3.174 Å, well above the sum of the Cu and O Van Der Waals radii (1.92 Å). The same situation has been found in a recent report.[182]

Complexes [Cu(L^{2Hex})]Cl_2 (**12**) and [Cu(L^{2Hex})]Br_2 (**13**) were prepared using ligand **9** and $CuCl_2 \cdot 2H_2O$ or $CuBr_2$, respectively, as starting materials, according to the procedure reported in **Scheme 27**.

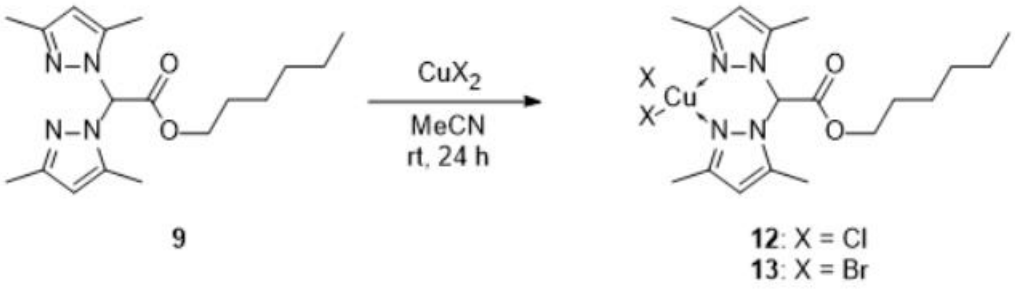

Scheme 27. Reaction for the synthesis of complexes **12** and **13**.

The FT-IR spectra showed all the expected bands for the complexes; in particular, weak and medium absorptions due to the C-H stretching were observed in the range 2859-3137 cm^{-1}. The asymmetric stretching of the C=O groups are detected as strong peaks at 1761 and 1756 cm^{-1}, respectively, in the range of the ester groups, without significant variations with respect to the absorption detectable in the free ligand (ν_{asym} C=O 1755 cm^{-1}), indicating that in the solid state the carbonyl group is not involved in the coordination of the metal. The ESI-MS

study was performed solubilizing complexes **12** and **13** in MeCN: the ESI-MS(+) spectra showed the peaks at *m/z* 430 and 476, attributable to the species $[(L^{2Hex})CuCl]^+$ and $[(L^{2Hex})CuBr]^+$, respectively, that confirm the complexes formation, while the ESI-MS(-) spectra showed the main peak at *m/z* 170 and 304, assignable to the $[CuX_3]^-$ species (X = Cl or Br, respectively).

Due to unsuccessful efforts in attempts to crystallize the compounds **11**, **12** and **13** to obtain crystals suitable for X-ray analysis, it has been chosen to exploit the X-ray Photoelectron Spectroscopy (XPS) and X-ray Absorption Fine Structure (XAFS) spectroscopy (in the near edge and in the extended regions) to achieve details about the electronic states (C, N, O, Cu) and the local coordination geometry in the complexes. These tests were performed, respectively, at the materials science beamline (MSB) and at the BEAR (Bending magnet for Emission Absorption and Reflectivity) beamline of the Elettra synchrotron radiation source (Trieste, Italy). The XPS data analysis results concerning C1s, N1s, O1s, Cl2p and Cu2p core levels (Binding Energy (BE), Full Width Half Maximum (FWHM) and assignments) confirmed the proposed molecular structures. The C1s signal can be always resolved by curve fitting analysis into three components corresponding, respectively, to aromatic and aliphatic C-C carbons (BE = 284.7 eV), to C-N carbons of the pyrazole-like rings and C-O of the carboxylate tail (BE = 286.6 eV) and to O-C=O carbon atoms of carboxylate (BE = 289 eV) tail. In addition, a small intensity signal attributed to C=O is individuated at about 288 eV and attributed to impurities always found on the surface of samples deposited in air. C1s spectra of the ligand **9** and the related coordination compound **12** are reported in **Figure 58a** and **Figure 58b**, respectively. N1s spectrum of the ligand **9** (**Figure 58c**) shows a couple of main signals at respectively 400.3 eV and 402.4 eV BE, indicative for the two types of nitrogen on the pyrazole rings, i.e. respectively amine-like and imine-like. As for the coordination compounds, it is expected that, when the two nitrogen atoms coordinate a metal ion, only the amine-like contribution appears, as reported in the literature for heterocycles coordinating metal ions (for example porphyrins or phthalocyanines),[190,191] as well as for pyrazole molecules anchored to copper substrates.[192] In excellent agreement with this prediction, in both complexes **12** (**Figure 58d**) and **10** a single N1s component can be observed at about 400.5 eV; it is attributed to the symmetrized nitrogen atoms coordinated to Cu(II). For the two coordination compounds **13** and **10**, Cu2p and Cl2p spectra were also collected and analyzed. Cl2p signals are noisy (as expected due to the low atomic percent of chlorine in the

proposed molecular structure); a couple of spin-orbit components is observed for both complexes at about 197.5 eV, as expected for chlorine atoms in metal coordination compounds.[193] Cu2p spectra of **12** and **10** are analogous, showing a couple of spin-orbit pairs, in excellent agreement with XANES data analysis. Both signals are indicative for Cu(II), respectively in coordination compounds[194] ($Cu2p_{3/2}$ at about 936 eV) and $CuCl_2$ salts or CuO ($Cu2p_{3/2}$ at about 933 eV), that can be due to residues arising by the synthesis procedure, but do not influence the coordination compounds molecular structure.

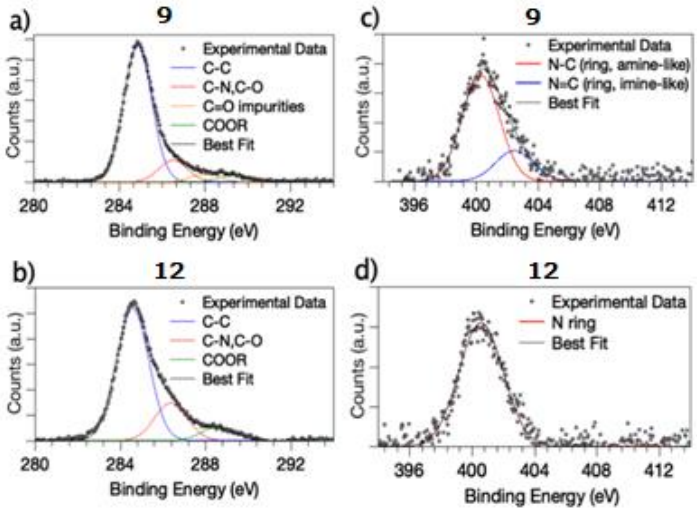

Fig. 58. a) XPS C1s core level spectrum of **9**; **b**) XPS C1s core level spectrum of **12**; **c**) XPS N1s core level spectrum of **9**; **d**) XPS N1s core level spectrum of **12**.

With the aim to gather further information about the functional groups presence and stability in the copper(II) coordination compounds, Near Edge X-ray Absorption Fine Structure (NEXAFS) spectroscopy measurements were also carried out at C and N K-edges. Spectra of **10**, **12** and **13** (that for sampling issues was difficult to measure with XPS) were collected in an experimental geometry at 30° incidence angle on the sample surface. Spectra of the C K-edge and N K-edge of the samples analysed are reported in **Figure 59**. Peak position and assignment of the main features detected in the C and N K-edge spectra of the analysed samples are also shown in **Table 26**.

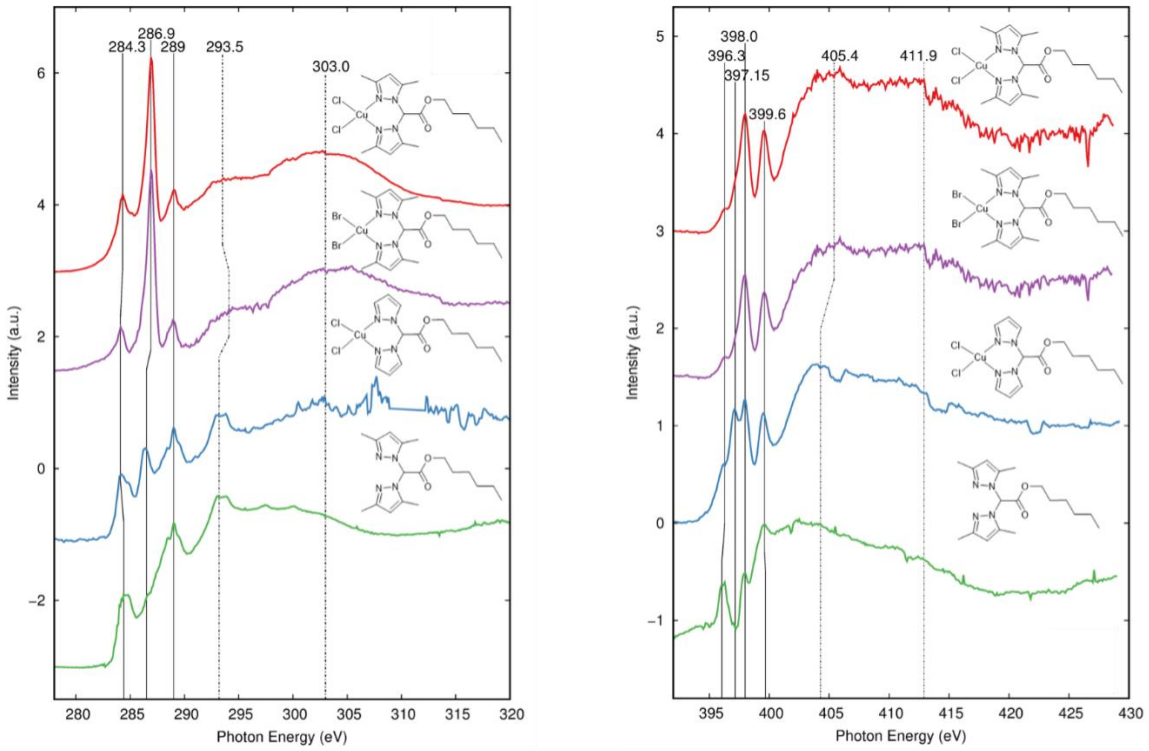

(a) **(b)**

Fig. 59. C K-edge (**a**) and N K-edge (**b**) NEXAFS spectra of samples **9**, **10**, **12** and **13**.

	9	**10**	**12**	**13**	**Assignment**
C K-edge	284.3	284.3	284.1	284.1	$\pi^*_{C=C}$
	286.5	286.9	286.9	286.5	$\pi^*_{C=N}$
	289.0	289.0	289.0	289.0	$\pi^*_{C=O}$
	293.2	293.5	294.1	293.2	σ^*_{C-C}
	303.0	303.0	303.0	303.0	$\sigma^*_{C=N}$
N K-edge	398.0	398.0	398.0	398.0	π^*_1
	399.6	399.6	399.6	399.6	π^*_2
	-	405.4	405.4	404.3	$\sigma^*_{C=N}$
	-	411.9	411.9	411.9	σ^*_{C-N}

Table 27. Peak position (eV) and relative assignment of the main features appearing in the C and N K-edge NEXAFS spectra of samples **9**, **10**, **12** and **13**.

The spectra of the three coordination compounds (particularly **12** and **13**) appear very similar, therefore they will be discussed together. For the C K-edge spectra the energy scale is referenced to the $\pi^*_{C=O}$ transition at 289 eV[195] while for the N K-edge spectra to the π^*_1

transition at 398 eV. In the C K-edge spectra, the features observed agree with the expected peaks reported in **Table 27**: below the edge C1s→π^* transitions originating respectively from C=C carbons and C=N carbons of the pyrazole rings ($\pi^*_{C=C}$ at 284.1 eV for **12** and **13** and at 284.3 eV for **10** and **9**, $\pi^*_{C=N}$ at 286.9 eV for **10** and **12** and 286.5 eV for **13** and **9**) and from the O-C=O carbon of the ester function ($\pi^*_{C=O}$ at 289 eV).[196,197] Above the edge, two large features are related to C1s→σ^* transitions of the alkyl side chains (σ^*_{C-C}) and of the pyrazole rings ($\sigma^*_{C=N}$). The features detected in the N K-edge NEXAFS spectra are mainly related to the pyrazole rings: below the edge a shoulder at 396.3 eV is observed, then two different N1s→π^* transitions (π^*_1 at 398 eV and π^*_2 at 399.6 eV) arising by two non-equivalent nitrogen atoms appear in the spectra, coherently with literature data reported for similar heterocyclic systems.[190,196] Above the edge, the two broad bands can be ascribed to $\sigma^*_{C=N}$ and σ^*_{C-N} resonances while the first two peaks appearing in **Figure 58** and not mentioned in **Table 27** correspond to impurities already observed in the literature.[198,199] The presence of all the expected signals in both C and N K-edges spectra confirms the stability of the ligands molecular structure after the coordination compounds formation.

XAS measurements were carried out at the XAFS beamline of the Elettra synchroton at Cu K-edge on complexes **10** and **12**. The analysis was carried out in the near edge (XANES) and extended (EXAFS) regions in order to achieve reliable and deep understanding about the average Cu local atomic structure and coordination chemistry. The analysis of the XANES features provides information about the average oxidation state of the absorber (Cu ion) and the local ligands geometry around it.

In **Figure 60** the normalized Cu K-edge XANES spectra of complexes **10** and **12** were reported and similar features can be observed. Accordingly to the literature[200-202] the main edge energy, the weak pre-edge peak at low energy and the pre-edge shoulder confirm the Cu(II) oxidation state, in agreement with XPS data analysis results. Comparing the experimental XANES spectra of **10** and **12** complexes with literature[203] XANES of Cu(II) sites having different local coordination chemistry, a close similarity can be seen between our data and those of Cu-glycine complex, suggesting for **10** and **12** data a roughly planar geometry.

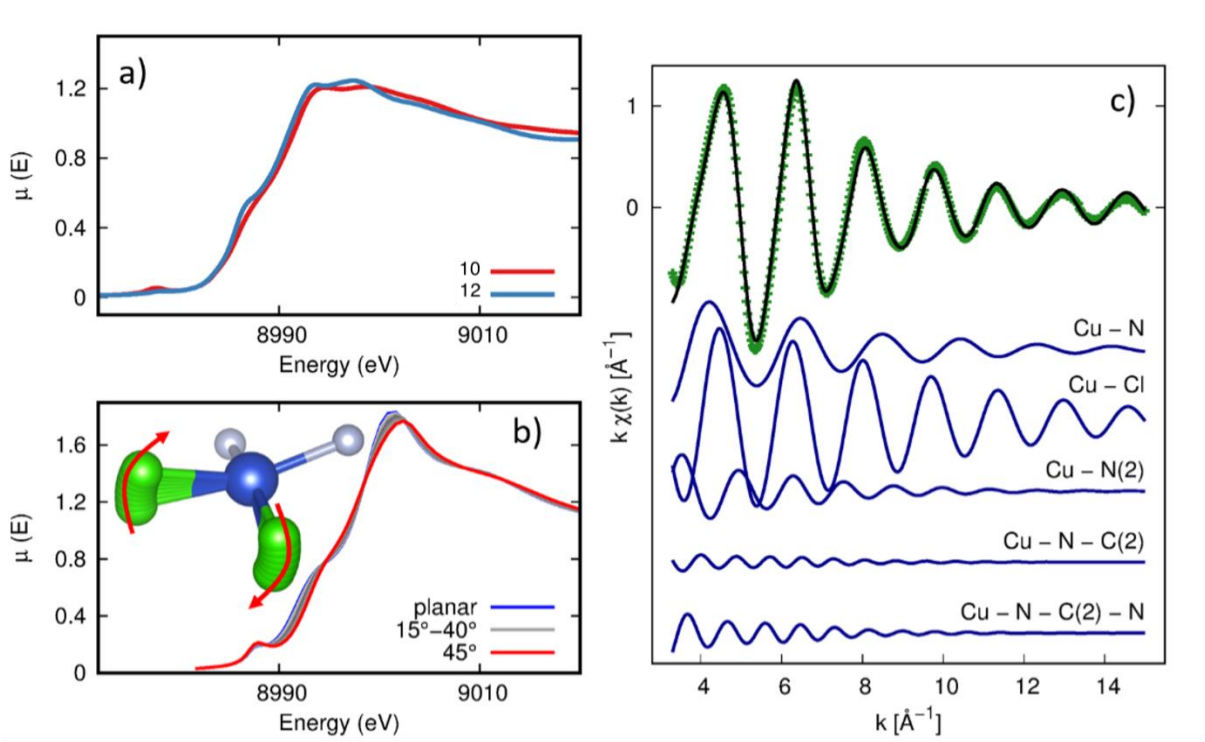

Fig. 60. a) Comparison of the Cu K-edge XANES spectra of complexes **10** (red) and **12** (blue); **b**) evolution of the XANES spectral features in $CuCl_2N_2$ model molecule as a function of distortions from a square planar geometry (see text); **c**) results of the quantitative EXAFS analysis in k space for complex **10**: k^2 weighed $k^2\chi(k)$ experimental data (green dots) and the best fit curve (black line) are presented. The k^2 weighed partial contributions χ_i^{th} are presented vertically shifted for sake of clarity.

Noticeably, although all the Cu-compounds present very similar features, looking at **Figure 60a** differences are quite evident: the pre-edge shoulder of **10** and the first peak of the edge appear less pronounced compared to **12**. To understand the origin of these differences in samples **12** and **10,** the *ab initio* XANES spectra of a simple model for the Cu local environment have been calculated using the FEFF 8.2[204] program. The model was a Cu absorber coordinated to 2 Cl and 2 N atoms in a square planar configuration. Then the Cl atom pair was rotated out of the structure evolving from the planar toward a tetragonal geometry. The behavior of the XANES spectra as a function of the angle Cl-pair (5 deg. steps) is reported in **Figure 60b** and it reveals an interesting behavior: as the two Cl atoms progressively tilt out of the plane $Cu\text{-}N_2$, the main white line peak broadens and decreases shifting toward high energies. At the same time the pre-edge shoulder becomes less pronounced and weaker. This behavior suggests a square planar coordination geometry for **10** and a tilted structure for **13**. Such a different behavior is likely due to the methyl groups

bounded to the pyrazole rings that, when they are present as in complex **13**, induce a steric distortion of the Cu coordination geometry allocated tilting the Cl atoms out of the square planar geometry. The EXAFS analysis provides further details about the local atomic structure around Cu in complexes and can be used to validate the coordination model after the synthesis procedure in case of complex molecules. The raw k^2 spectra were fitted in the k-space (3-15 $Å^{-1}$ range) and the results of the fit in k-space are reported in **Figure 60c** together with the partial contributions included in the fit. The first shell was made by the single scattering (SS) contribution of the 2 Cl and 2 N bounded to the central Cu, the second shell comes from the bond with the Cu-N(2) where N(2) is the furthest N atom in the pyrazole ring and the last two contributions are associated to the SS and multiple scattering (MS) to C(2) (furthest C atoms in the pyrazole ring) atoms through N which results relevant due to the almost aligned configuration. The quantitative investigation of the EXAFS region allowed to explore the nearest shells around Cu confirming that the Cu-complexes coordination took place accordingly to what expected from the synthesis procedure.

10.3.3 Application of complexes as catalysts

Copper complexes $[Cu(L^{1Hex})]Cl_2$ (**10**), $[Cu(L^{2Hex})]Cl_2$ (**12**) and $[Cu(L^{2Hex})]Br_2$ (**13**) were studied as catalysts for the oxidation of alkenes *via* the Kharasch-Sosnovsky reaction, based on previous experimental attempts using analogous copper(II) complexes bearing ligands with the methyl ester (L^{2Me}), in which the product was obtained just in traces. In particular, the hexyl derivative (L^{2Hex}) was chosen in order to increase the contact in a homogeneous mixture, avoiding the use of further solvents. Thus, in order to demonstrate the catalytic activity of complex $[Cu(L^{2Hex})]Cl_2$ (**12**), a series of preliminary tests was performed changing stoichiometry, temperature and solvents; they are focused on the oxidation of cyclohexenes to the corresponding ester using *t*-butylperbenzoate as oxidizing agent. After this screening, an interesting catalytic activity of complex **12** was actually observed, obtaining the best yield in the presence of 10 mol% of the complex, an excess of cyclohexene with respect to the perester (10:1) at 60°C (**Scheme 28**, **Table 28**, entry *j*).

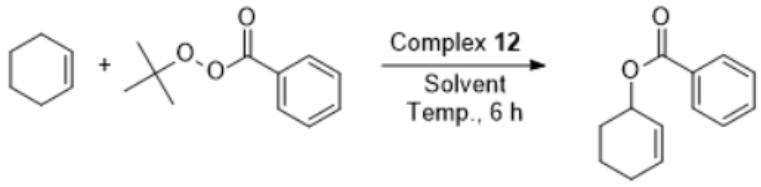

Scheme 28. Kharasch-Sosnovsky reaction performed with complex **12**.

Entry	12 mol%	Alkene:Perester Ratio	Solvent	Temperature (°C)	Product yield (%)[a]
A	20	3:1	CH_3CN[b]	rt	6
B	20	3:1	CH_3CN[b]	60	25
C	20	3:1	$CHCl_3$[b]	60	28
D	20	3:1	-	rt	25
E	20	3:1	-	60	40
F	20	3:1	-	80	29
G	20	10:1	-	60	65
H	20	7.5:1		60	59
I	20	5:1		60	54
J	10	10:1	-	60	68
K	5	10:1	-	60	40
L	1	10:1	-	60	31

Table 28. Study on the catalytic activity of complex **12** ([a] Yield of pure isolated product. [b] 1M concentration).

Once reaction conditions were optimized for complex **12**, the attention was turned on complex $[Cu(L^{2Hex})]Br_2$ (**13**). The latter complex showed better catalytic performance and in particular, working under the same reaction conditions, the reaction time decreased from 24 to 6 hours and the yield passed from 68 to 75%. A further significant improvement was recognized performing the reaction in a sealed vial, by which it was possible to minimize the variation of the concentration of the alkene due to the volatility of cyclohexene. Under these conditions and after some additional tests, the product was isolated in 85% of yield using only 5 mol% of complex **13** (**Scheme 29**, **Table 29**, entry *b*).

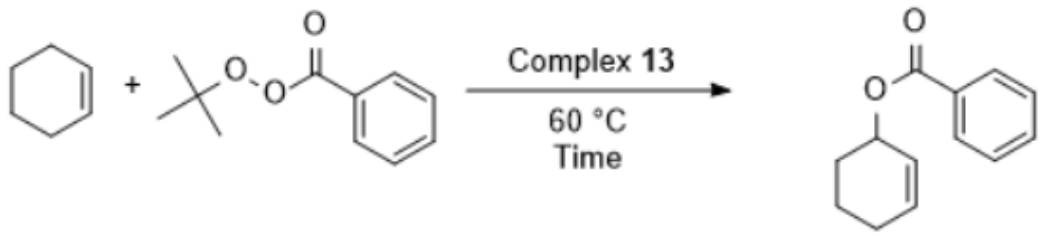

Scheme 29. Kharasch-Sosnovsky reaction performed with complex **13**.

Entry	13 mol%	Alkene:Perester Ratio	Time (h)	Product yield (%)[a]
A	10	10:1	3	84
B	5	5:1	6	85
C	1	5:1	24	73
D	-	5:1	24	-

Table 29. Additional tests performed in a sealed vial promoted by complex **13** ([a]Yield of pure isolated product).

Subsequently, based on previous optimization steps (**Table 28**, entry *b*), the catalytic activity of $[Cu(L^{1Hex})]Cl_2$ (**10**) was tested. However, this complex resulted less active then **13**, isolating the product in just 30% of yield. Nevertheless, satisfactory yields can be reached increasing the alkene:perester ratio to 10:1 and the amount of catalyst up to 20 mol%, obtaining 70% of yield after 24 hours at 60 °C. These results are probably due to the fact that the methyl groups slightly increase the solubility of complexes **12** and **13** in cyclohexene. A similar study was also performed under the same conditions with simple copper(II) salts, such as $CuCl_2$ and $CuBr_2$, obtaining very poor yields of the target compound, 15% and 18% respectively, after 24 hours at 60 °C.

Once proved the catalytic activity of these complexes and in particular identifying the complex $[Cu(L^{2Hex})]Br_2$ (**13**) as the most effective one, the optimised reaction conditions were tested on cyclopentene and cyclooctene, obtaining in both cases from good to excellent yields (**Figure 61**).

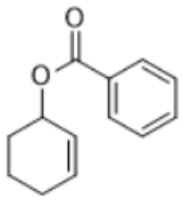

a) Yield: 85%

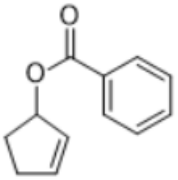

b) Yield: 85%

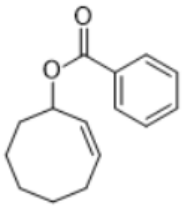

c) Yield: 90%

Fig. 61. Synthesis of oxygenate allylic compounds *via* Kharasch-Sosnovsky reaction using **13** as catalyst.

Regarding {[Cu(L^{1Hex})]Br(μ-Br)}$_2$ (**11**), the last of the series of the complexes bearing an esterified ligand with an hexyl chain, the crystallographic resolution has made to decide to test also this compound in the Kharasch-Sosnovsky reaction, even if complex **13** already proved to be the most effective one among the studied complexes, given its interesting dimeric structure. Starting from the results obtained with complex **13** (**Table 29**) a further strategy was developed, in order to reduce the amount of catalyst and increase the yield. A series of preliminary test were carried out to determine the catalytic activity of complex **11**. The starting point was related to the optimized reaction conditions described in **Table 29**. The reaction was performed using 5 mol% of the catalyst **11** leaving the reaction 6 hours at 60 °C, with an alkene:perester ratio of 5:1, achieving only 73% of yield (**Table 30**, entry *a*). After this first trial, several attempts were conducted and the best result was observed using 0.5 mol% of **11**, a slight excess of cyclohexene (alkene:perester ratio of 3:1) at 60 °C for 24 hours (**Table 30**, entry *h*). Using an alkene:perester ratio of 5:1, with 5 mol% of the catalyst and a 24 hour reaction time, the yield was almost quantitative (**Table 30**, entry *b*). This yield decreased a bit reducing the ratio to 3:1, due to the scarce and non-proportional amount of cyclohexene and *t*-butylperbenzoate (Luperox) (**Table 30,** entry *c*). A noteworthy upgrade was obtained carrying out the reaction with 1 mol% of **11**, for 24 hours at 60 °C: in this setting the yields were comparable with those obtained before (**Table 30**, entry *d* = 77% of yield and entry *e* = 74% of yield). So, based on above mentioned optimization steps, the catalytic activity of complex **11** was further developed, decreasing the amount to 0.5 mol%. Nonetheless, an almost quantitative yield can be reached increasing the alkene:perester ratio to 10:1, using 0.5 mol% of the catalyst and obtaining 95% of yield after 24 hours at 60 °C. A reduction of the ratio means a reduction of the amount of an alkene that could be, someway,

precious and not easily available, thus reducing waste of starting materials. Therefore, the use of a 3:1 ratio of cyclohexene:Luperox allowed to obtain a very good yield, up to 90% (**Scheme 30**, **Table 30**, entry *h*).

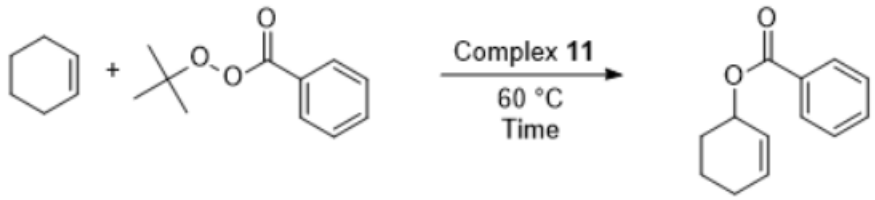

Scheme 30. Kharasch-Sosnovsky reaction performed with complex **11**.

Entry	11 mol%	Alkene:Perester Ratio	Time (h)	Product yield (%)[a]
A	5	5:1	6	73
B	5	5:1	24	95
C	5	3:1	24	79
D	1	5:1	24	77
E	1	3:1	24	74
F	0.5	10:1	24	95
G	0.5	5:1	24	90
H	0.5	3:1	24	90
I	0.5	1:1	48	33

Table 30. Study on the catalytic activity of complex **11** ([a]Yield of pure isolated product).

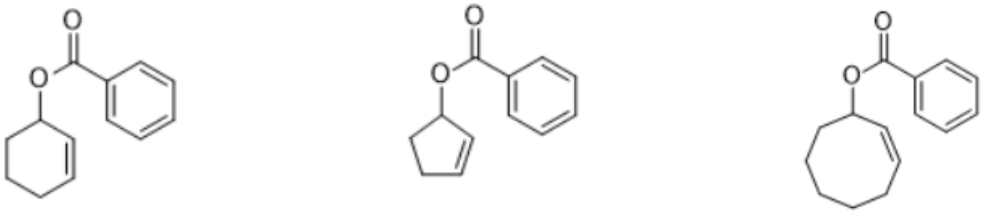

a) Yield: 90% b) Yield: 75% c) Yield: 57%

Fig. 62. Synthesis of oxygenate allylic compounds *via* Kharasch-Sosnovsky reaction using **11** as catalyst.

Finally, once confirmed the very virtuous catalytic performance of this complex, the optimised reaction conditions were tested on cyclopentene and cyclooctene, obtaining in both cases good yields (**Figure 62**).

10.4 Conclusion

Two new hexyl bis(pyrazol-1-yl) acetate ligands **8** and **9** were synthetised by the esterification reaction of the bis(pyrazol-1-yl) carboxylic acids. In addition, four copper complexes **10**-**13** were prepared from their reaction with $CuCl_2 \cdot 2H_2O$ and $CuBr_2$ in acetonitrile suspension, at room temperature. X-ray Photoelectron Spectroscopy data analysis and NEXAFS spectroscopy were performed on complexes with the aim to investigate the electronic and molecular structure of the ligands and the complexes and to gather further information about the functional groups presence and stability in the copper(II) coordination compounds, respectively. Finally, these complexes were successfully investigated as catalysts for the synthesis of oxygenate allylic compounds via Kharasch-Sosnovsky avoiding the use of any external agents, superstoichometric amount of reagents and long reaction times, which are the main limitations of Kharasch-Sosnovsky reaction. The use of complex **13** (5%mol) in 5:1 alkene peroxyester ratio and 6 h as reaction time led to 85% yield: these conditions were successively improved performing the reaction with complex **11**. In this case, the amount of catalyst and the alkene:peroxyester ratio were reduced to 0,5% mol and 3:1, respectively; the main advantages of this improved reaction are the major applicability spectrum to more expensive and les available starting materials and the reduce amount of generated waste products.

11. References

1) J. J. Berzelius, *Jahresberichte*, **12**, 63, 1833;
2) J. C. F. Williams, *J. Chem. Soc.*, **15**, Pt. 10, 1862;
3) A-V- Lourenço, *Compt. Rend.*, **51**, 365, 1860;
4) L. H. Baekeland, *Ind. Eng. Chem.*, **5**, 506, 1913;
5) https://www.nobelprize.org/prizes/chemistry;
6) H. Staudinger, *Chem. Ber.*, **57**, 1203, 1924;
7) H. Mark, G. S. Whitby (Eds.), *Collected Papers of Wallace Hume Carothers on High Polymeric Substances*, Wiley-Interscience, New York, 1940;
8) G. Natta, P. Pino, P. Corradini, F. Danusso, E. Mazzantini, G. Moraglio, *J. Am. Chem. Soc.*, **77**, 1708, 1955;
9) K. Ziegler, E. Holzkamp, H. Breil, H. Martin, *Angew. Chem.*, **67**, 541, 1955;
10) P. J. Flory, *Principles of Polymers Chemistry*, 2nd ed., Cornell University Press, Ithaca, N.Y., 1953;
11) Z. Zhou, S. Pesek, J. Klosin, M. S. Rosen, S. Mukhopadhyay, R. Cong, D. Baugh, B. Winniford, H. Brown, *Macromolecules*, **51**, 8443, 2018;
12) W. H. Carothers, *J. Amer. Chem. Soc.*, **51**, 2548, 1928;
13) M. L. Miller, *The Structure of Polymers*, Rheinhold, New York, 1966;
14) R. D. Deanin, *Polymer Structure, Properties and Applications*, Cahners Books, Boston, 1972;
15) H. F. Mark, N. R. Bikales, C. G. Overberger, G. Menges, J. I. Kroschwitz, *Encyclopedia of Polymer Science and Engineering*, **7**, 531-544, Wiley-Interscience, New York, 1987;
16) J. R. Wunsch, *Polystyrene: synthesis, production and applications*, iSmithers Rapra Publishing, 2000;
17) J. Brandup, E. H. Immergut, *Polymer Handbook, 3rd ed.*, Wiley-Interscience, New York, 1975;
18) A. Ledwith, A. M. North (Eds.), *Molecular Behaviour and the Development of Polymeric Materials*, Wiley-Interscience, New York, 1975;
19) A. V. Tobolsky, *Properties and Structure of Polymers*, Wiley-Interscience, New York, 1960;

20) G. L. Wilkes, *J. Chem. Educ.*, **58**, 880, 1981;
21) J. J. Aklonis, W. MacKnight, *Introduction to Polymer Viscoelasticity, 2nd ed.*, Wiley-interscience, 1983;
22) H. Tadokoro, *Structure of Crystalline Polymers*, Wiley-Interscience, New York, 1979;
23) P. H. Geil, E. Baer, Y. Wada, *The Solid State of Polymers*, Marcel Dekker, New York, 1974;
24) L. Mandelkern, *Crystallization of Polymers*, McGraw-Hill, New York, 1964;
25) L. R. G. Treolar, *The Physic of Rubber Elasticity, 3rd ed.*, Clarendon, Oxford, 1975;
26) H. H. Yang, *Kevlar® Aramid Fiber*, Wiley, Chichester, U.K., 1993;
27) D. Tanner, J. A. Fitzgerald, B. R. Phillips, *Angew. Chem. Int. Ed. Engl. Adv. Mater.*, **28**, 649, 1989;
28) N. R. Legge, G. Holden, H. E. Schroeder, *Thermopalstic Elastomers: A Comprehensive Rewiev*, Hanser-Gardner, 1989;
29) R. B. Seymour, G. B. Kauffman, *J. Chem. Educ.*, **69**, 967, 1992;
30) D.R. Paul, S. Newman, *Polymer Blends*, Academic Press, New York, 1978;
31) L. H. Sperling, *Macromol. Rev.*, **12**, 141, 1977;
32) J. A. Manson, L. H. Sperling, *Polymer Blends and Composites*, Plenum Press, New York, 1976;
33) G. Gozzellino, *Materie Plastiche*, Hoepli, 2007;
34) P. E Hurley, *Journal of Macromolecular Science: Part A*, **15:7**, 1279, 1981;
35) L. K. Opeke, *Tropical Tree Crops*, John Wiley and Sons, New York, 1982;
36) B. R. Buttery, S. G. Boatman, *Science*, **145**, 285, 1964;
37) H. De Livonniere, *IRRBD Technology Symposium on Quality and Consistency of Natural Rubber*, 1991, Manila, Philippines;
38) B. C. Sekhar, *Journal of Polymer Science*, **48**, 150, 133-150, 1960;
39) C. S. L. Baker, I. R. Gelling, R. Newell, *Rubber Chemistry and Technology*, **58**, 1, 1985;
40) A. Subramaniam, *Rubber Chemistry and Technology*, **45**, 1, 346, 1972;
41) S. Montes, J. L. White, *Rubber Chemistry and Technology*, **55**, 1354, 1982;
42) G. M. Bristow, *NR Technology*, **10**, 3, 53, 1979;
43) H. W. Greensmith, L. Mullins, A.G. Thomas, *The Chemistry and Physics of Rubber Like Substances*, Ed., L. Bateman, Maclaren and Sons Ltd., 1963;

44) D. Barnard, P. M. Lewis, *Natural Rubber Science and Technology*, Oxford University Press, 1988;
45) J. Witte, *Methods in Organic Chemistry: Macromolecular Compounds, Volume E20/1*, Eds., H. Bartl and J. Falbe, 1987;
46) ASTM D3053-04, Standard Terminology Relating to Carbon Black, 2004;
47) J. LeBras, E. Papirer, *Rubber Chem. Technol.*, **52**, 43, 1979;
48) M. B. Rodgers, W. H. Waddell, W. Klingensmith, *Kirk-Othmer Encyclopedia of Chemical Technology, 5th ed.*, John Wiley & Sons, 2004;
49) R. Alex, N. M. Mathew, P. P. De, S. K. De, *Kautsch. Gummi Kunsts.* **42**, 674, 1989;
50) E. M. Dannenberg, *Rubber chem. technol*., **48**, 410, 1975;
51) J. E. Mark, B. Erman, F. R. Eirich, *Science and Technology of Rubber*, *2nd ed.* Academic Press, 1994;
52) ASTM D611-12, Standard Test Methods for Aniline Point and Mixed Aniline Point of Petroleum Products and Hydrocarbon Solvents, 2016;
53) N. J. Morrison, M. Porter, *Rubber Chem. Technol.*, **57**, 63, 1984;
54) G. Oenslager, *Ind. Eng. Chem.*, **23**, 232, 1933;
55) L. Sebrell, C. Bedford, *US Patent 1 522 687*, 1925;
56) M. W Harmon, *US Patent 2 100 692*, 1937;
57) E. C. Gregg Jr., S. E. Katrenick, *Rubber Chem. Technol.*, **43**, 549, 1970;
58) K. A. J. Dijkhuis, J. W. M. Noordemeer, W. K. Dierkes, *Eur. Polym. J.*, **45**, 3302, 2009;
59) O. Bayer, *Angew. Chem.* **A59**, 275, 1947;
60) O. Bayer, Müller E., Petersen S., Piepenbrink H. F., Windemuth E., *Angew. Chem.***, 57**, 1950;
61) P. F. Bruins, *Polyurethane Technology*, Interscience Publishers, London, UK, 1969;
62) R. Herrington, K. Hock, *Flexible Polyurethane Foams*, *2nd Edition*, Dow Chemical Company, 1997;
63) G. Woods, *The ICI Polyurethanes Book*, *2nd Edition*, John Wiley & Sons, 1990;
64) S. G. Entelis, V. V. Evreinov, A. I. Kuzaev, *Reactive Oligomers*, Brill Publishers, 1988;
65) K. C. Frisch, J. H. Saunders, *Plastic Foams*, Marcel Dekker, 1972;

66) H. Saunders, K. C. Frisch in *Polyurethanes, Chemistry and Technology, High Polymers, Volume 14, Part II: Technology*, Interscience Publishers, 1964;
67) C. M. Barringer, *Bullettin HR-11*, 1956;
68) H. L. Heiss, J. H. Saunders, M. R. Morris, B. R. Davis, E. E. Hardy, *Ind. Eng. Chem.*, **46**, 1498, 1954;
69) E. Müller in *Houben-Weyl, Methoden der organischen Chemie, Vol. 14*, Thieme-Verlag;
70) ASTM D 907-82, *Annual Book of ASTM Standards*, 1984;
71) S. Ebnesajjad, *Handbook of Adhesives and Surface Preparation: Technology, Applications and Manufacturing*, Elsevier, 2011;
72) J. M. DeBell, W. C. Goggin, W. E. Gloor, *German Plastic Practice*, DeBell and Richar dson, 1946;
73) Farbenfabriken-Bayer, *U.S. patent 2,650,212*, 1953;
74) S. Petersen, *Liebigs Ann. Chem.*, **562**, 205, 1949;
75) G. Oertel, *Polyurethane Handbook*, Carl Hanser, 1985;
76) L. Maempel, *Adhesion*, **5**, 14, 1988;
77) ISO 6502-1, *Measurement of vulcanization characteristics using curemeters - Part 1: Introduction*, 2018;
78) ISO 6502-2, *Rubber - Measurement of vulcanization characteristics using curemeters - Part 2: Oscillating disc curemeter*, 2018;
79) ISO 2781, *Rubber, vulcanized or thermoplastic - Determination of density*, 2018;
80) ISO 4649, *Rubber, vulcanized or thermoplastic - Determination of abrasion resistance using a rotating cylindrical drum device*, 2017;
81) UNI EN ISO 20345, *Dispositivi di protezione individuale - Calzature di sicurezza*, 2012;
82) ISO 37-1, *Rubber, vulcanized or thermoplastic - Determination of tensile stress-strain properties*, 2017;
83) ISO 34-1, *Rubber, vulcanized or thermoplastic - Determination of tear strength - Part 1: Trouser, angle and crescent test pieces*, 2015;
84) ISO 868, *Plastics and ebonite - Determination of indentation hardness by means of a durometer (Shore hardness)*, 2003;
85) ISO 17708, *Footwear - Test methods for whole shoe - Upper sole adhesion*, 2018;

86) ISO 1817, *Rubber, vulcanized or thermoplastic - Determination of the effect of liquids*, 2015;
87) ISO 2878, *Rubber, vulcanized or thermoplastic - Antistatic and conductive products - Determination of electrical resistance*, 2017;
88) Inail, *Bollettino trimestrale denuncie di infortunio e malattie professionali*, periodo gennaio-dicembre 2021;
89) Y. S. Lee, S. H. Park, J. C. Lee, *J. Elastomers Plast.*, **48(8)**, 659, 2015;
90) Y. S. Lee, K. R. Ha, *World J. Text Eng. Technol.*, **5**, 77, 2019;
91) C. S. J. Cazin, *N-Heterocyclic Carbenes in Transition Metal Catalysis and Organocatalysis*; **Volume 32**, Springer Science & Business Media: Dordrecht, The Netherlands, 2011;
92) T. Rovis, S.P. Nolan, *Synlett.*, **24**, 1188, 2011;
93) L. A. Schaper, S.J. Hock, W. A. Herrmann, F. E. Kuehn, *Angew. Chem. int. Ed.*, **44**, 270, 2013;
94) Y. He, M.-F. Lv, C. Cai, *Dalton Trans.*, **41**, 12428, 2012;
95) Y. Li, X. Chen, Y. Song, L. Fang, G. Zou, *Dalton Trans.*, **40**, 2046, 2011;
96) K. D. Mjos, C. Orvig, *Chem. Rev.*, **114**, 4540, 2014;
97) S. B. Aher, P.N. Muskawar, K. Thenmozh, P.R. Bhagat, *Eur. J. Med. Chem.*, **81**, 408, 2014;
98) C. Ceresa, A. Bravin, G. Cavaletti, M. Pellei, C. Santini, *Curr. Med. Chem.*, **21**, 2237, 2014;
99) S. Budagumpi, R. A. Haque, S. Endud, G. U. Rehman, A.W. Salman, *Eur. J. Inorg. Chem.*, **2013**, 4367, 2013;
100) W. Liu, R. Gust, *Chem. Soc. Rev.*, **42**, 755, 2013;
101) C. A. Smith, M. R. Narouz, P. A. Lummis, I. Singh, A. Nazemi, C. H. Li, C. M. Crudden, *Chem. Rev.*, **119**, 4986, 2019;
102) L. Tschugajeff, M. Skanawy-Grigorjewa, A. Posnjak, *Z. Anorg. Chem.*, **148**, 37, 1925;
103) A. J. Arduengo, R. L. Harlow, M. Kline, *J. Am. Chem. Soc.*, **113**, 361, 1991;
104) W. A. Herrmann, M. Elison, J. Fischer, C. Kocher, G. R. J. Artus, *Angew. Chem. Int. Ed.*, **34**, 2371, 1995;
105) M. C. Perry, K. Burgess, *Tetrahedron: Asymmetry*, **14**, 951, 2003;

106) N. Fröhlich, U. Pidun, M. Stahl, G. Frenking, *Organometallics*, **16**, 442, 1997;

107) W. A. Herrmann, *Angew. Chem. Int. Ed.*, **41**, 1291, 2002;

108) X. L. Hu, Y. J. Tang, P. Gantzel, K. Meyer, *Organometallics*, **22,** 612–614, 2003;

109) N. M. Scott, R. Dorta, E. D. Stevens, A. Correa, L. Cavallo, S. P. Nolan, *J. Am. Chem. Soc.*, **127**, 3516, 2005;

110) A. A. D. Tulloch, A. A. Danopoulos, S. Kleinhenz, M. E. Light, M. B. Hursthouse, G. Eastham, *Organometallics*, **20**, 2027, 2007;

111) R. Dorta, E. D. Stevens, S. P. Nolan, *J. Am. Chem. Soc.*, **126**, 5054–5055, 2004;

112) C. A. Tolman, *Chem. Rev.*, **77**, 313, 1977;

113) A. Poater, B. Cosenza, A. Correa, S. Giudice, F. Ragone, V. Scarano, L. Cavallo, *Eur. J. Inorg. Chem.*, 1759, 2009;

114) P. de Frémont, N. Marion, S. P. Nolan, *Coord. Chem. Rev.*, **253**, 862, 2009;

115) F. E. Hahn, M. C. Jahnke, *Angew. Chem. Int. Ed.*, **47**, 3122, 2008;

116) A. J. Arduengo, J.R. Goerlich, W. J. Marshall, *J. Am. Chem. Soc.*, **117**, 11027, 1995;

117) A. Wacker, C. G. Yan, G. Kaltenpoth, A. Ginsberg, A. M. Arif, R. Ernst, H. Pritzkow, W. Siebert, *J. Organomet. Chem.*, **641**, 195, 2002;

118) A. Wacker, H. Pritzkow, W. Siebert, *Eur. J. Inorg. Chem.*, **6**, 843, 1998;

119) A. Weiss, H. Pritzkow, W. Siebert, *Eur. J. Inorg. Chem*., **2002**, 1607, 2002;

120) W. C. Liu, Y. H. Liu, T. S. Lin, S. M. Peng, C. W. Chiu, *Inorg. Chem.*, **56**, 10543, 2017;

121) A. Wacker, H. Pritzkow, W. Siebert, *Eur. J. Inorg. Chem.*, **5**, 789, 1999;

122) K. Okada, R. Suzuki, M. Oda, *J. Chem. Soc., Chem. Commun.*, **20**, 2069, 1995;

123) D. Vagedes, G. Erker, G. Kehr, K. Bergander, O. Kataeva, R. Fröhlich, S. Grimme, C. Mück-Lichtenfeld, *Dalton Trans.*, **7**, 1337, 2003;

124) I. I. Padilla-Martínez, M. D. J. Rosalez-Hoz, R. Contreras, S. Kerschl, B. Wrackmeyer, *Eur. J. Inorg. Chem.*, **127**, 343,1994;

125) C. Santini, M. Marinelli, M. Pellei, Eur. *J. Inorg. Chem*., **2016**, 2312, 2016;

126) R. Fränkel, C. Birg, U. Kernbach, T. Habereder, H. Noth, W. P. Fehlhammer, *Angew. Chem., Int. Ed.*, **40**, 1907, 2001;

127) A. Biffis, G. Gioia Lobbia, G. Papini, M. Pellei, C. Santini, E. Scattolin, C. Tubaro, *J. Organomet. Chem*, **693**, 3760, 2008;

128) G. Papini, G. Bandoli, A. Dolmella, G. Gioia Lobbia, M. Pellei, C. Santini, *Inorg. Chem. Commun.*, **11**, 1103, 2008;

129) G. Papini, M. Pellei, G. Gioia Lobbia, A. Burini, C. Santini, *Dalton Trans.*, 6985, 2009;

130) M. Meisters, J. T. VandeBerg, F. P. Cassaretto, H. Posvic, C. E. Moore, *Anal. Chim. Acta*, **49**, 481, 1970;

131) P. K. Bakshi, A. Linden, B. R. Vincent, S. P. Roe, D. Adhikesavalu, T. S. Cameron, O. Knop, *Can. J. Chem.*, **72**, 1273–1293, 1994;

132) J. Liu, J. Chen, J. Zhao, Y. Zhao, L. Li, H. Zhang, *Synthesis*, **17**, 2661–2666 ,2003;

133) G. M. Sheldrick, *Acta Crystallogr. Sect. A Found. Crystallogr.*, **64**, 112–122, 2007;

134) O. Dolomanov, L. J. Bourhis, R. Gildea, J. A. Howard, J. Puschmann, *J. Appl. Crystallogr.*, **42**, 339–341, 2009.

135) G. Bélanger-Chabot, S. M. Kaplan, P. Deokar, N. Szimhardt, R. Haiges, K. O. Christe, *Chem. - A Eur. J.*, **23**, 13087, 2017;

136) S. G. Ridlen, N. Kulkarni, H. V. R. Dias, *Inorg. Chem.*, **56**, 7237, 2017;

137) O. H. Winkelmann, O. Navarro, *Adv. Synth. Catal.*, **352**, 212, 2010;

138) D. P. Curran, A. Solovyev, M. M. Brahmi, L. Fensterbank, M. Malacria, E. Lacôte, *Angew. Chem. Int. Ed.*, **50**, 10294, 2011;

139) B. Wrackmeyer, *Annual Reports on NMR Spectroscopy*, **20**, 61, 1988;

140) R. G. Bergman, *Nature*, **446**, 391, 2007;

141) M. C. White, *Synlett.*, **23**, 2746, 2012;

142) J. Wencel-Delord, T. Dröge, F. Liu, F. Glorius, *Chem. Soc. Rev.*, **40**, 4740, 2011;

143) F. Ullmann, G. Wolfgang, Y. S. Yamamoto, F. T. Campbell, R. Pfefferkorn, J. Rounsaville, *Ullmann's Encyclopedia of Industrial Chemistry;* **Volume A3**, Wiley-VCH, 1985;

144) M. S. Kharasch, G. Sosnovsky, *J. Am. Chem. Soc.*, **80**, 75, 1958;

145) M. S. Kharasch, G. Sosnovsky, N. Yang, *J. Am. Chem. Soc.*, **81**, 5819–5824, 1959;

146) D. J. Rawlinson, G. Sosnovsky, *Synthesis*, **1972**, 1, 1972;

147) A- L. García-Cabeza, F. J. Moreno-Dorado, M. J. Ortega, F. M. Guerra, *Synthesis*, **48**, 2323, 2016;

148) N. Zhu, B. Qian, H. Xiong, H. Bao, *Tetrahedron Lett.*, **58**, 4125, 2017;

149) M. B. Andrus, J. C. Lashley, *Tetrahedron*, **58**, 845, 2002;

150) J. H. Delcamp, M. C. White, *J. Am. Chem. Soc.*, **128**, 15076, 2006;

151) V. Weidmann, W. Maison, *Synthesis*, **45 (16)**, 2201-2221, 2013;
152) K. J. Fraunhoffer, D. A. Bachovchin and M. C. White, *Org. Lett.*, **7**, 223-226, 2005;
153) J. Eames, M. Watkinson, *Angew. Chem. Int. Ed. Engl.*, **40**, 3567, 2001;
154) J. M. Brunel, O Legrand, G. Buono, *Comptes Rendus Acad. Sci. Ser. II C*, **2**, 19, 1999;
155) L. Aldea, J. I. Garcia, J. A. Mayoral, *Dalton Trans.*, **41**, 8285, 2012;
156) Q. Tan, M. Hayashi, *Adv. Synth. Catal.*, **350**, 2639, 2008;
157) S. Trofimenko, *J. Am. Chem. Soc.*, **88**, 1842, 1966;
158) A. Beck, B. Weibert, N. Burzlaff, *Eur. J. Inorg. Chem.*, **2001**, 521-527, 200;
159) N. Burzlaff, I. Hegelmann, B. Weibert, *J. Organomet. Chem.*, **626**, 16, 2001;
160) I. Alkorta, R. M. Claramunt, E. Díez-Barra, J. Elguero, A. d. l. Hoz, C. López, *Coord. Chem. Rev.*, **339**, 153, 2017;
161) A. Otero, J. Fernández-Baeza, A. Lara-Sánchez, L. F. Sánchez-Barba, *Coord. Chem. Rev.*, **257**, 1806, 2013;
162) T. Newhouse, P. S. Baran, *Angew. Chem., Int. Ed.*, **50**, 3362, 2011;
163) A. Otero, J. Fernández-Baeza, A. Lara-Sánchez, L. F. Sánchez-Barba, *Coord. Chem. Rev.*, **257**, 1806, 2013;
164) J. L. Rhinehart, K. A. Manbeck, S. K. Buzak, G. M. Lippa, W. W. Brennessel, *Organometallics*, **31**, 1943, 2012;
165) H. Kopf, B. Holzberger, C. Pietraszuk, E. Huebner, N. Burzlaff, *Organometallics*; **27**, 5894, 2008;
166) G. Türkoglu, S. Tampier, F. Strinitz, F. W. Heinemann, E. Hübner, N. Burzlaff, *Organometallics*, **31**, 2166, 2012;
167) T. Godau, S. M. Bleifuß, A. L. Müller, T. Roth, S. Hoffmann, F. W. Heinemann, N. Burzlaff, *Dalton Trans.*, **40**, 6547–6554, 2011;
168) J. Zhang, A. Li, T. S. A. Hor, *Organomet.*, **28**, 2935–2937, 2009;
169) P. Padnya, K. Shibaeva, M. Arsenyev, S. Baryshnikova, O. Terenteva, I. Shiabiev, A. Khannanov, A. Boldyrev, A. Gerasimov, D. Grishaev, D., *Molecules*, **26**, 2334, 2021;
170) B. M. L. Dioos, I. F. J. Vankelecom, P. A. Jacobs, *Adv. Synth. Catal.*, **348**, 1413, 2006;
171) M. I. Burguete, J. M. Fraile, J. I. García, E. García-Verdugo, C. I. Herrerías, S. V. Luis, J. A. Mayoral, *J. Org. Chem.*, **66**, 8893, 2001;

172) D. D. Mal, J. Kundu, D. Pradhan, *Chem. Cat. Chem.*, **13**, 362, 2021;

173) D. Tetour, M. Novotná, J. Hodacová, J. *Catalysts*, **11**, 41, 2021;

174) S. Alidori, G. Gioia Lobbia, G. Papini, M. Pellei, M. Porchia, F. Refosco, F. Tisato, S. L. Jason, C. Santini, *J. Biol. Inorg. Chem.*, **13**, 307, 2008;

175) C. Marzano, M. Pellei, D. Colavito, S. Alidori, G. Gioia Lobbia, V. Gandin, F. Tisato, C. Santini, *J. Med. Chem.*, **49**, 7317, 2006;

176) F. Benetollo, G. Gioia Lobbia, M. Mancini, M. Pellei, C. Santini, *J. Organomet. Chem.*, **690**, 1994, 2005;

177) M. Porchia, G. Papini, C. Santini, G. Gioia Lobbia, M. Pellei, F. Tisato, G. Bandoli, A. Dolmella, *Inorg. Chem.*, **44**, 4045, 2005;

178) M. Pellei, G. Gioia Lobbia, C. Santini, R. Spagna, M. Camalli, D. Fedeli, G. Falcioni, *Dalton Trans.*, 2822, 2004;

179) M. Pellei, V. Gandin, L. Marchiò, C. Marzano, L. Bagnarelli, C. Santini, *Molecules*, **24**, 1761, 2019.

180) C. K. Johnson, ORTEP, report ORNL-5138, Oak Ridge national laboratory, Oak Ridge, TN; 1976;

181) B. Kozlevčar, T. Pregelj, A. Pevec, N. Kitanovski, J. S. Costa, G. Van Albada, P. Gamez, J. Reedijk, *Eur. J. Inorg. Chem.*, **31**, 4977, 2008;

182) B. Quillian, W. E. Lynch, C. W. Padgett, A. Lorbecki, A. Petrillo, M. Tran, *J. Chem. Cryst.*, **49**, 1, 2019;

183) M. A. Romero, J. M. Salas, M. Quiros, M. P. Sanchez, J. Romero, D. Martin, *Inorg. Chem.*, **33**, 5477, 1994;

184) L. G. Lavrenova, V. N. Ikorskij, L. A. Sheludyakova, D. Y. Naumov, E. G. Boguslavskij, *Rus. J. Coord. Chem.*, **30**, 442, 2004;

185) L. Dobrzanska, D. J. Kleinhans, L. J. Barbour, *New J. Chem.*, **32**, 813, 2008;

186) A. Hoffmann, S. Herres-Pawlis, *Zeitschrift für Anorganische und Allgemeine Chemie*, **639**, 1426, 2013;

187) T. N. Andreeva, A. S. Lyakhov, L. S. Ivashkevich, S. V. Voitekhovich, Y. V. Grigoriev, O. A. Ivashkevich, *Zeitschrift für Anorganische und Allgemeine Chemie*, **641**, 2312, 2015;

188) I. I. Dyukova, T. A. Kuz'menko, V. Y. Komarov, T. S. Sukhikh, E. V. Vorontsova, L. G. Lavrenova, *Rus. J. Coord. Chem.*, **44**, 755, 2018;

189) C. F. Macrae, I. J. Bruno, J. A. Chisholm, P. R. Edgington, P. McCabe, E. Pidcock, L. Rodriguez-Monge, R. Taylor, J. Van De Streek, P. A. Wood, *J. App. Crystal.*, **41**, 466, 2008;

190) C. Battocchio, I. Fratoddi, G. Iucci, M. V. Russo, A. Goldoni, P. Parent, G. Polzonetti, *Mat. Sc. Eng. C*, **27**,1338, 2007;

191) G. Polzonetti, C. Battocchio, A. Goldoni, R. Larciprete, V. Carravetta, R. Paolesse, M. V. Russo, *Chem. Phys.*, **297**, 307, 2004;

192) J. Y. Jhuang, S. H. Lee, S. W. Chen, Y. H. Chen, Y. J. Chen, J. L. Lin, C. H. Wang, Y. W. Yang, *J. Phys. Chem. C*, **122**, 6195, 2018;

193) NIST, X-ray Photoelectron Spectroscopy Database, Version 4.1, National Institute of Standards and Technology, http://srdata.nist.gov/xps/;

194) T. Yoshida, K. Yamasaki, S. Sawada, *Bull. Chem. Soc. Jap.*, **51**, 1561, 1978;

195) D. A. Outka, J. Stöhr, R. J. Madix, H. H. Rotermund, B. Hermsmeier, J. Solomon, *Surf. Sc.*, **185**, 53, 1987;

196) A. V. Syugaev, A. N. Maratkanova, D. A. Smirnov, *J. Sol. St. Electrochem.*, **22**, 2127-2134, 2018;

197) J. Stöhr; *NEXAFS spectroscopy*, Springer Science & Business Media; 1992;

198) V. Secchi, S. Franchi, D. Ciccarelli, M. Dettin, A. Zamuner, A. Serio, G. Iucci, C. Battocchio, *ACS Biomat. Sc. & Eng.*, **5**, 2190, 2019;

199) V. Secchi, S. Franchi, M. Santi, A. Vladescu, M. Braic, T. Skála, J. Nováková, M. Dettin, A. Zamuner, G. Iucci, C. Battocchio, *Nanomat.*, **8**, 148, 2018;

200) G. Aquilanti, M. Giorgetti, M. Minicucci, G. Papini, M. Pellei, M. Tegoni, A. Trasatti, C. Santini, *Dalton Trans.*, **40**, 264, 2011;

201) M. Giorgetti, L. Guadagnini, S. G. Fiddy, C. Santini, M. Pellei, *Polyhedron*, **28**, 3600, 2009;

202) L. S. Kau, D. J. Spira-Solomon, J. E. Penner-Hahn, K. O. Hodgson, E. I. Solomon, *J. Am. Chem. Soc.*, **109**, 6433, 1987;

203) J. Chaboy, A. Muñoz-Páez, F. Carrera, P. Merkling, E. S. Marcos, *Phys. Rev. B*, **71**, 134208, 2005;

204) A. L. Ankudinov, B. Ravel, J. J. Rehr, S. D. Conradson, *Phys. Rev. B*, **58**, 7565, 1998.